Si recordamos la visión profética de Julio Verne en La isla misteriosa: "Creo que un día el agua será un carburante, que el hidrógeno y el oxígeno que la constituyen, utilizados solos o conjuntamente, proporcionarán una fuente inagotable de energía y de luz, con una intensidad que el carbón no puede; que, dado que las reservas de carbón se agotarán, nos calentaremos gracias al agua. El agua será el carbón del futuro". Aunque aquí Julio Verne quizá no estaba pensando en plantas, fotosíntesis, o biocombustibles derivados de ellas, aunque si parece que hubiese cierta conexión. Y es que el mundo no se está quedando sin energía, se está quedando sin tiempo para que la transición energética no sea un proceso traumático. La puesta a punto de nuevos sistemas de producción de energía, las inversiones necesarias, las infraestructuras, etc., son procesos muy lentos.

Los objetivos de este trabajo han sido marcados por el panorama actual de escasez de petróleo, a su creciente demanda y a la contaminación. Con el tiempo se consiguirá producir bioetanol de segunda generación económicamente viable, que será parte del amalgama de soluciones que acompañen a lograr una solución a dichos problemas. En este trabajo hemos hecho uso de herramientas de mejora genética clásica, biotecnológicas y de teledetección para poner en valor el uso de la biomasa lignocelulósica procedente de trigo, cebada y triticale como fuente alternativa de energía. Los resultados obtenidos han dado lugar a valiosas conclusiones entre las que principalmente han destacado, la gran variabilidad encotrada entre los numerosos genotipos evaluados para el factor del potencial de bioetanol, la posibilidad de usar con cierta precisión herramientas de teledetección para su evaluación y por último el posible efecto del gen BdGT43A silenciado en lineas de B. distachyon para el mismo factor. Con lo que seguro, a partir de aquí se darán lugar a nuevas investigaciones que podrían llegar a formar parte de la solución a nuestos probemas.

Francisco José Ostos Garrido

TESIS DOCTORAL

TESIS DOCTORAL

Mejora de trigo y triticale para la producción de bioetanol lignocelulósico usando herramientas clásicas y moleculares

TITULO: *MEJORA DE TRIGO Y TRITICALE PARA LA PRODUCCIÓN DE BIOETANOL LIGNOCELULÓSICO USANDO HERRAMIENTAS CLÁSICAS Y MOLECULARES*

AUTOR: *Francisco José Ostos Garrido*

Campus de Rabanales
Ctra. Nacional IV, Km. 396 A
14071 Córdoba

https://www.uco.es/ucopress/index.php/es/
ucopress@uco.es

UNIVERSIDAD
D
CÓRDOBA

Mejora de trigo y triticale para la producción de bioetanol lignocelulósico usando herramientas clásicas y moleculares

---

Breeding Wheat and Triticale for lignocellulosic bioethanol production using basic and molecular

Programa de Doctorado

Ingeniería agraria, alimentaria, forestal y de desarrollo rural sostenible

Autor

Francisco José Ostos Garrido

Dirigida por

Dr. Fernando Pistón Pistón

Dr. Sergio G. Atienza Peñas

Córdoba, 2019

Francisco José Ostos Garrido
ORCID: https://orcid.org/0000-0003-3528-1220

email: g12osgaf@gmail.com

INFORME RAZONADO DE LOS DIRECTORES DE LA TESIS

Título: Mejora de trigo y triticale para la producción de bioetanol lignocelulósico usando herramientas clásicas y moleculares
Doctorando: Francisco José Ostos Garrido

Esta tesis ha obtenido resultados relevantes para la mejora y el conocimiento de la biomasa lignocelulósica de trigo, triticale y cebada, destinada a la producción de bioetanol. Estos trabajos han requerido de un aprendizaje en distintos ámbitos tales como: la evaluación del material vegetal en campo y en invernadero bajo condiciones controladas, el desarrollo y puesta a punto de métodos de sacarificación para estimar el rendimiento en etanol lignocelulósico, manejo de técnicas moleculares, el diseño de experimentos y la aplicación de programas estadísticos para el tratamiento de los datos obtenidos.

Los resultados de la tesis han dado lugar ya a dos artículos publicados en revistas SCI, una de ellas en el primer decil, y a una tercera publicación aún bajo revisión. También dio lugar a una participación en un congreso internacional y a la aceptación como comunicación oral en otro congreso previsto para 2019.

Dichas contribuciones se reseñan a continuación:

Publicaciones

Ostos Garrido FJ, Pistón F, Gómez LD, McQueen-Mason SJ. “Biomass recalcitrance in barley, wheat and triticale straw: Correlation of biomass quality with classic agronomical traits.” *PLOS ONE.* November 2018. ISSN 1932-6203. doi:10.1371/journal.pone.e0205880.

Francisco J Ostos-Garrido, Ana I de Castro, Jorge Torres-Sánchez, Fernando Pistón, José M Peña. “High-throughput phenotyping of bioethanol potential

in cereals by using UAV-based multi-spectral imagery." Front. Plant Sci. - Technical Advances in Plant Science. Under revision

Whitehead C, **Ostos Garrido FJ**, Reymond M, Simister R, Distelfeld A, Atienza SG, et al. "A glycosyl transferase family 43 protein involved in xylan biosynthesis is associated with straw digestibility in *Brachypodium distachyon*." *New Phytol*. May 2018. doi : 10.1111/nph.15089.
(New Phytologist IF2017=7.433, Ranking: 4/791, D1 en Plant and animal science)

Congresos internacionales

Leonardo D. Gomez; Nguyen Duong; **Francisco J. Ostos Garrido**; Caragh Whitehead; Rachael Simister; Claire Halpin; Simon McQueen-Mason. Screening for novel genes to improve lignocellulosic biomass. *XIV Cell Wall Meeting. Chania, Grecia* Fecha:12-17/06/2016.

J.M Peña, **F. J. Ostos**, J. Torres-Sánchez, F Pistón, A.I. de Castro. An UAV-based system for phenotyping crop growth in wheat, barley and triticale fields trials. *The 12th European conference on precisión agricultura*. Previsto para las fechas 8-11 Julio 2019 Motpellier, Francia. Enviado como "Full paper" y bajo revisión. Aceptado como comunicación oral.

Por todo ello se autoriza la presentación de la tesis doctoral:

En Córdoba a _____ de _____ del 2019.

Firmas de los directores

Dr. Fernando Pistón Pistón	Dr. Sergio G. Atienza Peñas

A María Jesús,
Carlota y Javier

AGRADECIMIENTOS

Esta Tesis Doctoral se realizó en el Departamento de Mejora Genética Vegetal del Instituto de Agricultura Sostenible (CSIC) en Córdoba y ha sido financiada por una beca de Formación de Personal Investigador (FPI BES-2012-052455) del Ministerio de Ciencia e Innovación (MICINN) a cargo del proyecto AGL2011-22596.

RESUMEN

La impronta del ser humano sobre el medio ambiente es hoy una realidad. El problema medioambiental que se cierne sobre la globalidad del planeta se ha visto acelerado por la masiva emisión de gases de efecto invernadero que produce la quema de combustibles fósiles para la obtención de energía. Por otro lado esta la demanda de energía, que se ve incrementada año a año por el constante aumento de la población mundial. Además, a estas tensiones sobre la demanda de energía hay que sumar la escasez de petróleo que se preveé en el corto-medio plazo, pues como sabemos, se trata de una fuente de energía no renovable.

Es difícil encontrar alternativas energéticas viables que se adapten a las infraestructuras y necesidades energéticas actuales. Aun así, una de las alternativas más prometedoras para contribuir a paliar estos problemas, es el uso de la biomasa vegetal para la obtención de bioetanol. Pero a pesar de ser una muy buena opción, su uso supone destinar alimentos para la obtención de etanol. Esto provoca que los precios de los alimentos se encarezcan, creando un grave problema de abastecimiento y seguridad alimentaria en las poblaciones más desfavorecidas.

El uso de los biocombustibles genera un intenso debate por su efecto en los precios de los alimentos, como también en su posible papel en la mitigación de cambio climático, así como en el desarrollo agrícola. Estos temas de debate fueron tratados en la Conferencia de Alto Nivel sobre Seguridad Alimentaria Mundial: “Los Desafíos del Cambio Climático y la Bioenergía”, donde se evaluó detalladamente la perspectiva futura, riesgos y oportunidades que podrían generar los biocombustibles, y que quedó como tema central del informe de la FAO de 2008 acerca de “El estado mundial de la agricultura y a alimentación”.

La introducción del biocombustible de segunda generación, como aquellos que usan biomasa lignocelulósica para la producción de bioetanol, abre una posibilidad a la producción de un carburante menos contaminante que el petróleo, sin entrar en competencia directa por el alimento. La biomasa lignocelulósica para la producción de bioetanol proviene principalmente de residuos agrícolas como restos de poda, rastrojos, restos de madera, paja de maíz, trigo o arroz, bagazo (residuos de la caña de azúcar y el sorgo), etc. Esta biomasa es el principal componente de la pared celular de las plantas, que por sus características químicas y estructurales, es extremadamente resistente a la digestión enzimática necesaria

que se pretende hacer para liberar los azúcares atrapados en ella. Tan recalcitrante es esta estructura, que la bioconversión en etanol de esta materia prima hace que el proceso actualmente sea inviable económicamente. El principal objetivo pues, es que el proceso de producción de bioetanol llegue a ser económicamente viable, y para conseguirlo podemos hacerlo a través una digestión más eficiente mediante, o por la obtención de biomasa menos recalcitrantes y más fácilmente accesibles a las enzimas, o ambas.

Este trabajo ha abordado este reto mediante una búsqueda de materiales lignocelulósicos más fácilmente accesibles a las enzimas hidrolíticas. Para llevarlo a cabo se han usado herramientas de mejora clásicas y moleculares. Una colección de sesenta y seis genotipos de trigo, triticale y cebada se han caracterizado fenotípicamente a lo largo de su desarrollo. Los genotipos mostraron gran variabilidad para el factor sacarificación, que estuvo correlacionado negativamente con el contenido de lignina en la pared celular. Además, los resultados mostraron que éste y otros factores podrían ser evaluados con cierta precisión usando el tratamiento de imágenes con plataformas aéreas no tripuladas (UAV – unmanned aerial vehicle), antes de ser recolectadas, de forma rápida y no destructiva. Además, varios parentales provenientes de poblaciones de mapeo mostraron diferencias contrastantes para el grado de sacarificación. Por último, se hizo una selección de genes involucrados en la síntesis de componentes de pared y se silenciaron mediante micros-ARN (miARN) en *Brachypodium distachyon*. Las plantas transgénicas mostraron alteraciones en las células de pared en del tallo y en algunos componentes de pared que la forman, dando lugar a un mayor potencial de sacarificación y alteraciones en los principales componentes de la pared celular.

ABSTRACT

The imprint of the human being on the environment is today a reality. The environmental problem that hangs over the global nature of the planet has been accelerated by the massive emission of greenhouse gases produced by the burning of fossil fuels. On the other hand, this demand for energy increases every year due to the increase in world population. In addition, we must add to these tensions on demand, the shortage of oil that is expected in the short-medium term, as we know, it is a non-renewable source of energy.

The infrastructures and energy needs that we have today do not make it easy for us to find economically viable energy alternatives. Even so, one of the most promising alternatives to help alleviate these problems is the use of vegetable biomass for bioethanol production. But this, despite being a very good option, means entering into competition with food production. As a result, large increases in food prices could occur, creating a serious problem of supply and food security in the most disadvantaged populations.

The use of biofuels generates an intense debate because of its effect on food prices, as well as its possible role in mitigating climate change, as well as agricultural development. These topics were discussed at the High Level Conference on World Food Security: "The Challenges of Climate Change and Bioenergy", where the future perspective, risks and opportunities that could be generated by biofuels were evaluated in detail, and that remained as central topic to the 2008 FAO report on "The global state of agriculture and food".

The introduction of second-generation biofuels, which use lignocellulosic biomass for the production of bioethanol, opens up a possibility for the production of fuel without competing with food. The lignocellulosic biomass for the production of bioethanol comes mainly from agricultural residue such as pruning remains, stubble, wood remains, corn stover, wheat and rice straw, bagasse (residue from sugarcane and sorghum stalks), etc. The lignocellulosic biomass is the main component of the cell wall of plants, which due to its chemical and structural characteristics is extremely resistant to enzymatic digestion, which is intended to release the sugars trapped in it. So recalcitrant is this structure, that the bioconversion in ethanol of this raw material makes the process currently economically unfeasible. The main objective is that the bioethanol production process becomes

economically viable, to achieve this we could do it through a more efficient digestion using more efficient enzymes, by obtaining biomass less recalcitrant and more easily accessible to enzymes, or both.

This work has addressed this challenge through a search for lignocellulosic materials more easily accessible to hydrolytic enzymes. For its approach, classical and molecular improvement tools have been used. A collection of sixty-six genotypes of wheat, triticale and barley have been phenotypically characterized throughout their development. The genotypes showed great variability for the saccharification factor, which was negatively correlated with the lignin content in the cell wall. In addition, the results showed that this and other factors could be evaluated with good accuracy using the treatment of images with unmanned aerial platforms (UAV - unmanned aerial vehicle), before harvested, quickly and non-destructively. Moreover, several parents from mapping populations showed contrasting differences for the degree of saccharification. Finally, a tracking of genes involved in the synthesis of wall components was made, and it was observed that the silencing done with miRNA in Brachypodium distachyon produced alterations in the wall cells in the stem, giving rise to, higher degrees of saccharification and alterations the main wall components.

ÍNDICE GENERAL

ÍNDICE DE FIGURAS

ÍNDICE DE CUADROS

Capítulo 1

INTRODUCCIÓN

1.1. Conceptos básicos y antecedentes

Esta introducción dará comienzo con la definición de conceptos tan controvertidos y tan presentes hoy en día como son los conocidos "efecto invernadero", "cambio climático" y "calentamiento global". Éstos son a menudo mal usados principalmente por la clase política, así como por los medios de comunicación, dando lugar a malas interpretaciones y generando una gran controversia en la opinión pública.

En primer lugar, se define cambio climático como cualquier cambio significativo a largo plazo en la temperatura promedio, la precipitación y los patrones de viento. El clima se define por factores como niveles de radiación, composición atmosférica, movimiento de las corrientes oceánicas, etc.

El efecto invernadero se define como el efecto que se produce sobre la temperatura media de la tierra gracias a la radiación devuelta a la tierra por gases como el CO_2, CH_4, O_3, NO, NO_2 y vapor de agua en menor medida, conocidos como gases de efecto invernadero (GEI de aquí en adelante).

Las emisiones antropogénicas de GEI han aumentado de tal forma, que han alterado el equilibrio natural y calentando de media el planeta en unos 0,8° en los últimos 140 años (Fig 3.6 (a) y (b)). Este calentamiento es conocido como calentamiento global, y se ha visto acelerado por las emisiones antropogénicas de GEI, siendo 10 veces más veloz que en el cambio climático natural más rápido conocido, el final de la edad de hielo [1].

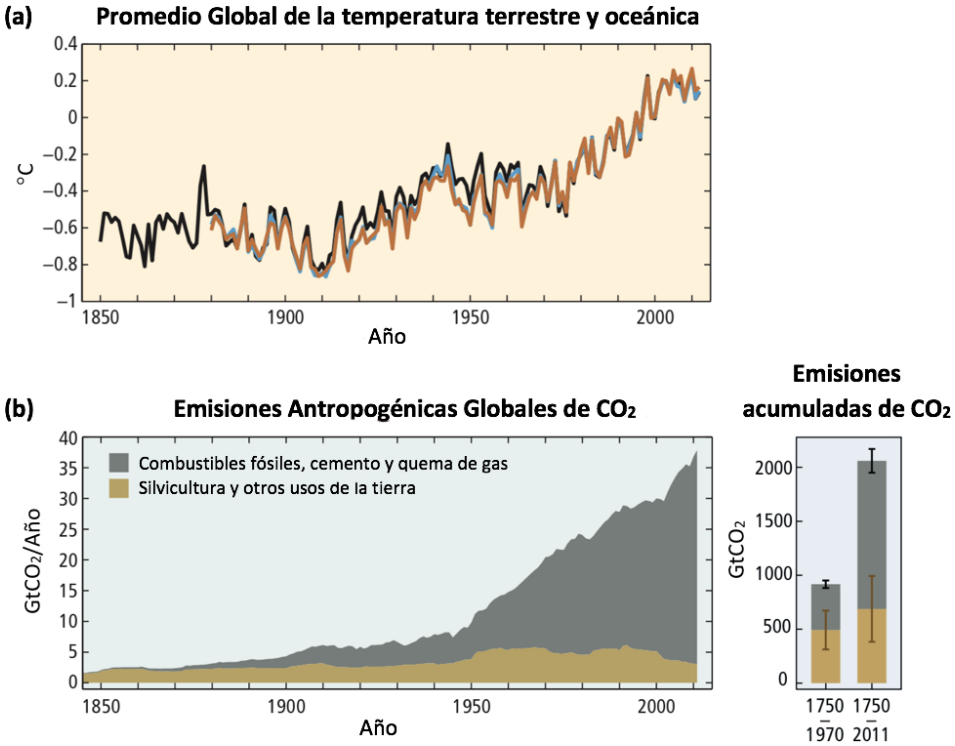

Figura 1.1: (a) Promedio anual y global de la temperatura en la superficie terrestre y oceánica en relación con el promedio durante el período de 1986 a 2005. Los datos mostrados con distintos colores en la imagen se corresponden con HadCRUT4 (version 4.1.1.0) en negro, NASA GISS en azul y NCDC MLOST (version 3.5.2) en naranja. (b) Emisiones antropogénicas anuales de dióxido de carbono (CO_2) (gigatonelada de CO_2 equivalente por año, GtCO_2/Año) procedentes de la quema de combustibles fósiles, producción de cemento, quema de pastos y otros usos de la tierra. Las emisiones acumuladas y sus incertidumbres se muestran como barras y bigotes, respectivamente, en el lado derecho. Ambas imagenes han sido tomadas y modificadas de [2] (`https://ar5-syr.ipcc.ch/`).

El término que define el proceso que conocemos como "efecto invernadero natural" fue descrito por primera vez en el año 1859 por el físico británico John Tyndall, pero fue una idea original de Joseph Fourier 30 años antes. Aunque nadie pudo demostrarlo hasta que Tyndall experimentó con las propiedades de absorción de los gases y vapores comúnmente encontrados en la atmósfera, con el objetivo de probar que absorbían diferentes cantidades de radiación [3]. Posteriormente, en 1897, Svante Arrhenius describió por primera vez el efecto de la contribución del dióxido de carbono sobre el efecto invernadero en un artículo titulado "On the Influence of Carbonic Acid in the Air upon the Temperature of the Ground" [4].

Estos GEI antropogénicos provienen principalmente de la producción energética basada en la quema de combustibles fósiles, la industria, el transporte y la cons-

trucción [2]. Por último, cabe reseñar que en 1938 Guy Stewart Callendar escribió un trabajo titulado: "The artificial production of carbon dioxide and its influence on temperature" [5], donde relacionaba la quema de combustibles fósiles con el calentamiento global a través de una modelización matemática, y que es actualmente conocido como el efecto Callendar [6].

1.2. Dependencia energética de los combustibles fósiles

Además de los problemas medioambientales a los que nos enfrentamos, y debido a la superpoblación e industrialización de países emergentes [7, 8], acecha en el horizonte un gran problema de desabastecimiento y distribución de energía. En el documento "World Energy Outlook, 2010" [9] que publica anualmente la Agencia Internacional de la Energía, fue situado en 2006 un cambio de tendencia en la extracción de petróleo a partir de los yacimientos conocidos (Fig 1.2). Este cambio de tendencia es conocido como "peak oil" y fue descrito por primera vez en 1949 por el geofísico Marion King Hubbert [10, 11].

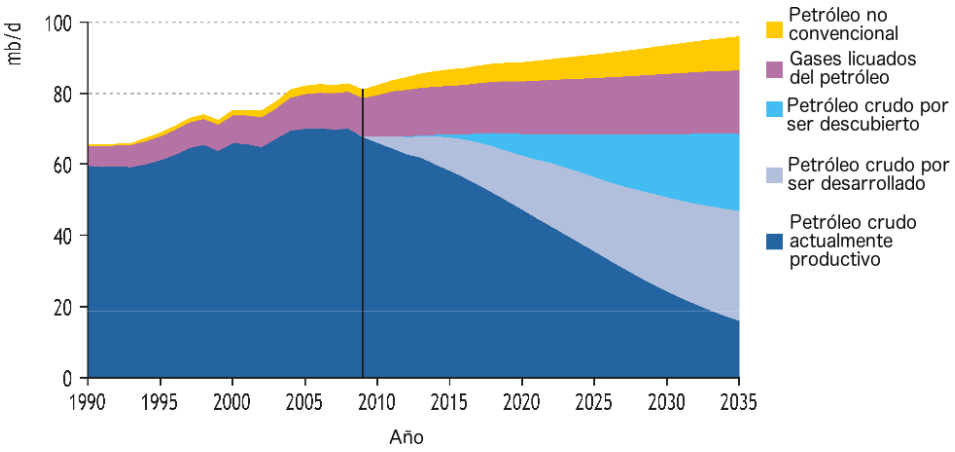

Figura 1.2: Producción de combustible por tipo. mb/d = millones de barriles diarios. (Imagen tomada y modificada de [9]).

La quema de combustibles fósiles produce aproximadamente el 81 % de la energía mundial [11] y es responsable del 80 % de las emisiones antropogénicas de gases de efecto invernadero (GEI) [12]. Del 81 % de la energía global suministrada por los combustibles fósiles, el 41 % proviene del petróleo, destinado en su mayor parte (92 %) al sector del transporte [11], por lo que una sustitución parcial de los combustibles utilizados en este sector por fuentes renovables podría ser de ayuda a superar la dependencia de estos combustibles fósiles.

Las políticas para aumentar la proporción de energía usada que provenga de fuentes renovables están en auge. Actualmente en la unión europea se fija para 2030 el objetivo de reducción de gases de efecto invernadero de almenos el 40 % respecto alos niveles de 1990 (https://ec.europa.eu/clima/policies/strategies/2030_es)

Si bien la generación de electricidad renovable se puede lograr utilizando energía solar, nuclear, eólica, geotérmica e hidroeléctrica, dichos recursos no biológicos no nos proporcionan un reemplazo de los combustibles derivados del petróleo. Es necesario, por tanto, hacer grandes esfuerzos en la búsqueda de fuentes energéticas alternativas, que sean renovables, sostenibles y respetuosas con el medio ambiente a la vez que viables en las actuales economías industriales y sociedades de consumo.

De cara a reemplazar una parte de los combustibles líquidos derivados del petróleo con una alternativa más neutra en cuanto a emisiones de gases de efecto invernadero, se han abordado distintas soluciones entre las que destaca el biocombustible líquido a partir de biomasa, donde el carbono liberado en la combustión se compensa con el que se fijó en la planta a través del proceso fotosintético. De ahí el interés en la producción y uso de combustibles a partir de las plantas cultivadas [13].

La biomasa, en términos energéticos hace referencia a toda materia orgánica originada en el proceso biológico, ya sea espontáneo o provocado, utilizable como fuente de energía, y que abarca un amplio rango de materias orgánicas con una gran heterogeneidad. La biomasa ha sido desde siempre la mayor fuente de energía para el ser humano y se estima que contribuye entre un 10 % y 14 % al abastecimiento de energía mundial [14].

El uso del bioetanol como combustible líquido para el transporte se ha incrementado rápidamente en las últimas décadas, mientras que su producción mundial se ha quintuplicado entre los años 2000 y 2014 (Fig 1.3). Esto ha sido debido a los nuevos retos medioambientales y económicos a los que se enfrenta la sociedad, que han provocado cambios políticos, que a su vez han puesto a disposición de los productores de energías renovables cuantiosas subvenciones y ayudas a su producción [12]. Desde 2006, Estados Unidos es el mayor productor de bioetanol a nivel mundial, cuya producción en el año 2014 supuso un 58 % del bieotanol total, siguiendole Brasil con un aporte del 28 % y en tercer lugar la Unión Europea con

un discreto 5,5 %.

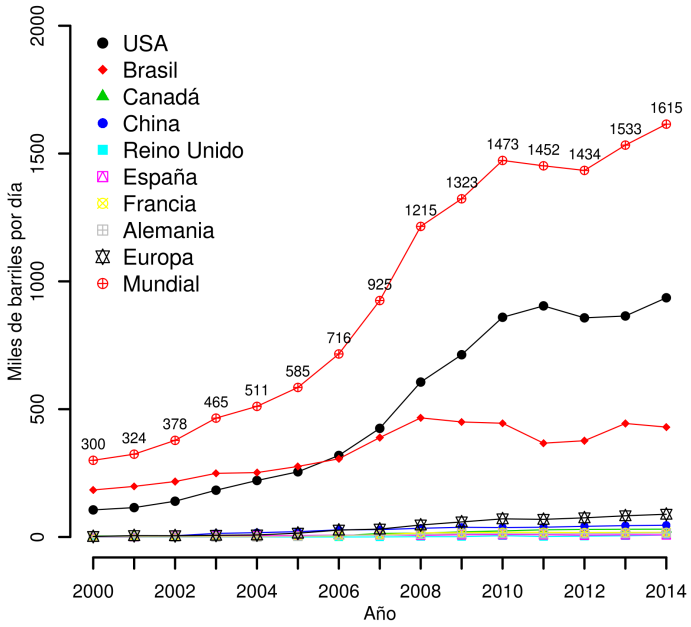

Figura 1.3: Producción de bioetanol mundial y países más significativos. Los datos están expresados en miles de barriles producidos por día Los datos se han tomado de U.S. Energy infromation Administration (`www.eia.gov`)

Las ventajas del uso de bioetanol en lugar de combustibles fósiles son varias:

La utilización de fuentes de energía renovables contribuye a disminuir la dependencia energética exterior y ayuda a la diversificación de las fuentes de energía. Las energías renovables no se agotan, no generan residuos de difícil tratamiento y reducen las emisiones de GEI.

La biomasa es una fuente de energía clave para el cumplimiento de los objetivos de utilización de energías renovables. Además, la biomasa presenta beneficios añadidos ya que permite un cierto grado de almacenamiento, constituyendo una alternativa realista para la sustitución parcial de los combustibles fósiles en el sector transporte a corto y medio plazo.

Favorece el mantenimiento y desarrollo del sector agrícola y forestal, y genera beneficios adicionales en el caso de la valorización energética de los residuos.

1.3. Tipos de Biocombustibles por el tipo de materia prima usada

Dependiendo del tipo de biomasa vegetal usada para la obtención de biocombustibles, podemos clasificalos como combustibles de primera, segunda o tercera generación. Las diferencias entre ellos se definen a continuación:

El biocombustible de **primera generación** (1G) se caracteriza principalmente porque es obtenido a partir de cultivos que son normalmente destinados a la alimentación humana o animal. El bioetanol 1G es producto de la fermentación de partes de la planta ricas en sustancias amiláceas y/o azucaradas como son las que encontramos en el grano de los cereales, en el tallo de la caña de azúcar e incluso en tubérculos como la patata. Estos azúcares son fácilmente accesibles a las enzimas, que tras su digestión quedan reducidos a monosacáridos para que finalmente sean transformados en la fermentación dando lugar al bioetanol.

La tecnología empleada en la producción del bioetanol 1G está bien desarrollada, es eficiente y está bien establecida en algunas partes del mundo, como por ejemplo, en Brasil, donde un programa gubernamental impulsó en 1975 la producción de bioetanol para el transporte a partir de caña de azúcar [15]. Desde el año 2000 hasta nuestros días el uso del bioetanol ha experimentado un rápido ascenso (Fig 1.3), no obstante, el bioetanol 1G es muy cuestionado principalmente por el uso de alimentos como materia prima, compitiendo directamente en disponibilidad y abastecimiento. La limitación de recursos disponibles para producir y alimentar a una población mundial en continuo crecimiento han dado lugar a una presión sobre el precio de los alimentos, haciendolos más difícilmente accesibles en muchas partes del mundo [16]. Por ejemplo, la limitación del recurso de la tierra es tal, que en el supuesto de que la destinásemos sólo a la producción de biocombustible a partir de una producción mundial de trigo, cebada, maíz, sorgo y caña de azúcar, tan solo podríamos abastecer un 19,4 % del combustible usado para el transporte [17]. Para hacernos una idea de como han afectado las tensiones sobre el precio de las materias primas durante la escalada en la producción de

bioetanol 1G en el periodo 2006-2013 (Fig 1.3), solo tenemos que fijarnos en cómo en estos años se han visto incrementados los precios del maíz y trigo en un 131 % y 177 % respectivamente [12].

Además del inconveniente que tiene la producción de bioetanol 1G sobre el coste y la accesibilidad a los alimentos, podemos destacar otra gran repercusión como es la que recae sobre el medio ambiente. Ésta última, se verá afectada principalmente por la alta demanda y subida del precio de materias primas y alimentos, haciéndola más atractiva a un productor o inversor en busca de beneficios netos más altos y conduciendo así a una deforestación masiva para disponer de mayor cantidad de tierra cultivable [18]. Asociada a esta deforestación van ligados otros factores negativos sobre el medio ambiente, como la pérdida de biodiversidad, uso de grandes cantidades de insumos para el desarrollo de los cultivos que sustituirían a la masa forestal, como son, agua, fertilizantes, pesticidas, abonos y combustibles fósiles, lo cual generaría más GEI de los que mitigaría el uso de los biocombustibles generados en esas tierras [18–20].

A la vista de estos inconvenientes, la insostenibilidad del sistema productivo de biocombustibles 1G, ha dado lugar a un interés en la obtención de bioetanol a partir de subproductos de cultivos agrícolas y residuos forestales como una alternativa más que, junto con otras muchas fuentes de energía, sea útil para sustituir a los combustibles fósiles.

El bioetanol de **segunda generación** (2G) es el que se obtiene a partir de una gran variedad de materiales procedentes de cultivos o partes de plantas que no son destinadas a la alimentación humana y que normalmente son considerados residuos agrícolas, forestales e incluso urbanos. Esta biomasa lignocelulósica está compuesta principalmente por la pared celular secundaria de las pantas, y encierra una matriz de polisacáridos (70-75 %) potencialmente convertibles en bioetanol [21]. Sin embargo, esta matriz de polisacáridos, dado el proceso evolutivo que han sufrido las plantas para resistir efectos bioticos y abioticos, es altamente reclacitrante y presenta gran resistencia a la liberación de los monosacáridos durante la digestión enzimática que se produce en el proceso de sacarificación.

El bioetanol procedente de la biomasa vegetal lignocelulósica es una alternativa muy prometedora como complemento o sustituto de los carburantes

líquidos de origen fósil [22], pero sin embargo, debido a las dificutades que opone esta biomasa a ser transformada en bioetanol son muchos los retos que aun quedan por superar para que sea una alternativa viable económicamente. Tan solo el 0,1 % aproximadamente del bioetanol producido actualmente es de segunda generación [12].

Finalmente, existe una **tercera generación** (3G) de biocombustibles, que son aquellos que se obtienen a partir de las algas. Esta biomasa procedente de las algas tienen un rendimiento productivo muy distinto en comparación a la biomasa lignocelulósica [23]. Usualmente, especies como la *Chlorella* destacan por su alto contenido en lípidos (alrededor de 60 a 70 %; [24]) y su alta productividad (7,4gr/L; [25]). Se sabe que la producción de biomasa a partir de algas es muy rápida en comparación con la biomasa lignocelulósica, sin embargo, la tecnología para la producción de biocombustibles a partir de algas se encuentra con grandes desafíos técnicos en los procesos de extracción de lípidos y de deshidratación, así como desafíos geográficos en zonas donde la temperatura está por debajo del punto de congelación durante gran parte del año [25].

1.4. Balance energético y emisiones de gases de efecto invernadero (GEI)

Enfrentar y conocer las diferencias en balances energéticos, así como la reducción de GEI que supondría el uso de biocombustibles 1G, 2G y de combustibles fósiles, es importante de cara ha poder comparar y evaluar el beneficio de usar unos frente a otros. Como veremos en las siguietes figuras, estos factores muestran un amplio rango de rendimientos por tipo de cultivo y superficie, que dependen principalmente del lugar, de la heterogeneidad de la biomasa, del ambiente y del tipo de tecnología de conversión en biocombustible [26].

El balance energético no es más que una comparación entre la energía fósil consumida por los insumos empleados en la producción del cultivo frente a la energía obtenida a partir de los productos del mismo. La energía fósil consumida se calcula como la suma de las energías necesarias para sembrar, cultivar y cosechar la materia prima, así como para convertirla en biocombustible y transportarla. Como vemos, el balance energético es relativo a la energía fósil que se emplea en la obtención del biocombustible, por lo que lo denominaremos como balance de energía fósil de aquí en adelante, y se calcula como el ratio entre la energía contenida en el biocombustible obtenido y la energía fósil empleada en su obtención [27]. Por

ejemplo, un valor para el balance energético fósil de 1 significa que se necesita la misma energía para producir un litro de biocombustible que de energía fósil, y un balance energético de combustible fósil de 2.0 significa que para obtener un litro de biocombustible se necesita la mitad de energía fósil, o que el biocombustible obtenido contiene el doble de energía fósil de la que se ha usado para producirlo.

Una vez aclarado este término, en la figura 1.4 podemos ver una representación gráfica de los balances de energía fósil para diferentes tipos de combustibles clasificados por el tipo de materia prima de la que proceden,los que nos permite describir la situación que ocupa cada uno. Por ejemplo, la gasolina y el diésel convencional alcancan balances de energía fósil <1, ya que parte de la energía consumida para la obtención de estos combustibles ha sido empleada en refinar el crudo para convertirlo en combustible y en el transporte hasta el usuario final. Por otro lado, todos los biocombustibles que muestran un balance de energía fósil mayor al de la gasolina y el diésel van a contribuir positivamente a la reducción de la dependencia de los combustibles fósiles. De hecho, todos los biocombustibles, tienen un balance de energía fósil mejor que el de los combustibles convencionales. También podemos observar que hay una gran variabilidad para los valores de balances de energía fósil dependiendo de la materia prima usada, y que podrían explicarse como la suma de diversos factores como es la variabilidad entre especies y/o cultivares de una misma especie, el ambiente, la localización, el manejo del cultivo, etc.

Por último, volviendo a la figura 1.4, podemos ver como la biomasa lignocelulósica alcanza los niveles más altos para el balance de energía fósil, aunque también es la que mayor variabilidad presenta. Esta variabilidad se puede explicar, en parte por la variabilidad natural que encontramos en los distintos residuos, ya sean agrícolas o forestales, sumada a la gran variabilidad que producen los sistemas de conversión de bioetanol.

De forma similar al balance de energía fósil y por tratarse de un término importante para determinar diferencias entre los distintos combustibles, podemos definir el efecto neto de cada uno de ellos sobre las emisiones de GEI. De forma general, los biocombustibles elaborados a partir de la biomasa deberían ser neutrales en cuanto a emisiones de GEI se refiere, ya que durante la combustión, sin entrar en análisis de otros factores implicados en la misma, se libera el dióxido de carbono que fue captado por la planta durante su crecimiento. Por el contrario, la quema

de los combustibles fósiles libera el dióxido de carbono que ha sido almacenado almacenado hace millones de años bajo la superficie de la tierra.

Pero si deseamos evaluar más detalladamente el balance sobre las emisiones de gases de efecto invernadero (GEI) de un biocombustible, sería necesario analizar las emisiones que producimos al sembrar, cosechar y transformar la materia prima en biocombustible, así como transportar este combustible hasta donde se vaya a almacenar y evaluar la cadena de distribución hasta el consumidor final, a lo que además hay que incluir los efectos de la combustión. Otro factor muy importante a tener en cuenta en la evaluación de la emisión de GEI son los cambios de uso de la tierra asociados a la producción de biocombustibles, como son por ejemplo, la deforestación para destinar la zona a producción de cultivos destinados a biocombustibles, los cultivos desplazados a otras tierras para implantar cultivos destinados a biocombustibles, etc. En general, cambios que provocan que el balance de las emisiones de GEI con respecto al cultivo o masa forestal previo necesite de algún tiempo para recuperar el carbono liberado en el cambio. [28–30]. En la figura 1.5 podemos ver los niveles de reducción de emisiones de GEI para distintos cultivos en comparación con los emitidos por combustibles fósiles. En esta figura podemos observar como las emisiones del etanol a partir de caña de azúcar y de los biocombustibles a partir de residuos lignocelulósicos (biocombustibles de 2ª generación), presentan unas buenas reducciones de emisiones de GEI, aunque estos últimos siguen siendo insignificantes a nivel comercial [27].

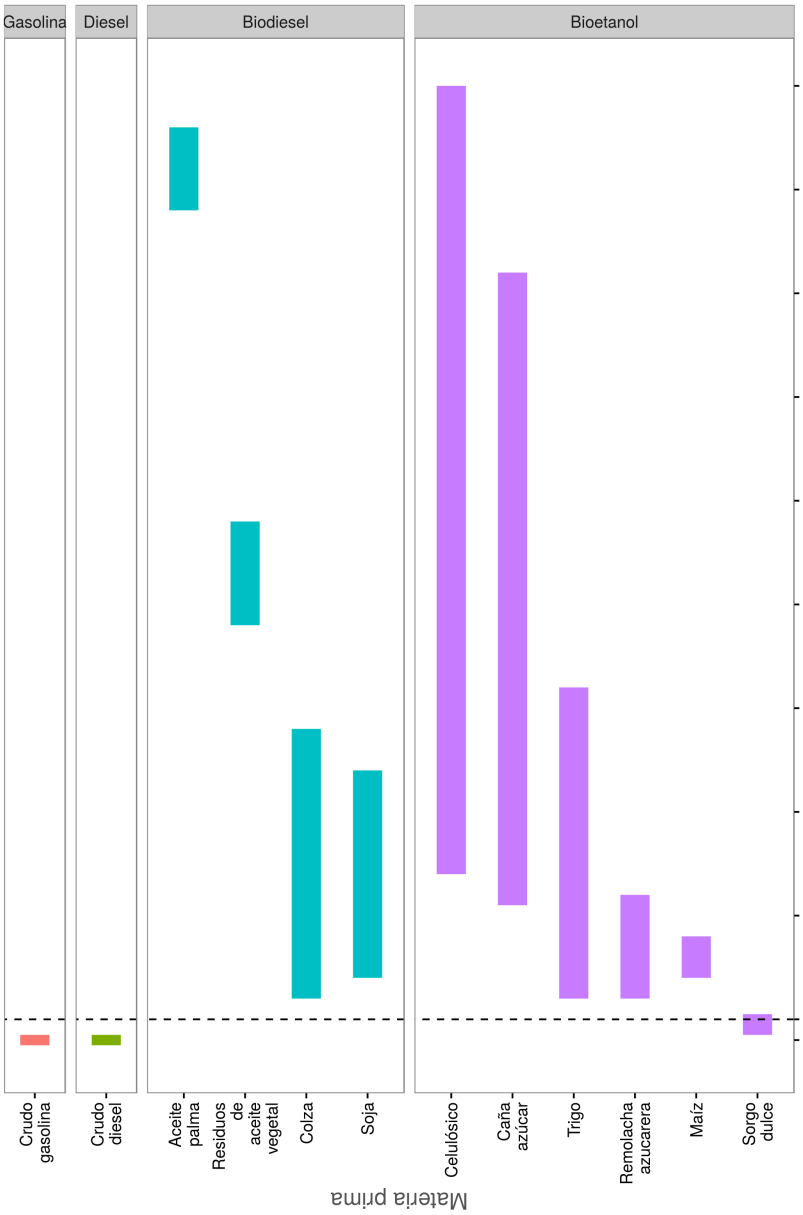

Figura 1.4: Balance de energía fósil [27].

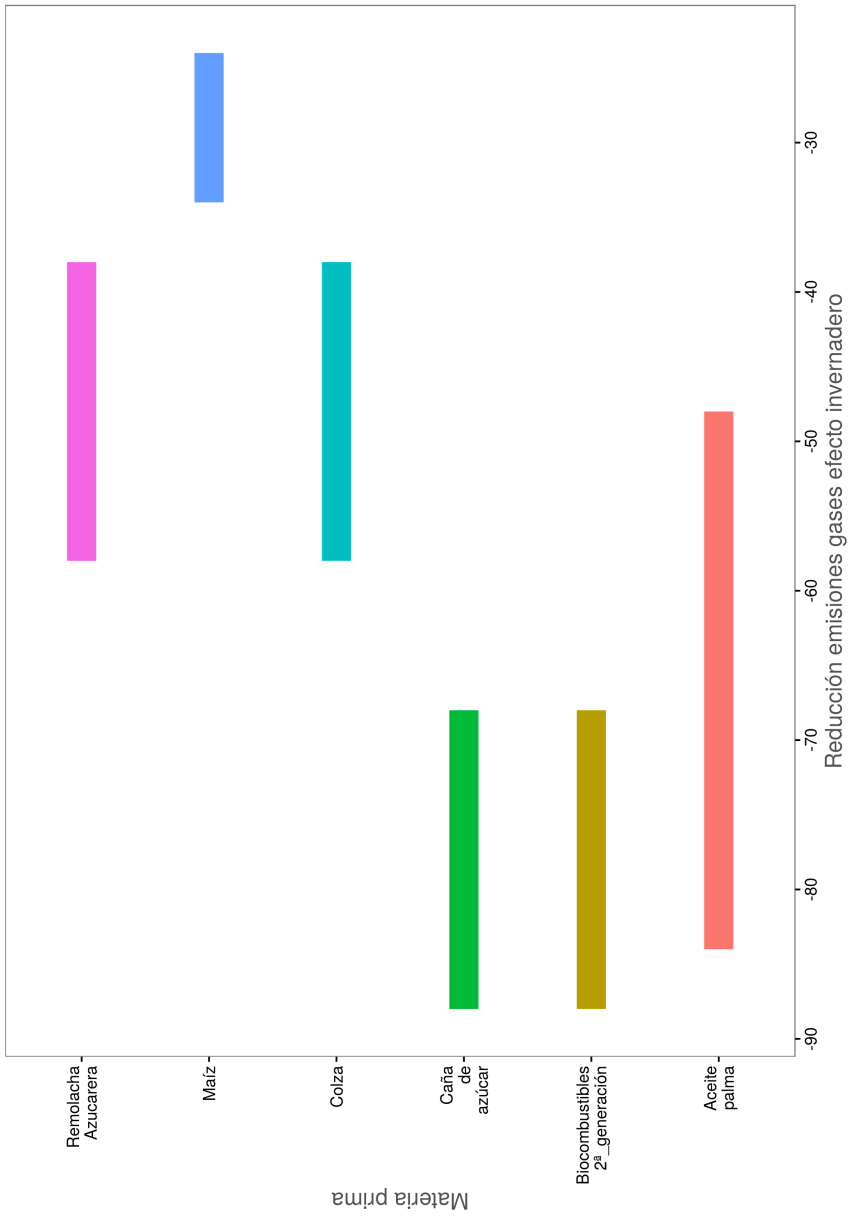

Figura 1.5: Reducción de emisiones de GEI (en %) comparado con los combustibles fósiles. [27]).

1.5. Composición y estructura de la pared celular

La biomasa lignocelulósica constituye la principal fuente renovable de materia orgánica en la tierra, encontrándose principalmente en las paredes celulares de las plantas, justo en la capa gruesa y reforzada de la pared celular secundaria de las mismas. Aproximadamente el 70-75 % de esta lignocelulosa está compuesta por polisacáridos potencialmente convertibles en monosacáridos que serán fermentados para dar lugar al bioetanol [21].

Las capas y componentes de la pared celular se depositan en un cierto orden durante su formación (figura 1.7) [31, 32], formando una estructura compuesta por múltiples capas (figura 1.6), las cuales difieren mucho en cuanto a función, grosor y disposición. Las pectinas y hemicelulosas son los primeros componentes en depositarse, formando la capa más externa de la pared celular llamada lámina media (LM figura 1.6), siendo esta capa la responsable de la unión entre células [33, 34]. Después de la división celular comienza la síntesis de la celulosa, permitiendo la deposición de microfibrillas dentro de las redes de hemicelulosa y pectinas, conformando la pared celular primaria. Esta pared celular primaria, rodea a las células vegetales durante su crecimiento y división, proporcionando resistencia mecánica y capacidad de expansión de las células. Las microfibrillas de celulosa en la pared celular primaria están orientadas aleatoriamente (figura 1.6 d).

Una vez se ha completado el alargamiento celular en células como los vasos del xilema, floema y esclereidas, comienza la formación de la pared celular secundaria. Las pectinas dejan de ser sintetizadas y depositadas, mientras que la síntesis hemicelulosas y celulosas continúa engrosando la pared celular, estableciendose una pared celular secundaria compuesta por tres capas: S1, S2 y S3. En las capas S1 y S3 las microfibrillas tienen una orientación casi transversal al eje de la célula (60° a 80°C), sin embargo en la capa S2 las microfibrillas se orientan longitudinalmente (figura 1.6 c) [35, 36]. Esta disposición de fibras longitudinales y transversales parece ser la responsable de la resistencia y flexibilidad de los tallos en las plantas [32].

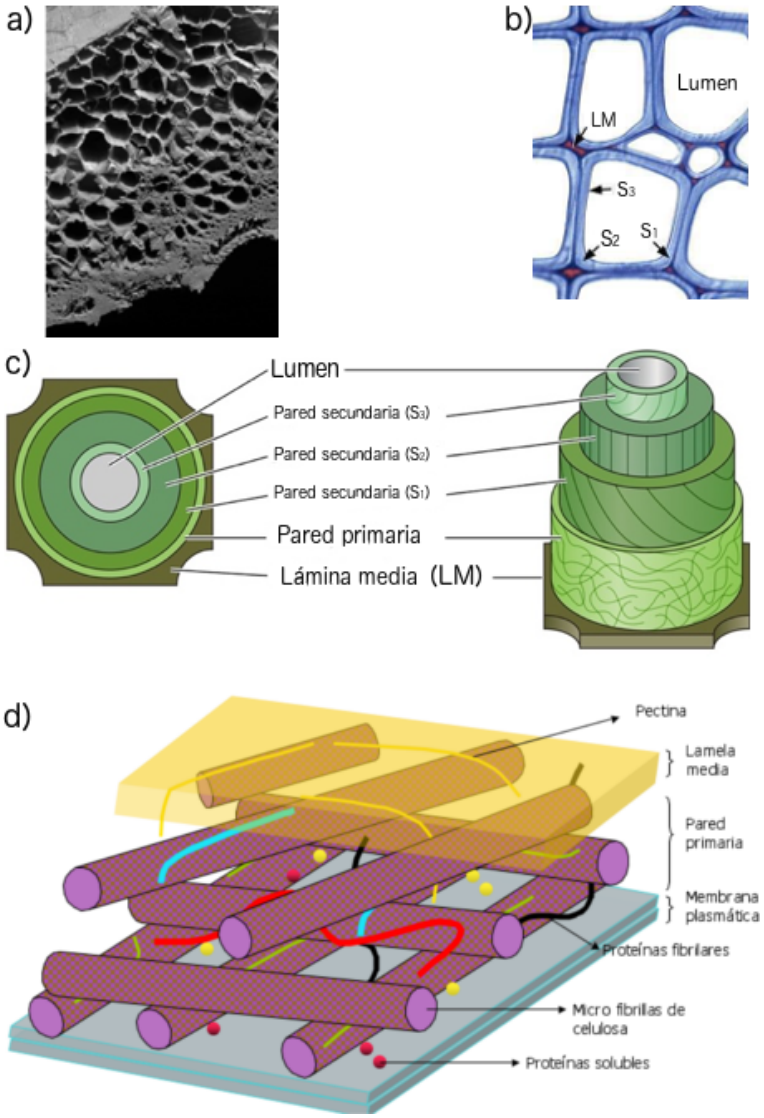

Figura 1.6: Modelo simplificado de la estructura de la pared celular vegetal. (a) Imagen transversal de paja de trigo tomada con microscopio electrónico, el tejido vivo disminuye de tamaño hacia el exterior del tallo, aumentando el grosor de la pared (imagen tomada de [37]), (b) sección transversal de traqueidas de madera temprana (imagen tomada de [38]) (c) estructura consistente en las tres capas principales: lamela media (LM), pared celular primaria y pared celular secundaria. En la pared celular secundaria se describen tres capas secundarias, externa (S1), media (S2) e interna (S3) (Imagen modificada de [39]). (d) Esquema de la pared celular primaria (Fuente: `https://es.wikipedia.org/wiki/Pared_celular`

En dicotiledóneas, la hemicelulosa cambia de xiloglucanos a xilanos en el cambio de formación de pared primaria a secundaria respectivamente. Sin embargo, en gramíneas, el xilano es la única hemicelulosa sintetizada, y es depositada en

	Dicotiledoneas	Monocotiledoneas	Maderas Blandas	Maderas Duras
Celulosa	45-50 %	35-45 %	25-30 %	40-55 %
Hemicelulosa	20-30 %	40-50 %	20-30 %	20-35 %
Lignina	7-10 %	20 %	25-35 %	18-25 %

Fuentes: [21, 31, 41–43]

Tabla 1.1: Composición en porcentaje de los principales componentes de pared celular de diferentes fuentes de biomasa lignocelulosica.

paredes primarias y secundarias. La lignina solo se comienza a depositar una vez que la pared primaria ha terminado de formarse y hasta después de la muerte celular [31, 40].

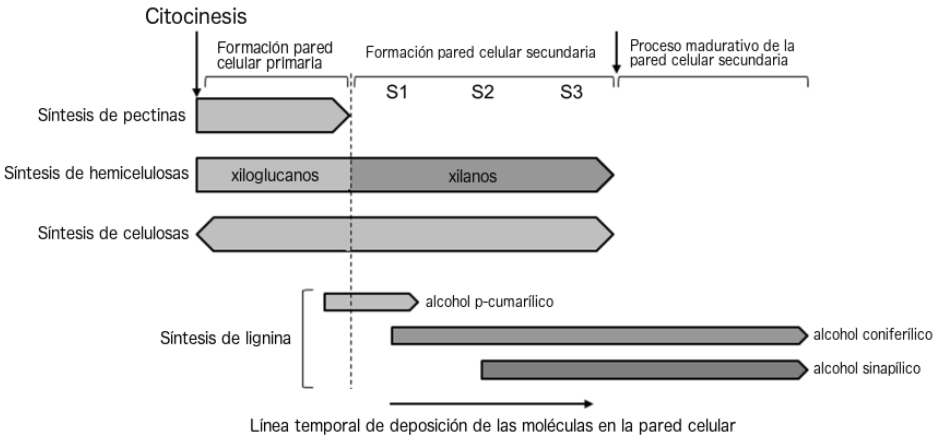

Figura 1.7: Línea temporal de deposición de celulosa, hemicelulosa, pectinas y lignina durante la formación de la pared celular vegetal (Imagen modificada de [31]).

Los tres polímeros principales que componen la biomasa lignocelulósica ordenados de mayor a menor proporción son la celulosa, hemicelulosa y lignina. Otros componentes menores incluyen proteínas, extractos y minerales inorgánicos. Como podemos ver en la tabla 1.1, estos pueden variar notablemente dependiendo del origen de la materia prima.

La Celulosa

La celulosa destaca por ser el componente principal en la pared celular, que comprende alrededor de un tercio de la masa total de la gran mayoría de las plantas [31]. Se trata de un homopolímero lineal de unidades de glucosa ($C_6H_{12}O_6$) unidas

entre sí en forma de unidades de D-anhidroglucopiranosa a través de enlaces β-1,4-O-glucosídico (figura 1.8). Estas unidades monoméricas unidas entre sí por enlaces glicosídicos forman un tipo de polímero conocido como glucano, y múltiples cadenas de glucanos unidas por enlaces de hidrógeno y fuerzas de Van der Waals [44, 45] quedan dispuestas en matrices cristalinas paralelas para conformar las microfibrillas de celulosa. De estructura lineal, rígida e insoluble en agua, cada molécula de celulosa comprende entre 5.000 y 10.000 unidades de glucosa [46].

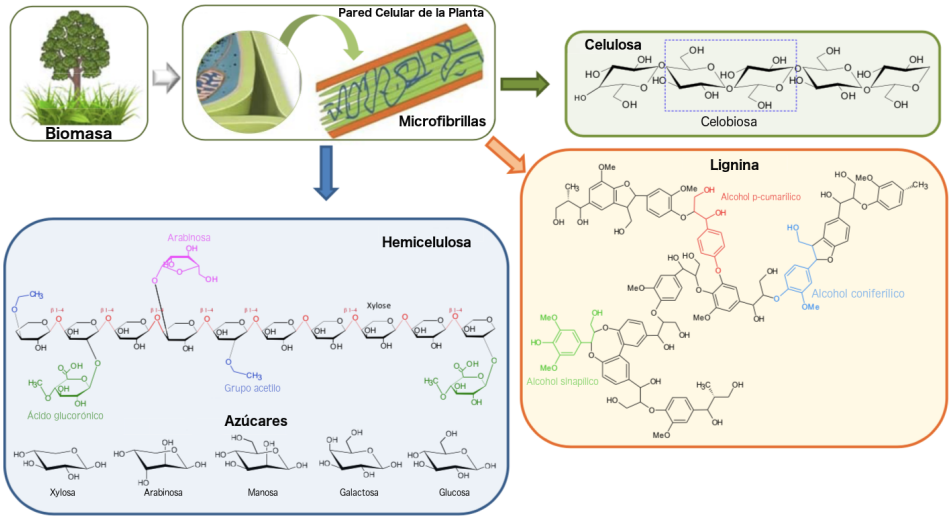

Figura 1.8: Estructura y principales componentes de la pared celular vegetal (Imagen modificada de [47]).

La celulosa es el componente más importante de la pared celular para la producción de bioetanol, pues contiene grandes cantidades de glucosa que podrían fermentarse fácilmente a etanol una vez que hubieran sido liberadas de la estructura del polisacárido. Sin embargo, la cristalinidad de este polisacárido es un factor que lo hace extremadamente inaccesible a las enzimas digestivas y al agua que se requiere para la hidrólisis de los enlaces glucosídicos.

Alterando la celulosa para incrementar la sacarificación Se han observado correlaciones negativas entre la cristalinidad de celulosa y la tasa inicial de hidrólisis para una celulosa cristalina purificada (Avicel) [48], residuos de maíz [49], y entre la cristalinidad de la celulosa y el rendimiento potencial de la hidrólisis entre distintas variedades de *Sorghum bicolor* [50]. Por otro lado, se ha observado un mayor potencial de sacarificación en plantas de *Arabidopsis thaliana* con una

reducción en la cristalinidad de la celulosa, causada por mutaciones en los genes implicados en la ruta de síntesis de la celulosa [51]. Otra solución para aumentar el potencial de la sacarificación es aumentar el contenido total de celulosa en la pared celular [52]. La composición de la celulosa es la misma para todas las especies de plantas y los factores que la afectan podrían ser también los mismos o muy parecidos, siendo pues su conocimiento de gran importancia en todos los residuos que potencialmente sean convertibles en bioetanol.

La hemicelulosa

La hemicelulosa está formada por un conjunto muy heterogéneo de polisacáridos como son los xilanos, xiloglucanos, mananos, glucomananos y β-(1-3,1-4)-glucanos. Estos polisacáridos hemicelulósicos forman cadenas principales del mismo monosacárido unidos con enlaces β-1,4. Estas moléculas además tienen cadenas laterales y ramificaciones que evitan la formación de estructuras cristalinas [31, 53] (figura 1.9).

Hemicelulosas y celulosas forman una red polimérica que probablemente tenga lugares de unión específicos a lo largo de la microfibrilla de celulosa [54]. La hemicelulosa parece tener una función plastificante, permitiendo la extensibilidad de la pared celular manteniendo las fibrillas separadas entre sí y actuando a su vez como un lugar de actividad para las expansinas [55]. Las clases, ramificaciones y abundancia de las hemicelulosas varían ampliamente en función de la especie vegetal, tipo de célula y etapa de desarrollo de la planta. En las paredes celulares de las gramíneas, la mayor parte de la hemicelulosa está compuesta por xilanos. En gramíneas, los glucoronoarabinoxilanos (GAX) están formados por un eje principal de xilano con muchas sustituciones de residuos de arabionsa y cadenas laterales de galactosilo, GlcA, MeGlcA, xilosa y ácido ferúlico. Los GAX pueden llegar a constituir de un 20 a un 40 % de las paredes celulares primarias, y de un 40 a un 50 % de las secundarias [56].

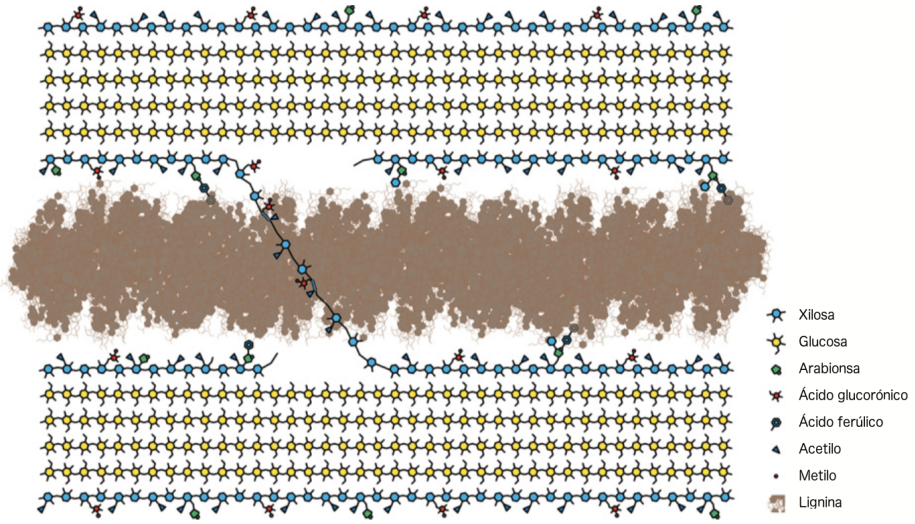

Figura 1.9: Modelo hipotético de la red de hemicelulosa-celulosa en la pared celular de las gramíneas. Las moléculas de hemicelulosa (glucuronoarabinoxilano), que se muestran en azul, se pueden unir a secciones de la microfibrilla de celulosa, mostrada en amarillo, a través de enlaces de hidrógeno. Las moléculas de hemicelulosa pueden abarcar dos o más microfibrillas de celulosa, uniéndolas entre sí. (Figura está adaptada de [57]).

Alterando la hemicelulosa para incrementar la sacarificación Mutantes en el gen xilema irregular (*irx*) ya sea con inserciones T-DNA o mediante silenciamiento de ARN de glicosiltransferasas implicadas en la síntesis de xilanos, en *A. thaliana* y en álamo, han mostrado un contenido de glucoronoxilanos reducido en las paredes celulares secundarias y un aumento significativo de la sacarificación en comparación con el control (WT) [58–60]. También en álamo se ha descrito una reducción en hemicelulosa como resultado de la sobreexpresión de xilanasa y xiloglucanasa, mostrando un aumento de casi el doble de sacarificación que en el WT [61]. Se han observado también correlaciones positivas entre la eliminación de hemicelulosas mediante extracción química y la accesibilidad a la celulosa con la hidrólisis enzimática [62, 63]. En estos trabajos se vio incrementada la liberación de glucosa demostrando así que las hemicelulosas forman parte del retículo de las microfibrillas de celulosa y de lignina, haciendo más difícil el acceso a la celulosa por parte de las celulasas.

Lignina

La lignina se encuentra en las paredes celulares secundarias, y aparece una vez se ha completado la expansión celular. Su función es principalmente estructural,

fortaleciendo la pared celular proporcionando rigidez, resistencia y aumentando su hidrofobicidad, representando así una barrera formidable ante plagas y patógenos, así como para las enzimas que degradan la pared celular [64, 65]. La lignina es, en proporción, la tercera fracción mayoritaria de la biomasa lignocelulósica y está formada de monómeros (monolignoles) polimerizados oxidativamente por radicales libres, diferenciándose de la mayoría de los polímeros biológicos que son polimerizados por enzimas. Las moléculas de lignina están compuestas de cientos de monómeros [31] formando compuestos complejos tridimensionales en los que los enlaces entre monómeros se pueden dar en múltiples posiciones, dificultando así la digestión enzimática [66]. Los monómeros que forman la lignina se diferencian entre sí por las diferentes sustituciones que presenta el anillo aromático. Así el alcohol *p*-cumarílico que da lugar a las unidades *p*-hidroxifenilo (H), no presenta ningún sustituyente; el alcohol coniferílico que da lugar a las unidades guayacilo (G) presenta un grupo metoxilo en la posición 3 del anillo aromático y el alcohol sinapílico que da lugar a las unidades siringilo (S) presenta dos grupos metoxilo en posiciones 3 y 5 de dicho anillo. La lignocelulosa de gimnoespermas (maderas blandas) se caracteriza por estar formada mayoritariamente por unidades G, mientras que la lignina de angiospermas leñosas (maderas duras) está formada por unidades G y S. La alta proporción de unidades S derivadas del alcohol sinapílico en maderas duras determina la estructura y características de este tipo de lignina menos polimerizada y con un menor grado de condensación. De esta forma las maderas duras son más fáciles de deslignificar que las maderas blandas. Este polímero racémico forma múltiples isómeros, lo cual significa que estás moléculas de lignina nunca serán idénticas [67], careciendo de una estructura repetida a la que las enzimas líticas específicas puedan atacar con eficacia. Hasta ahora, todas las enzimas de degradación de lignina caracterizadas parecen funcionar mediante una oxidación indirecta de los radicales libres [68].

Alterando la lignina para incrementar la sacarificación El efecto de la lignina sobre la sacarificación ha sido investigado profundamente, lo que ha dado a los investigadores una compresión relativamente buena de la biosíntesis y el papel que juega este elemento en la pared celular vegetal. Se ha demostrado que la digestibilidad enzimática de la biomasa lignocelulósica está afectada por factores como la cantidad, estructura y composición de la lignina.

El contenido de lignina Hay diversos estudios que han demostrado que la alteración de la expresión de biosíntesis de monolignoles conduce a la alteración en la cantidad de lignina depositada en la pared celular, que a su vez ha demostrado afectar significativamente a la sacarificación. En el trabajo de [69] se demostró que, en seis líneas transgénicas de alfalfa (*Medicago sativa* L.), cada una regulada negativamente por un gen diferente de biosíntesis de lignina, aparecía una fuerte correlación negativa entre contenido de lignina y azúcares liberados mediante hidrólisis enzimática. En otro trabajo similar en *A. thaliana*, 20 plantas mutantes para 10 genes distintos implicados en la ruta de biosíntesis de monómeros de lignina, se mostró que el contenido de lignina afectaba significativamente al rendimiento de la sacarificación [70]. Otros estudios recientes como en chopo [71, 72], pastos [73], en *A. thaliana* [74, 75], alfalfa [76], y otros en diferentes especies [77], han mostrado como reduciendo la expresión de enzimas implicadas en la ruta de síntesis de monolignoles se producen menores cantidades de lignina depositada en la pared celular, efecto directamente correlacionado con el potencial de sacarificación.

Composición y estructura de la Lignina La composición y estructura de la lignina ha sido abordada por un gran número de trabajos, demostrando que este factor tiene un impacto significativo en la sacarificación de la biomasa lignocelulósica. Pero a menudo es difícil distinguir entre los efectos del contenido de lignina y su composición porque las modificaciones en la síntesis de enzimas de monolignoles a menudo tienen efectos sobre ambos factores, contenido y composición de la lignina. Por ejemplo, en los trabajos de [70, 78] se obtuvieron resultados que demostraban que una regulación a la baja de cinamato-4-hidroxilasa, 4-cumarato-CoA ligasa, ácido cafeico-O-metiltransferasa, resultaban en una mayor sacarificación con una reducción de lignina y un cambio en la composición, con un mayor ratio de las unidades repetidas Siringilo (S):Guayacilo (G). Por otro lado [79] obtuvo resultados que mostraban como en una población de álamo, la correlación negativa entre sacarificación y contenido en lignina solo se observaba para muestras con un ratio S:G<2. Sin embargo, para ratios S:G mayores, el incremento de sacarificación era proporcional a las unidades de S en la lignina, teniendo el contenido de esta última un menor efecto. En el trabajo de [80, 81] se observó como en la biomasa lignocelulósica al someterse a un pretratamiento antes de la hidrólisis, el contenido de lignina no mostraba correlación alguna con la sacarificación, mientras que el efecto de la relación S:G sí que se hacía evidente, y curiosamente

solo se observaba cuando se usaba el pretratamiento, lo que sugiere que la lignina modificada permite una mayor depolimerización durante el pretratamiento. Otros trabajos importantes en los que se ha destacado la importancia de la composición de la lignina sobre la recalcitrancia de la biomasa lignocelulósica han sido algunos como el de [82] en el que una alta sacarificación se atribuye a que la lignina tiene una alta proporción de unidades S; el trabajo de [83] donde se propone que la lignina rica en unidades S es más fácilmente digerible por el tipo de enlaces que se dan entre estas unidades y no permitiendo otros enlaces más energéticos. Otros autores han descrito como afecta la proporción de monómeros tipo H en lignina, el cual está presente en muy poca cantidad en la lignina natural, y que mediante silenciamiento de algunas rutas metabólicas conocidas de unidades S y G sobre lignina se ha observado una correlación entre sacarificación e incremento en la proporción de unidades H [69, 84].

Pectinas

Las pectinas son otros polisacáridos que se diferencian de las hemicelulosas en que contienen altas proporciones de ácido D-galacturónico. En la pared primaria de dicotiledóneas y monocotiledóneas no gramíneas, las pectinas están en una proporción del 20-35 %, solo un 5 % en la pared primaria de gramíneas y una pequeñísima proporción de aproximadamente 0,1 % en la pared secundaria de dicotiledóneas y gramíneas [21]. Como la biomasa lignocelulósica está principalmente compuesta de pared celular secundaria, estos polisacáridos de pared serán descritos brevemente, para una revisión más profunda de la estructura y síntesis de las pectinas en la pared celular ver [85]. Existen tres tipos de pectinas en las paredes celulares vegetales: Homogalaturonanos (HG), Ramnogalacturonanos-I (RGI) y Ramnogalacturonanos-II (RGII). En general, estos tres componentes aparecen en un 65 % en el caso de HG, entre el 20-30 % de RGI y un 10 % de RGII [86].

Proteínas estructurales

Al igual que ocurre en las pectinas, las proteínas estructurales están presentes en muy bajas cantidades en las paredes celulares secundarias de las plantas (monocotiledóneas y dicotiledóneas) [21]. El papel que juegan estas proteínas en la pared celular será pues brevemente discutido. En la pared celular vegetal se distinguen cinco principales clases de proteínas estructurales: extensinas, proteínas ricas en glicina (GRPs), proteínas ricas en prolina (PRPs), lectinas solanáceas y las proteí-

nas de arabinogalactano (AGPs) [86]. Se piensa que las extensinas desempeñan un papel importante en la pared celular vegetal, fortaleciéndola y creando una barrera contra infecciones y patógenos. Se ha demostrado que se acumulan en la pared celular y se entrelazan en respuesta al etileno, a heridas mecánicas y a la invasión de patógenos [87–89].

1.6. Proceso de producción de bioetanol lignocelulósico

En la bioconversión de materias lignocelulósicas se diferencian cuatro pasos principales: reducción de tamaño de la biomasa, pretratamiento, hidrólisis y conversión a productos finales como biocombustibles [90], donde el principal reto en la producción de etanol es facilitar la digestión, mediante el tratamiento previo, a las enzimas que actúan en el proceso de hidrólisis.

Pretratamiento

Cuando en la etapa de hidrólisis de la celulosa se emplean catalizadores enzimáticos, debido a las características estructurales de los materiales lignocelulósicos anteriormente mencionados, el pretratamiento es una etapa crucial. La incubación de materiales celulósicos en presencia de preparaciones de celulasas resulta generalmente en unos rendimientos de hidrólisis enzimática (HE) inferiores al 20 %, debido a que la fuerte asociación de la celulosa con la lignina constituye una verdadera barrera física a la penetración de las enzimas [91]. Existen diferentes tecnologías de pretratamiento de la biomasa lignocelulósica, que pueden ser clasificadas según su naturaleza en pretratamientos físicos, químicos, biológicos y fisicoquímicos [92]. Dentro de los pretratamientos físicos se engloba la molienda que utiliza fuerzas de impacto y cizalla para disminuir la cristalinidad de la celulosa [92]. Los pretratamientos químicos emplean diferentes agentes como el ozono, ácidos, álcalis, peróxido y solventes orgánicos. Entre los diferentes pretratamientos químicos, el pretratamiento con ácido diluido ha sido el más estudiado y mejora significativamente la hidrólisis enzimática [93]. Los pretratamientos biológicos implican el uso de microorganismos como los hongos de la podredumbre blanca, parda o blanda, capaces de degradar la lignina y hemicelulosa [94]. Entre los pretratamientos físico-químicos la explosión por vapor (EV) ha sido el pretratamiento más ampliamente utilizado para la biomasa lignocelulósica [95]. Junto a la EV, el pretratamiento con agua caliente en fase líquida (ACL) y la explosión por vapor con amoniaco (AFEX, del inglés “amonia fiber explosion”) también se muestran

como pretratamientos físico-químicos eficientes para la biomasa lignocelulósica [96]. El pretratamiento AFEX es similar a la EV. La biomasa se impregna con amoniaco a alta presión y el pretratamiento se realiza a temperaturas por debajo de 100ºC [97]. De entre todos los pretratamientos mencionados, los físicos como la molienda, los químicos como la ozonólisis y los biológicos, no parecen adecuados para su desarrollo a escala comercial debido su elevado coste energético. Sin embargo, la EV, el ACL, el pretratamiento con ácido diluido y el AFEX se consideran pretratamientos con potencial para su implementación a escala comercial [97].

Hidrólisis enzimática

El material insoluble obtenido tras el pretratamiento está formado principalmente por celulosa y lignina, ya que gran parte los azúcares hemicelulósicos son solubilizados durante el mismo. Con el fin de romper las cadenas de celulosa en monómeros de glucosa, se emplean diversas enzimas que se conocen con el nombre de celulasas. La hidrólisis enzimática (HE) constituye una de las etapas limitantes del proceso global de producción de etanol. Las principales dificultades al realizar la HE de la biomasa lignocelulósica están relacionadas con la baja actividad específica de las enzimas actualmente disponibles, lo que conlleva el empleo de altas dosis de celulasas, y con la propia naturaleza de la lignocelulosa. Es por este último inconveniente que el pretratamiento es una etapa crucial en los procesos de producción de etanol mediante HE. En el proceso de obtención de etanol a partir de biomasa, la HE puede realizarse antes de la fermentación (hidrólisis y fermentación separadas, HFS) o simultáneamente a ésta, (SFS).

Fermentación

Cuando la fermentación se emplea en el proceso de producción de bioetanol a partir de biomasa lignocelulósica, los azúcares liberados durante la hidrólisis enzimática son fermentados con la consiguiente producción de etanol y CO_2. El microorganismo comúnmente empleado a nivel industrial en los procesos de fermentación alcohólica es la levadura *Saccharomyces cerevisiae*, ya que puede usar todo tipo de hexosas y produce etanol con unos rendimientos cercanos al máximo teórico (0,51 gramos de etanol por gramo de azúcar). Además, si se emplea en procesos de producción de etanol a partir de lignocelulosa, muestra gran tolerancia a los productos tóxicos generados durante el pretratamiento. No obstante, *S. cerevisiae* presenta una gran limitación cuando se quiere utilizar en la fermentación de

los azúcares hemicelulósicos ya que no es capaz de fermentar pentosas, como la xilosa, que también están presentes en los materiales lignocelulósicos. De ahí el interés de utilizar en este proceso microorganismos capaces de fermentar de forma eficiente todo tipo de azúcares. Además, el microorganismo empleado debe ser también capaz de tolerar los posibles tóxicos generados durante el pretratamiento [98].

1.7. Objetivos

El objetivo general de este trabajo es determinar los factores que permitan obtener un residuo lignocelulósico de cereales, que sea más fácilmente accesible para la enzima durante la fase del proceso de hidrólisis enzimática, mediante la manipulación de los entrecruzamientos entre hemicelulosa y lignina de las paredes celulares, abaratando los costes del proceso de producción y obtenido una mayor liberación de azúcares fermentables para la producción de etanol lignocelulósico. Los objetivos concretos que se persiguen en este trabajo son:

I El primer objetivo de este trabajo es evaluar la variabilidad de los azúcares fermentables liberados en diferentes genotipos de trigo (*Triticum durum* L., *Triticum aestivum* L.), cebada (*Hordeum vulgare* L.) y de triticale (X *Triticosecale* Wittmack).

II El segundo objetivo es el de proponer un sistema de fenotipado basado en UAV capaz proporcionar una clasificación de genotipos en términos de potencial de bioetanol con valor para facilitar el proceso de toma de decisiones en el contexto de los programas de fitomejoramiento.

III El último objetivo de este trabajo es determinar la posible función de una selección genes potencialmente involucrados en la síntesis de xilanos de la pared celular, así como su efecto sobre la sacarificación.

Referencias

[1] Myles Allen, Vicente Barros, John Broome, Wolfgang Cramer, Renate Christ, John Church, Leon Clarke, Qin Dahe, Purnamita Dasgupta, Navroz Dubash, Ottmar Edenhofer, Ismail Elgizouli, Christopher Field, Piers Forster, Pierre Friedlingstein, Jan Fuglestvedt, Luis Gomez-Echeverri, Stephane Hallegatte, Gabriele Hegerl, Mark Howden, Kejun Jiang, Blanca Jimenez Cisneros, Vladimir Kattsov, Hoesung Lee, Katharine Mach, Jochem Marotzke, Michael Mastrandrea, Leo Meyer, Jan Minx, Yacob Mulugetta, Karen O'Brien, Michael Oppenheimer, RK Pachauri, Joy Pereira, Ramón Pichs-Madruga, Gian-Kasper Plattner, Hans-Otto Pörtner, Scott Power, Benjamin Preston, NH Ravindranath, Andy Reisinger, Keywan Riahi, Matilde Rusticucci, Robert Scholes, Kristin Seyboth, Youba Sokona, Robert Stavins, Thomas Stocker, Petra Tschakert, Detlef van Vuuren, Jean-Pascal van Ypersele, Gabriel Blanco, Michael Eby, Jae Edmonds, Marc Fleurbaey, Reyer Gerlagh, Sivan Kartha, Howard Kunreuther, Joeri Rogelj, Michiel Schaeffer, Jan Sedláček, Ralph Sims, Diana Ürge-Vorsatz, David Victor, and Gary Yohe. *{IPCC fifth assessment synthesis report - Climate Change 2014 synthesis report}*. Intergovernmental Panel on Climate Change (IPCC), November 2014.

[2] R. K. Pachauri, M. R. Allen, V. R. Barros, J. Broome, W. Cramer, R. Christ, J. A. Church, L. Clarke, Q. Dahe, P. Dasgupta, N. K. Dubash, O. Edenhofer, I. Elgizouli, C. B. Field, P. Forster, P. Friedlingstein, J. Fuglestvedt, L. Gomez-Echeverri, S. Hallegatte, G. Hegerl, M. Howden, K. Jiang, B. Jimenez Cisneroz, V. Kattsov, H. Lee, K. J. Mach, J. Marotzke, M. D. Mastrandrea, L. Meyer, J. Minx, Y. Mulugetta, K. O'Brien, M. Oppenheimer, J. J. Pereira, R. Pichs-Madruga, G.-K. Plattner, Hans-Otto Pörtner, S. B. Power, B. Preston, N. H. Ravindranath, A. Reisinger, K. Riahi, M. Rusticucci, R. Scholes, K. Seyboth, Y. Sokona, R. Stavins, T. F. Stocker, P. Tschakert, D. van Vuuren, and J.-P. van Ypserle. *Climate Change 2014: Synthesis Report. Contribution of Working Groups I, II and III to the Fifth Assessment Report of the Intergovernmental Panel on Climate Change*. IPCC, Geneva, Switzerland, 2014.

[3] Mike Hulme. On the origin of 'the greenhouse effect': John Tyndall's 1859 interrogation of nature. *Weather*, 64(5):121–123, May 2009.

[4] S. Arrhenius and Edward S. Holden. ON THE INFLUENCE OF CARBONIC ACID IN THE AIR UPON THE TEMPERATURE OF THE EARTH. *Publications of the Astronomical Society of the Pacific*, 9(54):14–24, 1897. 00014.

[5] G. S. Callendar. The artificial production of carbon dioxide and its influence

on temperature. *Quarterly Journal of the Royal Meteorological Society*, 64(275):223–240, April 1938. 00591.

[6] Mark Carey. Review of The Callendar Effect: The Life and Work of (1898-1964), the Scientist Who Established the Carbon Dioxide Theory of Climate Change, ; Intimate Universality: Local and Global Themes in the History of Weather and Climate, James Rodger Fleming. *Environmental History*, 13(1):158–160, 2008. 00000.

[7] Andreas Uihlein and Liselotte Schebek. Environmental impacts of a lignocellulose feedstock biorefinery system: An assessment. *Biomass and Bioenergy*, 33(5):793–802, May 2009. 00114.

[8] A. Denny Ellerman, Henry D. Jacoby, and Annelène Decaux. *The Effects on Developing Countries of the Kyoto Protocol and CO2 Emissions Trading*. World Bank Publications, 1998. 00101 Google-Books-ID: JtrUajRXapcC.

[9] IEA. *World Energy Outlook 2010*. Organisation for Economic Co-operation and Development, Paris, November 2010. 00004.

[10] M. King Hubbert. Energy from Fossil Fuels. *Science*, 109(2823):103–109, February 1949. 00002.

[11] IEA IEA. World energy outlook 2011. *Int. Energy Agency*, page 666, 2011. 00073.

[12] I. E. A. Bioenergy. From 1st-to 2nd-Generation BioFuel technoloGies. *An overview of current industry and RD&D activities. IEA-OECD*, 2008. 00014.

[13] Wolfhart Dürrschmidt and Michael van Mark. *Renewable Energy Employment Effects: Impact of the Expansion of Renewable Energy on the German Labour Market.* Federal Ministry for the Environment, Nature, Conservation and Nuclear Safety, Berlin, 2006. 00003.

[14] Peter McKendry. Energy production from biomass (Part 1): Overview of biomass. *Bioresource Technology*, 83(1):37–46, May 2002. 02395.

[15] José Goldemberg. The Brazilian biofuels industry. *Biotechnology for Biofuels*, 1:6, May 2008. 00261.

[16] Lian Pin Koh and Jaboury Ghazoul. Biofuels, biodiversity, and people: Understanding the conflicts and finding opportunities. *Biological Conservation*, 141(10):2450–2460, October 2008. 00421.

[17] Biswo N. Poudel, Krishna P. Paudel, Govinda Timilsina, and David Zilberman. Providing Numbers for a Food versus Fuel Debate: An Analysis of a Future Biofuel Production Scenario. *Applied Economic Perspectives and Policy*, 34(4):637–668, December 2012. 00017.

[18] Renton Righelato and Dominick V. Spracklen. Carbon Mitigation by Biofuels or by Saving and Restoring Forests? *Science*, 317(5840):902–902, August 2007. 00458.

[19] Petr Havlík, Uwe A. Schneider, Erwin Schmid, Hannes Böttcher, Steffen Fritz, Rastislav Skalský, Kentaro Aoki, Stéphane De Cara, Georg Kindermann, Florian Kraxner, Sylvain Leduc, Ian McCallum, Aline Mosnier, Timm Sauer, and Michael Obersteiner. Global land-use implications of first and second generation biofuel targets. *Energy Policy*, 39(10):5690–5702, October 2011. 00455.

[20] Angela Karp and Goetz M. Richter. Meeting the challenge of food and energy security. *Journal of Experimental Botany*, 62(10):3263–3271, June 2011. 00085.

[21] John Vogel. Unique aspects of the grass cell wall. *Current Opinion in Plant Biology*, 11(3):301–307, June 2008. 00284.

[22] Maelor Davies, Malcolm Campbell, and Robert Henry. The role of plant biotechnology in bio-energy production. *Plant Biotechnology Journal*, 8(3):243–243, 2010.

[23] Liam Brennan and Philip Owende. Biofuels from microalgae—A review of technologies for production, processing, and extractions of biofuels and co-products. *Renewable and Sustainable Energy Reviews*, 14(2):557–577, February 2010.

[24] Yanna Liang, Nicolas Sarkany, and Yi Cui. Biomass and lipid productivities of <Emphasis Type="Italic">Chlorella vulgaris</Emphasis> under autotrophic, heterotrophic and mixotrophic growth conditions. *Biotechnology Letters*, 31(7):1043–1049, July 2009.

[25] Chun-Yen Chen, Kuei-Ling Yeh, Rifka Aisyah, Duu-Jong Lee, and Jo-Shu Chang. Cultivation, photobioreactor design and harvesting of microalgae for biodiesel production: A critical review. *Bioresource Technology*, 102(1):71–81, January 2011.

[26] Kelsey Gerbrandt, Pei Lin Chu, Allison Simmonds, Kimberley A Mullins, Heather L MacLean, W Michael Griffin, and Bradley A Saville. Life cycle assessment of lignocellulosic ethanol: a review of key factors and methods affecting calculated GHG emissions and energy use. *Current Opinion in Biotechnology*, 38:63–70, April 2016. 00000.

[27] FAO and Organización de las Naciones Unidas para la Agricultura y la Alimentación. *El estado mundial de la agricultura y la alimentación 2008: BIOCOMBUSTIBLES: perspectivas, riesgos y oportunidades*. 2008. 00000.

[28] Land Clearing. the Biofuel Carbon Debt Fargione, Joseph; Hill, Jason; Tilman, David; Polasky, Stephen; Hawthorne, Peter. *Science (Washington, DC, United States)*, 319(5867):1235–1238, 2008. 00064.

[29] John Pickett, D. Anderson, D. Bowles, T. Bridgwater, P. Jarvis, N. Mortimer, M. Poliakoff, and J. Woods. Sustainable biofuels: prospects and challenges. *The Royal Society, London, UK*, 2008. 00055.

[30] Tim Searchinger. The impacts of biofuels on greenhouse gases: how land use change alters the equation. *Policy Brief. Washington, DC, The German Marshall Fund of the United States*, 2008. 00019.

[31] Peter Albersheim, Alan Darvill, Keith Roberts, Ron Sederoff, and Andrew Staehelin. *Plant Cell Walls*. Garland Science, April 2010. Google-Books-ID: vCsWBAAAQBAJ.

[32] Takayoshi Higuchi. *Biosynthesis and biodegradation of wood components*. Elsevier, December 2012. Google-Books-ID: Wp04UtqNXA4C.

[33] Elizabeth M. Lord and Jean-Claude Mollet. Plant cell adhesion: A bioassay facilitates discovery of the first pectin biosynthetic gene. *Proceedings of the National Academy of Sciences*, 99(25):15843–15845, December 2002.

[34] Mazz Marry, Keith Roberts, S. Juliet Jopson, I. Max Huxham, Michael C. Jarvis, Julia Corsar, Eoin Robertson, and Maureen C. McCann. Cell-cell adhesion in fresh sugar-beet root parenchyma requires both pectin esters and calcium cross-links. *Physiologia Plantarum*, 126(2):243–256, February 2006.

[35] H. Abe, R. Funada, H. Imaizumi, J. Ohtani, and K. Fukazawa. Dynamic changes in the arrangement of cortical microtubules in conifer tracheids during differentiation. *Planta*, 197(2):418–421, September 1995.

[36] A. K. M. A. Prodhan, R. Funada, J. Ohtani, H. Abe, and K. Fukazawa. Orientation of microfibrils and microtubules in developing tension-wood fibres of Japanese ash (<Emphasis Type="Italic">Fraxinus mandshurica</Emphasis> var. <Emphasis Type="Italic">japonica</Emphasis>). *Planta*, 196(3):577–585, June 1995.

[37] Mads A. T. Hansen, Jan Bach Kristensen, Claus Felby, and Henning Jørgensen. Pretreatment and enzymatic hydrolysis of wheat straw (Triticum aestivum L.) – The impact of lignin relocation and plant tissues on enzymatic accessibility. *Bioresource Technology*, 102(3):2804–2811, February 2011.

[38] Da Re and Cristina Verónica. *Relevamiento de cepas argentinas de hongos ligninolíticos para su aplicación en procesos biotecnológicos ligados a la industria celulósico-papelera*. Text, Facultad de Ciencias Exactas y Naturales. Universidad de Buenos Aires, 2016.

[39] Johanna Rytioja, Kristiina Hildén, Jennifer Yuzon, Annele Hatakka, Ronald P. de Vries, and Miia R. Mäkelä. Plant-Polysaccharide-Degrading Enzymes from Basidiomycetes. *Microbiology and Molecular Biology Reviews : MMBR*, 78(4):614–649, December 2014.

[40] Lloyd A. Donaldson. Lignification and lignin topochemistry — an ultrastructural view. *Phytochemistry*, 57(6):859–873, July 2001.

[41] M. Abramson, O. Shoseyov, S. Hirsch, and Z. Shani. Genetic Modifications of Plant Cell Walls to Increase Biomass and Bioethanol Production. In *Advanced Biofuels and Bioproducts*, pages 315–338. Springer, New York, NY, 2013.

[42] Rubin Shmulsky and P. David Jones. *Forest Products and Wood Science: An Introduction*. John Wiley & Sons, July 2011. Google-Books-ID: BBrsBgAAQBAJ.

[43] Roger M. Rowell. *Handbook of Wood Chemistry and Wood Composites, Second Edition*. CRC Press, September 2012. Google-Books-ID: QMn6rsl_PPgC.

[44] Yoshiharu Nishiyama, Paul Langan, and Henri Chanzy. Crystal Structure and Hydrogen-Bonding System in Cellulose from Synchrotron and Neutron Fiber Diffraction. *Journal of the American Chemical Society*, 124(31):9074–9082, August 2002.

[45] Yoshiharu Nishiyama, Junji Sugiyama, Henri Chanzy, and Paul Langan. Crystal Structure and Hydrogen Bonding System in Cellulose from Synchrotron X-ray and Neutron Fiber Diffraction. *Journal of the American Chemical Society*, 125(47):14300–14306, November 2003.

[46] Mark Crocker. *Thermochemical Conversion of Biomass to Liquid Fuels and Chemicals*. Royal Society of Chemistry, 2010. Google-Books-ID: MZyl15Cz3PAC.

[47] S. I. Mussatto. *Biomass Fractionation Technologies for a Lignocellulosic Feedstock Based Biorefinery*. Elsevier, February 2016. Google-Books-ID: LrZ7BgAAQBAJ.

[48] Mélanie Hall, Prabuddha Bansal, Jay H. Lee, Matthew J. Realff, and Andreas S. Bommarius. Cellulose crystallinity–a key predictor of the enzymatic hydrolysis rate. *The FEBS journal*, 277(6):1571–1582, March 2010.

[49] Lizbeth Laureano-Perez, Farzaneh Teymouri, Hasan Alizadeh, and Bruce E. Dale. Understanding factors that limit enzymatic hydrolysis of biomass. *Applied Biochemistry and Biotechnology*, 124(1-3):1081–1099, March 2005.

[50] Joshua P. Vandenbrink, Roger N. Hilten, K. C. Das, Andrew H. Paterson, and Frank Alex Feltus. Analysis of Crystallinity Index and Hydrolysis Rates in the Bioenergy Crop <Emphasis Type="Italic">Sorghum bicolor</Emphasis>. *BioEnergy Research*, 5(2):387–397, June 2012.

[51] Darby Harris, Jozsef Stork, and Seth Debolt. Genetic modification in cellulose-synthase reduces crystallinity and improves biochemical conversion to fermentable sugar. *GCB Bioenergy*, 1(1):51–61, February 2009. 00051.

[52] Sara Andersson-Gunnerås, Ewa J. Mellerowicz, Jonathan Love, Bo Segerman, Yasunori Ohmiya, Pedro M. Coutinho, Peter Nilsson, Bernard Henrissat, Thomas Moritz, and Björn Sundberg. Biosynthesis of cellulose-enriched tension wood in Populus: global analysis of transcripts and metabolites identifies biochemical and developmental regulators in secondary wall biosynthesis. *The Plant Journal: For Cell and Molecular Biology*, 45(2):144–165, January 2006.

[53] Marta Busse-Wicher, Thiago C F Gomes, Theodora Tryfona, Nino Nikolovski, Katherine Stott, Nicholas J Grantham, David N Bolam, Munir S Skaf, and Paul Dupree. The pattern of xylan acetylation suggests xylan may interact with cellulose microfibrils as a twofold helical screw in the secondary plant cell wall of Arabidopsis thaliana. *The Plant Journal*, 79(3):492–506, August 2014.

[54] Yong Bum Park and Daniel J. Cosgrove. A Revised Architecture of Primary Cell Walls Based on Biomechanical Changes Induced by Substrate-Specific Endoglucanases. *Plant Physiology*, 158(4):1933–1943, April 2012.

[55] Sarah E. C. Whitney, Mike J. Gidley, and Simon J. McQueen-Mason. Probing expansin action using cellulose/hemicellulose composites. *The Plant Journal*, 22(4):327–334, May 2000.

[56] Henrik Vibe Scheller and Peter Ulvskov. Hemicelluloses. *Annual Review of Plant Biology*, 61(1):263–289, 2010.

[57] Poppy E. Marriott, Leonardo D. Gómez, and Simon J. McQueen-Mason. Unlocking the potential of lignocellulosic biomass through plant science. *New Phytologist*, 209(4):1366–1381, March 2016. 00007.

[58] David Brown, Raymond Wightman, Zhinong Zhang, Leonardo D. Gomez, Ivan Atanassov, John-Paul Bukowski, Theodora Tryfona, Simon J. McQueen-Mason, Paul Dupree, and Simon Turner. Arabidopsis genes IRREGULAR

XYLEM (IRX15) and IRX15l encode DUF579-containing proteins that are essential for normal xylan deposition in the secondary cell wall. *The Plant Journal*, 66(3):401–413, May 2011.

[59] Chanhui Lee, Quincy Teng, Wenlin Huang, Ruiqin Zhong, and Zheng-Hua Ye. Down-regulation of PoGT47c expression in poplar results in a reduced glucuronoxylan content and an increased wood digestibility by cellulase. *Plant & Cell Physiology*, 50(6):1075–1089, June 2009. 00095.

[60] Pia Damm Petersen, Jane Lau, Berit Ebert, Fan Yang, Yves Verhertbruggen, Jin Sun Kim, Patanjali Varanasi, Anongpat Suttangkakul, Manfred Auer, Dominique Loqué, and Henrik Vibe Scheller. Engineering of plants with improved properties as biofuels feedstocks by vessel-specific complementation of xylan biosynthesis mutants. *Biotechnology for Biofuels*, 5(1):84, November 2012.

[61] Rumi Kaida, Tomomi Kaku, Kei'ichi Baba, Masafumi Oyadomari, Takashi Watanabe, Koji Nishida, Toshiji Kanaya, Ziv Shani, Oded Shoseyov, and Takahisa Hayashi. Loosening Xyloglucan Accelerates the Enzymatic Degradation of Cellulose in Wood. *Molecular Plant*, 2(5):904–909, September 2009.

[62] Geoffrey Moxley, Armindo Ribeiro Gaspar, Don Higgins, and Hui Xu. Structural changes of corn stover lignin during acid pretreatment. *Journal of Industrial Microbiology & Biotechnology*, 39(9):1289–1299, September 2012.

[63] Z. J. Wang, J. Y. Zhu, Ronald S. Zalesny, and K. F. Chen. Ethanol production from poplar wood through enzymatic saccharification and fermentation by dilute acid and SPORL pretreatments. *Fuel*, 95:606–614, May 2012.

[64] Louise Jones, A. Roland Ennos, and Simon R. Turner. Cloning and characterization of irregular xylem4 (irx4): a severely lignin-deficient mutant of Arabidopsis. *The Plant Journal*, 26(2):205–216, April 2001.

[65] Scott E. Sattler and Deanna L. Funnell-Harris. Modifying lignin to improve bioenergy feedstocks: strengthening the barrier against pathogens?†. *Frontiers in Plant Science*, 4, April 2013.

[66] Wout Boerjan, John Ralph, and Marie Baucher. Lignin Biosynthesis. *Annual Review of Plant Biology*, 54(1):519–546, 2003.

[67] John Ralph, Junpeng Peng, Fachuang Lu, Ronald D. Hatfield, and Richard F. Helm. Are Lignins Optically Active? *Journal of Agricultural and Food Chemistry*, 47(8):2991–2996, August 1999.

[68] Jean-Claude Sigoillot, Jean-Guy Berrin, Mathieu Bey, Laurence Lesage-Meessen, Anthony Levasseur, Anne Lomascolo, Eric Record, and Eva Uzan-Boukhris. Chapter 8 - Fungal Strategies for Lignin Degradation. In Lise Jouanin and Catherine Lapierre, editors, *Advances in Botanical Research*, volume 61 of *Lignins*, pages 263–308. Academic Press, January 2012.

[69] Fang Chen and Richard A. Dixon. Lignin modification improves fermentable sugar yields for biofuel production. *Nature Biotechnology*, 25(7):759–761, July 2007. 00769.

[70] Rebecca Van Acker, Ruben Vanholme, Véronique Storme, Jennifer C. Mortimer, Paul Dupree, and Wout Boerjan. Lignin biosynthesis perturbations affect secondary cell wall composition and saccharification yield in Arabidopsis thaliana. *Biotechnology for Biofuels*, 6:46, 2013. 00066.

[71] Rebecca Van Acker, Jean-Charles Leplé, Dirk Aerts, Véronique Storme, Geert Goeminne, Bart Ivens, Frédéric Légée, Catherine Lapierre, Kathleen Piens, Marc C. E. Van Montagu, Nicholas Santoro, Clifton E. Foster, John Ralph, Wim Soetaert, Gilles Pilate, and Wout Boerjan. Improved saccharification and ethanol yield from field-grown transgenic poplar deficient in cinnamoyl-CoA reductase. *Proceedings of the National Academy of Sciences*, 111(2):845–850, January 2014.

[72] Douyong Min, Quanzi Li, Hasan Jameel, Vincent Chiang, and Houmin Chang. The Cellulase-Mediated Saccharification on Wood Derived from Transgenic Low-Lignin Lines of Black Cottonwood (<Emphasis Type="Italic">Populus trichocarpa</Emphasis>). *Applied Biochemistry and Biotechnology*, 168(4):947–955, October 2012.

[73] Chunxiang Fu, Xirong Xiao, Yajun Xi, Yaxin Ge, Fang Chen, Joseph Bouton, Richard A. Dixon, and Zeng-Yu Wang. Downregulation of Cinnamyl Alcohol Dehydrogenase (CAD) Leads to Improved Saccharification Efficiency in Switchgrass. *BioEnergy Research*, 4(3):153–164, September 2011.

[74] Serge Berthet, Nathalie Demont-Caulet, Brigitte Pollet, Przemyslaw Bidzinski, Laurent Cézard, Phillipe Le Bris, Nero Borrega, Jonathan Hervé, Eddy Blondet, Sandrine Balzergue, Catherine Lapierre, and Lise Jouanin. Disruption of LACCASE4 and 17 Results in Tissue-Specific Alterations to Lignification of Arabidopsis thaliana Stems. *The Plant Cell*, 23(3):1124–1137, March 2011.

[75] Kewei Zhang, Mohammad-Wadud Bhuiya, Jorge Rencoret Pazo, Yuchen Miao, Hoon Kim, John Ralph, and Chang-Jun Liu. An Engineered Monolignol 4-O-Methyltransferase Depresses Lignin Biosynthesis and Confers Novel Metabolic Capability in Arabidopsis[C][W][OA]. *The Plant Cell*, 24(7):3135–3152, July 2012. 00000.

[76] Marc-Olivier Duceppe, Annick Bertrand, Sivakumar Pattathil, Jeffrey Miller, Yves Castonguay, Michael G. Hahn, Réal Michaud, and Marie-Pier Dubé. Assessment of Genetic Variability of Cell Wall Degradability for the Selection of Alfalfa with Improved Saccharification Efficiency. *BioEnergy Research*, 5(4):904–914, December 2012.

[77] B. M. Goff, P. T. Murphy, and K. J. Moore. Comparison of common lignin methods and modifications on forage and lignocellulosic biomass materials. *Journal of the science of food and agriculture.*, 92(4):751–758, March 2012.

[78] Dianging Guo, Fang Chen, John Wheeler, John Winder, Susan Selman, Michael Peterson, and Richard A. Dixon. Improvement of in-rumen digestibility of alfalfa forage by genetic manipulation of lignin O-methyltransferases. *Transgenic Research*, 10(5):457–464, October 2001. 00133.

[79] Michael H. Studer, Jaclyn D. DeMartini, Mark F. Davis, Robert W. Sykes, Brian Davison, Martin Keller, Gerald A. Tuskan, and Charles E. Wyman. Lignin content in natural Populus variants affects sugar release. *Proceedings of the National Academy of Sciences*, 108(15):6300–6305, April 2011. 00238.

[80] Xu Li, Eduardo Ximenes, Youngmi Kim, Mary Slininger, Richard Meilan, Michael Ladisch, and Clint Chapple. Lignin monomer composition affects Arabidopsis cell-wall degradability after liquid hot water pretreatment. *Biotechnology for Biofuels*, 3(1):27, December 2010.

[81] Shawn D. Mansfield, Kyu-Young Kang, and Clint Chapple. Designed for deconstruction–poplar trees altered in cell wall lignification improve the efficacy of bioethanol production. *The New Phytologist*, 194(1):91–101, April 2012. 00066.

[82] Angela Ziebell, Kristen Gracom, Rui Katahira, Fang Chen, Yunqiao Pu, Art Ragauskas, Richard A. Dixon, and Mark Davis. Increase in 4-Coumaryl Alcohol Units during Lignification in Alfalfa (Medicago sativa) Alters the Extractability and Molecular Weight of Lignin. *Journal of Biological Chemistry*, 285(50):38961–38968, December 2010.

[83] John Ralph, Mirko Bunzel, Jane M. Marita, Ronald D. Hatfield, Fachuang Lu, Hoon Kim, Paul F. Schatz, John H. Grabber, and Hans Steinhart. Peroxidase-dependent cross-linking reactions of p-hydroxycinnamates in plant cell walls. *Phytochemistry Reviews*, 3(1-2):79–96, January 2004. 00200.

[84] Ruben Vanholme, Igor Cesarino, Katarzyna Rataj, Yuguo Xiao, Lisa Sundin, Geert Goeminne, Hoon Kim, Joanna Cross, Kris Morreel, Pedro Araujo, Lydia Welsh, Jurgen Haustraete, Christopher McClellan, Bartel Vanholme, John Ralph, Gordon G. Simpson, Claire Halpin, and Wout Boerjan. Caffeoyl

Shikimate Esterase (CSE) Is an Enzyme in the Lignin Biosynthetic Pathway in Arabidopsis. *Science*, 341(6150):1103–1106, September 2013.

[85] Debra Mohnen. Pectin structure and biosynthesis. *Current Opinion in Plant Biology*, 11(3):266–277, June 2008.

[86] A. M. Showalter. Structure and function of plant cell wall proteins. *The Plant Cell*, 5(1):9–23, January 1993.

[87] D. J. Bradley, P. Kjellbom, and C. J. Lamb. Elicitor- and wound-induced oxidative cross-linking of a proline-rich plant cell wall protein: a novel, rapid defense response. *Cell*, 70(1):21–30, July 1992.

[88] Gerrit-Jan van Holst and Joseph E. Varner. Reinforced Polyproline II Conformation in a Hydroxyproline-Rich Cell Wall Glycoprotein from Carrot Root. *Plant Physiology*, 74(2):247–251, February 1984.

[89] Jay E. Mellon and John P. Helgeson. Interaction of a Hydroxyproline-Rich Glycoprotein from Tobacco Callus with Potential Pathogens. *Plant Physiology*, 70(2):401–405, August 1982.

[90] Andrew Carroll and Chris Somerville. Cellulosic Biofuels. *Annual Review of Plant Biology*, 60(1):165–182, 2009.

[91] Lee R. Lynd, Paul J. Weimer, Willem H. van Zyl, and Isak S. Pretorius. Microbial Cellulose Utilization: Fundamentals and Biotechnology. *Microbiology and Molecular Biology Reviews*, 66(3):506–577, September 2002. 03601.

[92] Ye Sun and Jiayang Cheng. Hydrolysis of lignocellulosic materials for ethanol production: a review. *Bioresource Technology*, 83(1):1–11, May 2002.

[93] Badal C. Saha, Loren B. Iten, Michael A. Cotta, and Y. Victor Wu. Dilute acid pretreatment, enzymatic saccharification and fermentation of wheat straw to ethanol. *Process Biochemistry*, 40(12):3693–3700, December 2005.

[94] R.P. Tengerdy and G. Szakacs. Bioconversion of lignocellulose in solid substrate fermentation. *Biochemical Engineering Journal*, 13(2–3):169–179, March 2003.

[95] Ignacio Ballesteros, MaJosé Negro, JoséMiguel Oliva, Araceli Cabañas, Paloma Manzanares, and Mercedes Ballesteros. Ethanol Production From Steam-Explosion Pretreated Wheat Straw. In JamesD. McMillan, WilliamS. Adney, JonathanR. Mielenz, and K.Thomas Klasson, editors, *Twenty-Seventh Symposium on Biotechnology for Fuels and Chemicals*, ABAB Symposium, pages 496–508. Humana Press, 2006. 00244.

[96] Maria José Negro, Paloma Manzanares, Ignacio Ballesteros, Jose Miguel Oliva, Araceli Cabañas, and Mercedes Ballesteros. Hydrothermal Pretreatment Conditions to Enhance Ethanol Production from Poplar Biomass. In Brian H. Davison, James W. Lee, Mark Finkelstein, and James D. McMillan, editors, *Biotechnology for Fuels and Chemicals*, Applied Biochemistry and Biotechnology, pages 87–100. Humana Press, 2003. 00171.

[97] Nathan Mosier, Charles Wyman, Bruce Dale, Richard Elander, Y. Y. Lee, Mark Holtzapple, and Michael Ladisch. Features of promising technologies for pretreatment of lignocellulosic biomass. *Bioresource Technology*, 96(6):673–686, April 2005. 03830.

[98] Bärbel Hahn-Hägerdal, Kaisa Karhumaa, César Fonseca, Isabel Spencer-Martins, and Marie F. Gorwa-Grauslund. Towards industrial pentose-fermenting yeast strains. *Applied Microbiology and Biotechnology*, 74(5):937–953, April 2007. 00502.

Capítulo 2

BIOMASS RECALCITRANCE IN BARLEY, WHEAT AND TRITICALE STRAW: CORRELATION OF BIOMASS QUALITY WITH CLASSIC AGRONOMICAL TRAITS

Published as:

Ostos Garrido FJ, Pistón F, Gómez LD, McQueen-Mason SJ. "Biomass recalcitrance in barley, wheat and triticale straw: Correlation of biomass quality with classic agronomical traits." *PLOS ONE.* November 2018. ISSN 1932-6203. doi:10.1371/journal.pone.e0205880.

2.1. Abstract:

The global production of cereal straw as an agricultural by-product presents a significant source of biomass, which could be used as feedstock for the production of second generation biofuels by fermentation. The production of sugars for fermentation is an important measure of straw quality and in its suitability for biofuel production. In this paper, we present a characterization of straw digestibility from a wide range of cereal. Our main objective is to evaluate the variability of fermentable sugars released from different species including wheat (*Triticum durum* L., *Triticum aestivum* L.), barley (*Hordeum vulgare* L.) and triticale (X *Triticosecale Wittmack*). To this end, we adapted a saccharification method (IAS Method) capable of detecting significant differences of released sugars between cultivars and species, while using separately another method that would serve as a control and with which we could contrast our results (CNAP method). ANOVA analyses revealed that barley has a higher saccharification potential than wheat and triticale and shows more variation between genotypes. Thus, populations derived from crosses among them such as Steptoe × Morex and OWB Dominant × OWB Recessive hold potential for the identification of genetic basis for saccharification-related traits. The correlation of glucose released between the two methods was moderate (R^2 = 0.57). An evaluation of the inter- and intra- specific correlation between a number of chemical and agronomical parameters and saccharification suggests that the cell wall thickness and lignin content in straw could be used in breeding programs for the improvement of the saccharification potential. Finally, the lack of correlation

between grain yield and saccharification suggests that it would be possible to make a selection of genotypes for dual purpose, low recalcitrance and grain yield.

2.2. Introduction

Widespread burning of fossil fuels produces approximately 81 % of the world's energy, of which 41 % comes from oil, mostly destined (92 %) to the transport sector [1]. The environmental consequences of burning fossil fuels, and the threat of a shortage of energy due to finite oil reserves are well documented [2]. In response, the use of bioethanol as a liquid fuel has triggered a fivefold increase in ethanol production since 2000 [3]. Current commercial biofuel supply relies on first-generation biofuel production, which, although efficient, requires food and feed commodities as a feedstock and as such, poses a potential threat to food security. Although first generation biofuels can be produced efficiently, they use food and feed commodities as a feedstock posing a potential threat to food security. In addition, the cultivation of such feedstocks requires high agrochemical inputs that increase the carbon footprint of biofuels [4]. The development of second-generation biofuels from agricultural waste presents a valuable alternative as it can be obtained as a by-product from food crops [5]. At present, cereal straw is treated as a residue and is usually burnt or incorporated into the soil, but these by-products (including wheat, barley, rice, corn, oat, cotton straw, and bagasse from sugar cane, and totaling approximately 3 billion metric tons annually) present a great potential energy source [6]. Second generation bioethanol production from lignocellulosic biomass requires the conversion of lignocellulose into simple sugars, in three stages [7]: size reduction, thermochemical pretreatment and hydrolysis. The ease with which a biomass is hydrolyzed, also known as saccharification potential, can be used to evaluate recalcitrance of biomass in breeding programs. In this paper, two saccharification methods have been used, one developed by the Instituto de Agricultura Sostenible, (IAS hereinafter) and another procedure, which is widely used, [8] used as a control (Centre for Novel Agricultural Products, CNAP hereinafter).

Pretreatment serves to improve the accessibility of the hydrolysing enzymes to the lignocellulose feedstock. Each pretreatment process is optimised to the biomass to

be hydrolyzed since this has a specific effect on the cellulose, hemicellulose and lignin fraction [9]. Due to the great variability in the composition of lignocellulosic materials, it is necessary to adapt the saccharification method to the properties of the biomass. The pretreatment conditions should be chosen in accordance with the configuration of the process selected for the subsequent hydrolysis and fermentation steps. This process, besides being crucial in the conversion of biomass to bioethanol, is considered as the second most expensive after the feedstock cost [9].

The variability in the cell wall degradability of lignocellulosic material can be affected by many factors such as genetic [10, 11], morphological [12, 13], environmental [14, 15], experimental technique for releasing sugars [16], and crop harvesting [17, 18]. To fully evaluate all sources of variability, it is advisable to take a multi-phase and multi-environment approach [19] with different experimental methods [16].

The deliberate modification of cell-wall properties is challenging considering the high number of genes involved. Indeed, recent findings in *Arabidopsis thaliana* estimate that 10–15 % of plant genes are related to cell-wall biology [20]. This is not surprising since cell walls are essential to plants, contributing to pest and disease resistance and providing mechanical support to plant tissues. Consequently, breeding programs for bioethanol production should aim for a balance between saccharification potential and agronomic performance.

A number of biofuel research initiatives have developed high throughput methods for pretreatment and enzymatic hydrolysis (HTPH) to evaluate the saccharification properties of large collections of germplasm with high potential for the production of second generation biofuels [8, 21–23].

The aims of this work are to evaluate the variation in sugar yield from straw obtained from wheat, barley and triticale cultivars under rain-fed environments and to select parental genotypes to develop mapping populations to detect QTL for saccharification.

2.3. Material and methods

Plant material

Four cereal species were studied: Hordeum vulgare L., Triticum aestivum L., Triticum durum L. and X Triticosecale Wittmack (Table 2.1). Triticale, barley

and wheat lines were obtained from either the National Small Grains Collection (NSGC) of the United States Department of Agriculture-Agricultural Research Service (USDA-ARS) (https://www.ars.usda.gov/pacific-west-area/aberdeen-id/small-grains-and-potato-germplasm-research/docs/national-small-grains-collection/) or from the Barley and Wild Plant Resource Center, Okayama University (http://earth.lab.nig.ac.jp). When available, accessions used as parental lines in mapping populations were selected with a dual purpose: Firstly, to allow for the identification of mapping populations suitable for studying the genetic bases of saccharification, and secondly to give a fair representation to the variability available in each species, as parental lines are normally selected to be as divergent as possible.

Accession name(a)	Species	Accession number
Apex**	H. vulgare	PI600966
Azumamugi***	H. vulgare	J698
Cebada Capa**	H. vulgare	PI539113
Clipper**	H. vulgare	PI349366
Dicktoo**	H. vulgare	CIho 5529
Franka**	H. vulgare	PI574293
Franklin**	H. vulgare	PI373729
Fredrickson**	H. vulgare	CIho 13647
Golden Promise**	H. vulgare	PI467829
Igri**	H. vulgare	PI406263
Kanto Nakate Gold***	H. vulgare	J518
Ko A**	H. vulgare	PI383935
L94**	H. vulgare	CIho 11797
Lina**	H. vulgare	PI584808
Mokusekko 3**	H. vulgare	PI420938
Morex**	H. vulgare	Ciho 15773
OWB dominant**	H. vulgare	GSHO3450
OWB recessive**	H. vulgare	GSHO3451
Stander**	H. vulgare	PI564743
Steptoe**	H. vulgare	CIho 15229
Vada**	H. vulgare	PI280422
Anza*	T. aestivum	NA

Sigue en la página siguiente...

Accession name(a)	Species	Accession number
Avocet**	T. aestivum	PI464644
BobWhite*	T. aestivum	NA
Caledonia**	T. aestivum	PI610188
Cayuga**	T. aestivum	PI595848
CIGM90.248**	T. aestivum	PI610750
Excalibur**	T. aestivum	PI572701
JAYPEE**	T. aestivum	PI592760
Kanqueen**	T. aestivum	PI401539
M6**	T. aestivum	PI83534
McNeal**	T. aestivum	PI574642
Opata85**	T. aestivum	PI591776
OS9A**	T. aestivum	PI658243
P91193**	T. aestivum	GSTR 10001
P92201**	T. aestivum	GSTR 10002
Penawawa**	T. aestivum	PI495916
Perico*	T. aestivum	NA
QCB36**	T. aestivum	PI658244
Renan**	T. aestivum	PI564569
SS550**	T. aestivum	GSTR 12501
TAM107-R7**	T. aestivum	GSTR 11601
Thatcher**	T. aestivum	CItr 10003
UC1110**	T. aestivum	GSTR 13501
USG 3209**	T. aestivum	PI617055
Amadina**	T. durum	GSTR 12701
Avalon**	T. durum	PI446910
CO940610**	T. durum	GSTR 10702
Grandin*5/ND614-A**	T. durum	GSTR 10401
IDO444**	T. durum	GSTR 12902
Jupateco 73S**	T. durum	GSTR 10501
NY18/Clark's Cream 40-1**	T. durum	GSTR 10402
Rio Blanco**	T. durum	PI531244
Rugby**	T. durum	CItr 17284
UC1113 Yr36 Gpc-B1**	T. durum	PI638741

Sigue en la página siguiente...

Accession name(a)	Species	Accession number
Weebill 1**	T. durum	GSTR 10502
Armadillo 130**	X Triticosecale	PI583701
Currency**	X Triticosecale	PI483066
Drira**	X Triticosecale	PI520478
Juanillo 95**	X Triticosecale	PI520488
Kramer**	X Triticosecale	PI476216
Navojoa**	X Triticosecale	PI520421
Rahum**	X Triticosecale	PI422269
Wapiti**	X Triticosecale	PI511870
Yoreme Tehuacan 75**	X Triticosecale	PI519876
Zebra**	X Triticosecale	PI429031

Table 2.1: Plant material used in this work. More information on the genotypes can be found at https://npgsweb.ars-grin.gov/gringlobal/search.aspx.
(a) Plant material availability:
* IAS-CSIC;
** USDA-ARS, National Small Grains Germplasm Research Facility, Aberdeen, ID 83210, USA.;
*** Barley and Wild Plant Resource Center. Institute of Plant Science and Resources. Okayama University, Kurashiki, 710-0046, Japan.

Field trials and sample processing

Three field trials, which were designed in three completely randomized blocks, were conducted in Córdoba (37.85981, -4.796895). Each field trial included sixty-six accessions belonging to four different species: barley (*Hordeum vulgare* L.) common wheat (*T. aestivum*), durum wheat (*T. durum*) and triticale (*Triticosecale*) (Table 2.1). Each plot consisted of four plants separated by 15cm with an inter-plot distance of 30cm and an inter-furrow distance of 50cm. The straw harvested included leaves and stems; and it was harvested at maturity for each genotype. Samples were chopped using a grinder before processing was performed using a cyclonic mill (Cyclotec 1093, Foss-Tekator) with a 1mm sieve.

Phenotyping

The all genotypes were scored for: plant height at different stages of growth, total plant biomass, grain yield, biomass yield and stem wall thickness at several internodes. All determinations but plant height was taken at harvest.

Theoretical ethanol yield calculation

The theoretical ethanol yield was calculated considering the total biomass conversion per surface area unit (ha), according to the National Renewable Energy Laboratory Standards (NREL) [24]. Theoretical ethanol was conducted through the following formula:

$$f(Glu, Biomass) = \frac{Glu \cdot 0{,}511 \cdot Biomass}{1000} \tag{2.1}$$

Where Glu: Glucose released (µL/mgDW), Biomass: Theoretical biomass (Kg/ha), produced by genotype from the quantity of straw in plots of 0.3 square meters, 0.511: theoretical ethanol yield conversion.

Saccharification systems

Both systems to determine saccharification were calibrated based on previous knowledge for near optimal hydrothermal pretreatment of straw and optimal enzyme loading [25, 26].

IAS method Assays to determine saccharification involved three main steps: pretreatment, hydrolysis and sugar detection. The conditions established by Gomez et al. [8] and Santoro et al. [23] were adapted for sample processing in a single 2 mL tube as used by Santoro et al [23]. Briefly, 20 mg of ground straw were loaded into 2 mL screw-cap tubes. A pretreatment solution (6.25 mM) NaOH was used as described by Santoro et al. [23] using 1.5 mL of pretreatment solution and incubated at 90°C for 3 h in a water bath, then cooled on ice. Enzymatic hydrolysis was performed using an enzyme cocktail with a 4:1 ratio of Celluclast: Novozyme 188 (Novozymes, Bagsvaerd, Denmark) [8]. Hydrolysis was performed during 20 h with constant shaking, at 50°C in a 0.5 M sodium citrate buffer at pH 4.5. Different enzyme concentrations were assayed to optimize the digestion in a single tube (Fig S2.4), the concentration selected as optimal to determine differences between genotypes was 0.05 (µL/mg DW. Nine serial dilutions were established from a maximum enzyme concentration of 2 (µL/mg of dry weight (DW). The determination of sugars released after hydrolysis was carried out using the glucose oxidase/peroxidase (GOPOD) kit (K-Gluc, Megazyme, Ireland). The assay volumes were reduced to allow the procedure to be performed in 96-well ELISA plates. Glucose determination was performed using 8 (µL of the digestion

reaction mixture and 240 (µL of the GOPOD assay reagent followed by incubation at 50°C during 20 min. The yield of glucose was analyzed using 96 well plates. Absorbance readings were determined at 490 nm in a BioTek ELx800 Absorbance Microplate Reader (BioTek Instruments, Inc.). The adapted protocol used at IAS was validated with the saccharification protocol described by Gomez et al. [8].

CNAP method 96-well plates containing biomass underwent saccharification analysis using a liquid handling platform (Tecan Evo 200; Tecan Group Ltd.) which pretreated the samples with 0.5N NaOH at 90°C for 20 min, followed by enzymatic hydrolysis 50°C for 8 hours. The enzyme cocktail contained commercially available Celluclast and Novozyme 188 (Novozymes A/S, Bagsvaerd, Denmark) at a ratio of 4:1 at an enzyme loading of 22.5 Filter Paper Units (FPU)/g. The reducing sugars released during hydrolysis were determined using a colorimetric assay involving 3-methyl-2-benzothiazolinone hydrozone (MTBH) [8]. Each plate contained standard reactions of 50 nmol, 100 nmol, and 150 nmol of glucose. Change in color was read with a Tecan Sunrise microplate absorbance reader at 620 nm.

Lignin determination

Lignin content was quantified using the acetyl bromide method according to Foster et al. [27]. Briefly, 3mg of biomass alcohol insoluble residue (AIR) were weighed into a 5 mL volumetric flask, and 250 (µL of freshly prepared acetyl bromide solution (25 % v/v acetyl bromide in glacial acetic acid) was added. Samples were incubated at 50°C for 2h, followed by a further 1h, mixing every 15min. Samples were taken to 5 mL with glacial acetic acid and mixed. The absorption was read using a Shimadzu UV 1800 spectrophotometer (http://www.shimadzu.com) at 280nm. Lignin content was (µg x mg^{-1} cell wall) determined using the following formula 2.2:

$$\text{Lignin Content} = \frac{\text{Absorbance}}{(\text{Coefficient x Path length})} \cdot \frac{\text{Total volume}}{\text{Biomass weight}} \cdot 100. \qquad (2.2)$$

The coefficient used for grasses was 17.75.

Statistical analyses

All statistical analyses were conducted with the software **R** version 3.2.3 [28]. Data was adjusted to a linear model with the function lm and the significance was established using analysis of the variance (ANOVA) (function aov, package agricolae [29]. Differences between species or genotypes were determined by Tuckey HSD test ($P \leq 0.05$) (function LSD.test, agricolae package). Pearson correlations were calculated with cor function (stats package) and all boxplot and art-graph were depicted with boxplot function (ggplot2 package [30]). The main assumptions of linear model were confirmed using the Shapiro-Wilk test for normal distribution (function shapiro.test, stats package [28] and by the Levene test for homogeneity of variances (function leveneTest, package car [31]) and variables were transformed if required.

2.4. Results and discussion

Variation of the saccharification potential in a range of cereal cultivars

To assess the differences in recalcitrance among species and cultivars of triticale, wheat (*T. durum* and *T. aestivum*) and barley, all samples were analysed for saccharification potential using the IAS and CNAP methods described above. Glucose yields were standardized using inter-plate checks to control inter-plate variance. ANOVA analysis revealed significant differences among species, barley being the species with the highest saccharification potential (Fig 2.1A).

To validate the results obtained through IAS method, a biological replicate of each sample was analysed using the CNAP method, as control. The correlation of standardized glucose yields between IAS and CNAP methods was moderate (R^2 = 0.5688) but it is significantly higher than the values reported by Lindedam et al. [16] for two high throughput systems (R^2 = 0.2139), differences between IAS and CNAP could be due to the different methods used for the quantification of the sugars released. IAS determines only glucose, while CNAP determines all sugars as reducing sugars. Lindedam et al. [16] analysed three different methods, but only reported their best correlation which implies that the other correlations were lower. Both methods used here show that barley presents the highest saccharification potential (Fig 2.1B). Further analyses were conducted to evaluate the relative recalcitrance among genotypes for each genus/species (Table 2.2).

Significant differences were detected among barley, wheat and triticale genotypes. In the screening of the 66 cultivars of wheat, barley and triticale, we are able to

identify a large variability in the enzymatic hydrolysis of the cell walls of straw. The variability for saccharification among cultivars of different species ranged between 47.09 µg/mg DW and 89.62 µg/mg DW (mean values) using the IAS method, and from 51.59 to 85.07 µg/mg DW using the CNAP method. The variance coefficients (CV) between all genotypes in this trial were 14.7 % and 12.2 % for the IAS and CNAP methods, respectively. *H. Chilense* had a coefficient of variation of 11.6 % and 8.54 %, *T. Aestivum* of 9.6 % and 7.6 %, *T. Durum* of 15.1 % and 7.82 %, and *Triticosecale* of 9.8 % and 6.2 %, respectively. The differences between methods for CVs between cultivars of each species are always higher for the IAS method. This could be explained to a large extent because in the IAS method only one 96-well plate could be assayed each time, whereas in the high-throughput method of CNAP a larger number of plates per assay (usually six). In terms of variability in cell wall saccharification, similar results have been previously reported in other collections of different cultivars [11, 14, 32]. The block factor was also significant in the ANOVA analysis, but it is likely related to a short flooding period during the growing season. A significant block effect was also reported by [19] due to a short period of drought stress. Taken together, these results suggest that the water balance during the crop cycle could marginally affect the release of glucose. In the present work we do not have the possibility of separating the environmental effect of experimental error, but environmental interactions on the degradability of the cell wall have been previously investigated [10, 14]. However, several genotypes differing in biomass recalcitrance to enzymatic hydrolysis have been used as parental lines in mapping populations for different traits. These mapping populations constitute a valuable resource for barley genetic studies. Indeed, since the development of the Steptoe x Morex and OWB populations [33] they have been successfully used for genetic mapping, including regulatory genes [34] or resistance to leaf stripe [35]. Furthermore, both mapping populations were used to develop a consensus SNP genetic linkage map in barley [36]. Given the contrasting saccharification potential of the parental lines, the barley mapping populations Steptoe × Morex, Vada × Steptoe, OWB Dominant × Steptoe, OWB Dominant × OWB Recessive, and Lina × L94, could be used to identify the genetic factors underlying differential recalcitrance (Fig 2.2A). Similarly, the IDO444 × Rio Blanco mapping population [37] could be used in wheat (Fig 2.2C). However, only the OWB populations and Steptoe × Morex should be considered for mapping purposes since the CNAP method did not detect significant differences at $p < 0.05$

between the other parental listed above.

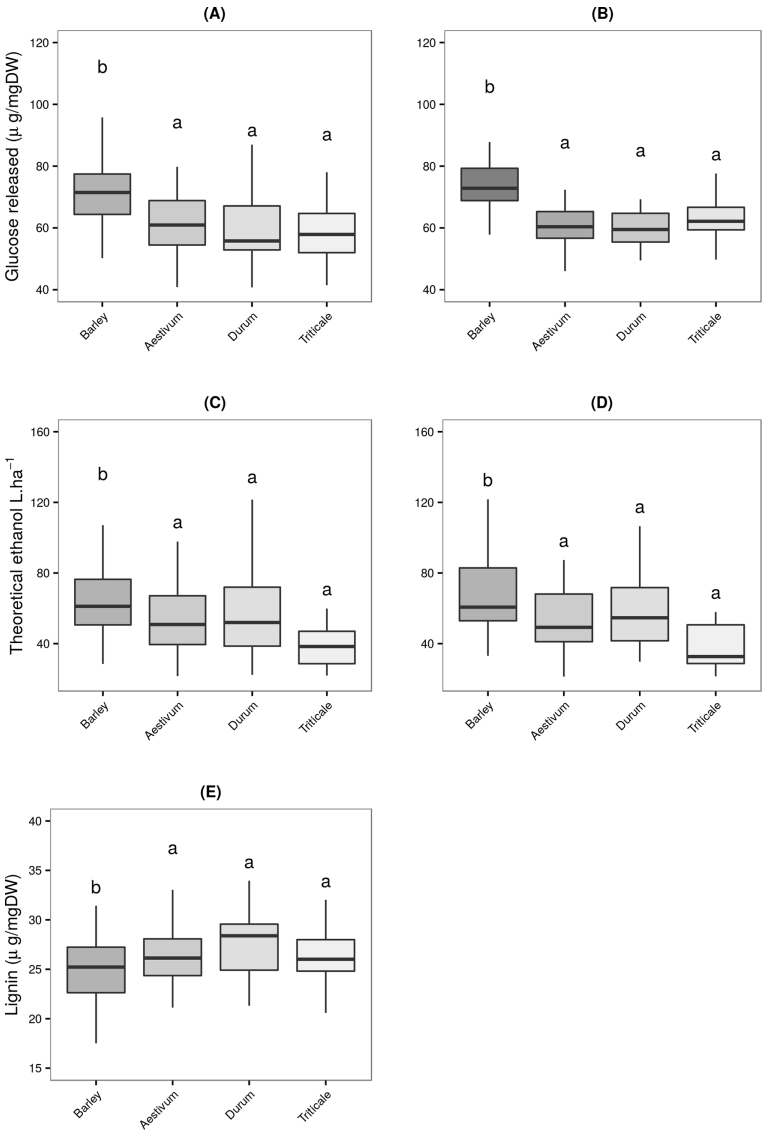

Figure 2.1: Comparative yield of glucose released in barley, wheat and triticale under different saccharification conditions. Boxplot of glucose's quantification released for wheat, barley and triticale under different saccharification conditions. (a) IAS; (b) CNAP. Mean (line), $25^{th} - 75^{th}$ percentile (box) and $10^{th} - 90^{th}$ percentile (whiskers) of glucose released for each genus. For each saccharification method, bars with different letters are significantly different (ANOVA, Tuckey HSD test, P≤0.05).

T.aestivum	Glucose Yield	*T.durum*	Glucose yield	*Barley*	Glucose Yield	*Triticale*	Glucose Yield
Caledonia	75.11 a	Avalon	78.4 a	OWB recessive	98.00 a	Juanillo 95	68.32 a
Kanqueen	68.94 ab	NY18/Clark's Cream 40-1	69.55 ab	Steptoe	89.62 ab	Currency	65.5 ab
Excalibur	68.6 abc	IDO444	66.05 abc	Apex	83.24 abc	Yoreme Tehuacan 75	63.38 abc
SS550	67.93 abc	Rugby	63.59 abc	Golden Promise	79.56 abc	Armadillo 130	59.53 abcd
USG3209	67.41 abcd	UC1113 YR36 Gpc-B1	63.52 abc	Capa	76.95 bcd	Drira	58.69 abcd
Avocet	66.94 abcd	Jupateco	58.15 bcd	Lina	75.57 bcd	Rahum	56.48 abcd
Cayuga	66.45 abcd	GRA614A	56.04 bcd	Fredrickson	73.10 bcd	Zebra	55.07 abcd
McNeal	65.37 abcd	Amadina	53.45 bcd	Clipper	73.07 bcd	Navajoa	54.05 bcd
QCB36	64.68 abcd	Weebill_1	53.27 bcd	Azumamugi	72.07 bcd	Wapiti	51.36 cd
P92201	64.58 abcd	CO940610	50.06 cd	Dicktoo	71.60 bcd	Kramer	47.76 d
Renan	63.59 abcd	Rio Blanco	47.1 d	Igri	71.55 bcd		
P91193	63.57 abcd			Mokusekko	69.71 bcd		
CIGM90.248	62.71 abcd			Koa	67.44 bcd		
OS9A	62.33 abcd			OWB dominant	66.49 cd		
Penawawa	59.83 bcd			Stander	65.84 cd		
M6	59.79 bcd			Franka	65.44 cd		
UC1110	57.44 bcd			Morex	65.34 cd		
Thatcher	57.23 bcd			Kanto Nakte Gold	64.88 cd		
Jaypee	56.07 bcd			Vada	64.33 cd		
TAM107 R7	56 bcd			Franklin	62.06 cd		
Anza	55 bcd			L94	52.41 d		
Opata85	53.61 cd						
Bobwhite	51.1 d						
Perico	50.72 d						

Table 2.2: Mean values of total sugar released (μg/mgDW) for sixty-six accessions under IAS-CSIC saccharification conditions. Post-hoc test independently for all genotypes in each. The Study in Wheat was made with LSD test ($p \leq 0.05$) with Benjamini-Yekutieli p-values adjust. Values with same letter are not significantly different at level 0.05.

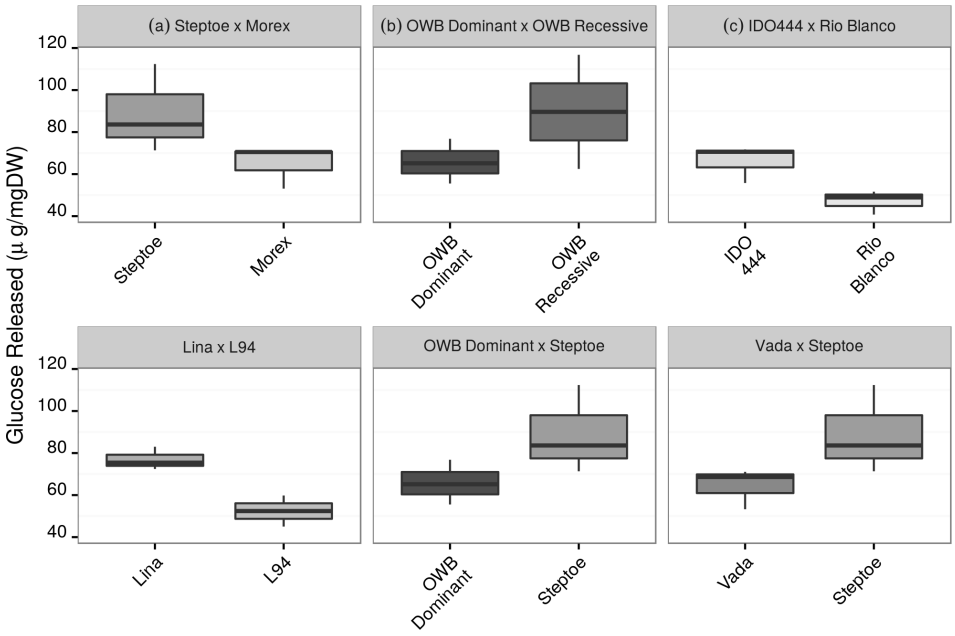

Figure 2.2: Yield of glucose released in selected barley and wheat lines. Boxplot of glucose's quantification. Mean (line), 25^{th}-$75th$ percentile (box) and 10^{th}-90^{th} percentile (whiskers) of glucose released for each genotype. Each graph (a to f) shows significant differences at significance level of 0.05 (using IAS-CSIC saccharification conditions) between parental lines used for the development of mapping populations in the literature. Differences shown in graphs a and b were also significant using the CNAP saccharification conditions, and differences shown in graph c was the only one significant different for wheat.

Determinants of sugar yield

Fig 2.3 shows the degree of correlation between a number of phenotypic characters and saccharification in all genotypes. Lignin content presents a significant negative correlation with sugar yield (r = -0.55) for all genotypes (Fig 2.3A), which is in agreement with previous results by Lindedam et al. [38]. When we compared the top 10 genotypes for biomass yield (Fig 2.3B), we found a stronger Pearson correlation (r = -0.82) and a better relationship between saccharification and lignin content. These results are comparable to previous findings in *Solanum pennellii* by Caruso et al. [39], transgenic alfalfa lines by Chen et al. [40] and *Arabidopsis thaliana* by Van Acker et al [41]. Collectively these results suggest that lignin content should be considered in breeding for saccharification potential. In the current study we observed a negative correlation (r = -0.79) between plant height and saccharification using the CNAP method and a positive correlation between plant height and lignin content (r = 0.65) (Fig 2.3B), both correlations for high

biomass yield selected lines. This relationship between plant height and plant cell wall recalcitrance could be due to the requirement of increased lignin for mechanical stiffness with the consequent reduction in saccharification. Similar results were showed by [11] and [42]. The negative correlation between plant height and degradability could also partly be explained by higher plants having relatively smaller leaf fraction. For correlation analysis with all samples, we could not see correlation between height and degradability; this fact could be explained because breeding programs for semi-dwarf cultivars may in fact have affected the degradability of modern cultivar [43]. ILPave (Average for straw wall thickness for largest internode) and PePave (Average for straw wall thickness for peduncle) showed a significant negative correlation with degradability, theoretical ethanol and number of nodes, and also showed a positive correlation between thickness and lignin content (Fig 2.3A). Generally, barley has a higher number of nodes and low wall thickness, which is consistent with high saccharification and low lignin content results showed in Fig 2.1. Differences in lignin content in cell wall of one genotype of wheat, one barley, and one triticale straw, have been reported previously, showing that barley contains less lignin than wheat [44, 45].

Our results obtained from many genotypes for each species are in agreement with previous reports and extend the observation across genotypes. Plants with the same height and stems with low wall thickness will have more short internodes, implying more numbers of nodes, and consequently are less susceptible to lodging. Correlations between lodging resistance, thickness and number of nodes were shown by Jezowski et al. [46], Tandon et al. [47], and Brady et al. [48] On the other hand, as reported Saint Pierre et al. [49] thickness is an ideal factor to maximize water soluble carbohydrate reserves, and it appears to be important under water limited conditions, where these could be mobilized for grain filling. ILPave and PePave were uncorrelated with plant height and grain yield, hence allowing breeding for that character without compromising high grain yield. Moreover, we could assess that grain yield and saccharification are not correlated (Fig 2.3A), establishing a degree of independence between these two traits.

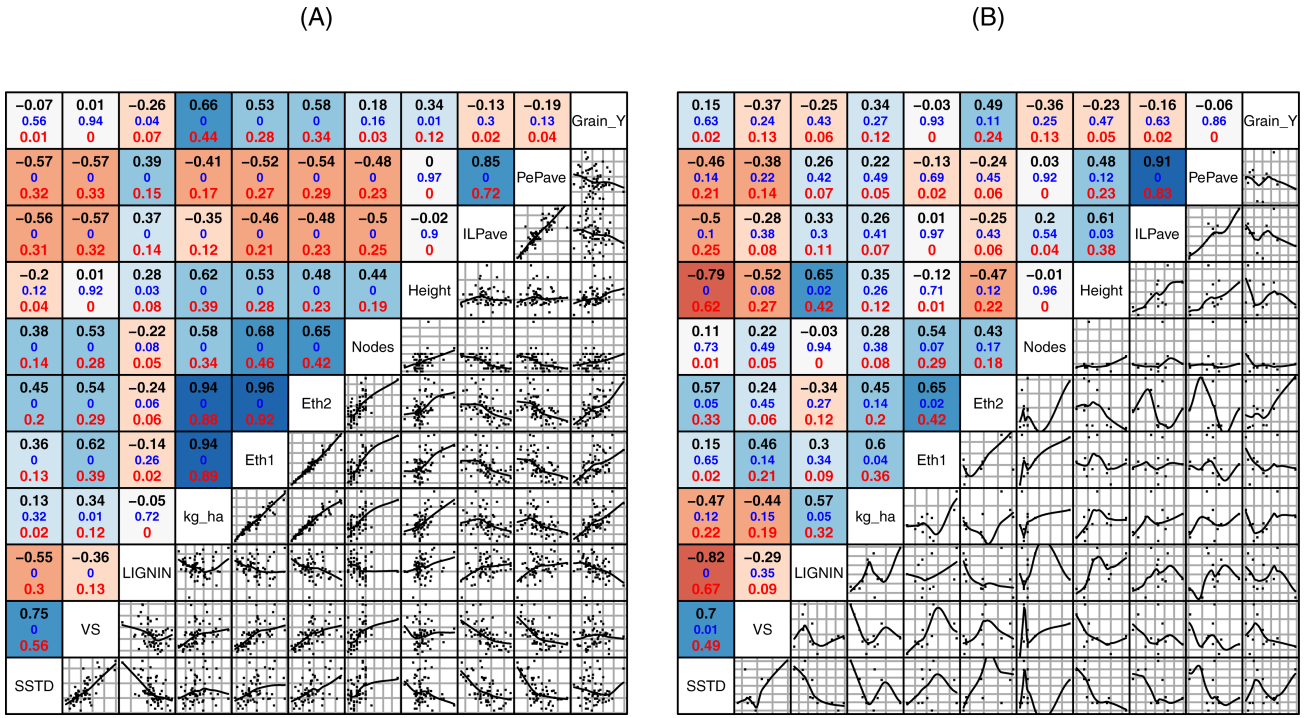

Figure 2.3: Scatter Plot and Pearson's correlation coefficient matrix for comparison among phenotyping, saccharification and theoretical ethanol data. Pairwise correlation analyses were performed for all assayed genotypes (a) and the 10 best genotypes for biomass yield (b). The upper panel above the diagonal shows Pearson's correlation coefficients, p-value and regression coefficient. The lower panel below the diagonal gives their scatter plot. (SSTD = Saccharification standardized values under CNAP conditions, VS = Saccharification standardized values under IAS-CSIC conditions, Kg ha = estimated weight of straw by hectare, Eth1 = Theoretical ethanol calculated with CNAP's saccharification values and estimated biomass, Eth2 = Theoretical ethanol calculated with IAS-CSIC's saccharification values and estimated biomass, ILPave = Average for straw wall thickness for largest internode, PePave = Average for straw wall thickness for peduncle, and Grain Y = grain yield).

2.5. Final remarks

In the current work we analysed a collection of wheat (*T. durum* and *T. aestivum*), barley and triticale genotypes in order to investigate interspecific and intraspecific differences. The methodology adapted at IAS could be useful for genotype selection in biomass quality since it shows a good degree of concordance with previous methodologies. Thus, it would be useful for the identification of improved varieties with good saccharification potential in a breeding program. Collectively, our results indicate that barley is a better source of lignocellulosic material for bioethanol production than wheat and triticale. The ranking of genotypes was slightly different with IAS and CNAP methods, but the most contrasting genotypes were picked up by both methodologies. Interestingly, some of the most dissimilar genotypes have been used to develop mapping populations in barley. For instance, both Steptoe × Morex and OWB Dominant × OWB Recessive barley mapping populations would be good tools for the identification of the genetic basis of saccharification-related traits. Finally, correlation analyses suggest that sugars released, lignin content and its correlation with straw wall thickness would be good predictors of biomass degradability in breeding programs. Furthermore, the lack of correlation between grain yield and saccharification suggests that it would be possible to select genotypes with low recalcitrance and high grain yield for dual use (grain and energy).

2.6. Supporting information

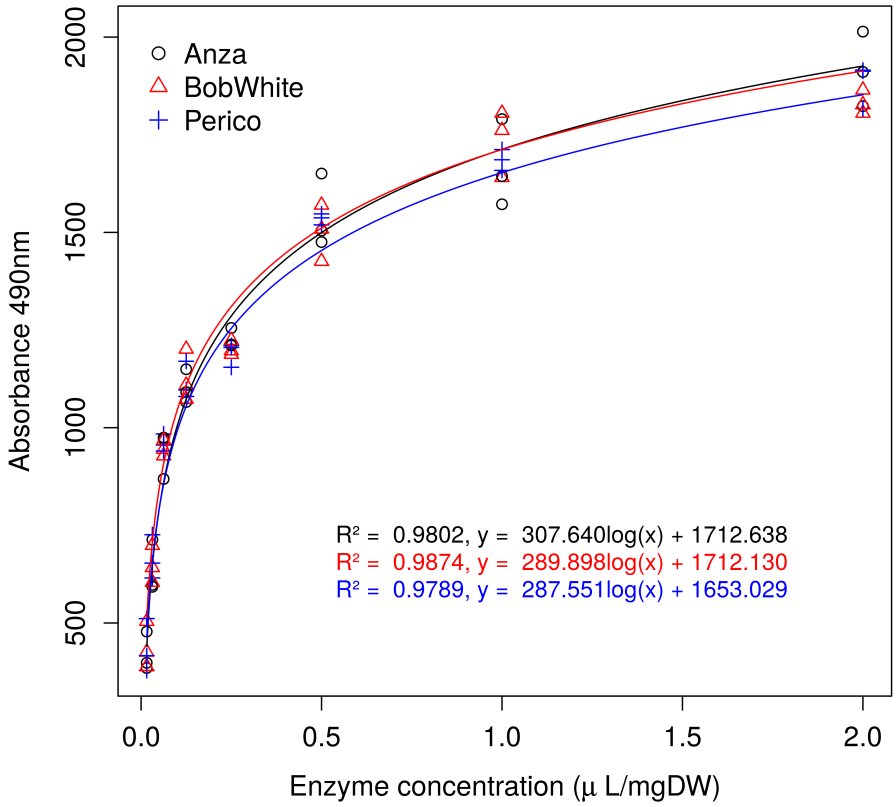

Figure 2.4: Enzyme optimization.Glucose released in wheat genotypes (Anza, Bobwhite and Perico) with different concentrations of enzyme cocktail. R^2 values correspond to different wheat genotypes and enzyme concentrations between 2 and 0.0078 µL/mg DW.

Referencias

[1] IEA IEA. World energy outlook 2011. *Int. Energy Agency*, page 666, 2011. 00073.

[2] IEA. *World Energy Outlook 2010*. Organisation for Economic Co-operation and Development, Paris, November 2010. 00004.

[3] I. E. A. Bioenergy. From 1st-to 2nd-Generation BioFuel technoloGies. *An overview of current industry and RD&D activities. IEA-OECD*, 2008. 00014.

[4] Jason Hill, Erik Nelson, David Tilman, Stephen Polasky, and Douglas Tiffany. Environmental, economic, and energetic costs and benefits of biodiesel and ethanol biofuels. *Proceedings of the National Academy of Sciences*, 103(30):11206–11210, July 2006. 02173.

[5] M. R. Ercolano, L. D. Gomez, A. Andolfi, R. Simister, C. Troise, G. Angelino, C. Borrelli, S. J. McQueen-Mason, A. Evidente, L. Frusciante, and G. Caruso. Residual biomass saccharification in processing tomato is affected by cultivar and nitrogen fertilization. *Biomass and Bioenergy*, 72:242–250, January 2015.

[6] Tong-Qi Yuan and Run-Cang Sun. Chapter 7.3 - Modification of Straw for Activated Carbon Preparation and Application for the Removal of Dyes from Aqueous Solutions. In *Cereal Straw as a Resource for Sustainable Biomaterials and Biofuels*, pages 239–252. Elsevier, Amsterdam, 2010. 00002.

[7] Andrew Carroll and Chris Somerville. Cellulosic Biofuels. *Annual Review of Plant Biology*, 60(1):165–182, 2009.

[8] Leonardo D. Gomez, Caragh Whitehead, Abdellah Barakate, Claire Halpin, and Simon J. McQueen-Mason. Automated saccharification assay for determination of digestibility in plant materials. *Biotechnology for Biofuels*, 3(1):23, October 2010.

[9] Nathan Mosier, Charles Wyman, Bruce Dale, Richard Elander, Y. Y. Lee, Mark Holtzapple, and Michael Ladisch. Features of promising technologies for pretreatment of lignocellulosic biomass. *Bioresource Technology*, 96(6):673–686, April 2005. 03830.

[10] B. S. Capper. Genetic variation in the feeding value of cereal straw. *Animal Feed Science and Technology*, 21(2):127–140, October 1988. 00062.

[11] Jacob Wagner Jensen, Jakob Magid, Jens Hansen-Møller, Sven Bode Andersen, and Sander Bruun. Genetic variation in degradability of wheat straw and potential for improvement through plant breeding. *Biomass and Bioenergy*, 35(3):1114–1120, March 2011. 00009.

[12] K. B. Duguid, M. D. Montross, C. W. Radtke, C. L. Crofcheck, S. A. Shearer, and R. L. Hoskinson. Screening for sugar and ethanol processing characteristics from anatomical fractions of wheat stover. *Biomass and Bioenergy*, 31(8):585–592, 2007. 00027.

[13] A. Tolera, B. Tsegaye, and T. Berg. Effects of variety, cropping year, location and fertilizer application on nutritive value of durum wheat straw. *Journal of Animal Physiology and Animal Nutrition*, 92(2):121–130, 2008. 00008.

[14] E. R. (Rowett Research Inst Orskov. Consistency of differences in nutritive value of straw from different varieties in different seasons. ILCA, 1988. 00017.

[15] S. C. Rao. Regional environment and cultivar effects on the quality of wheat straw. *Agronomy journal*, 1989. 00007.

[16] Jane Lindedam, Sander Bruun, Henning Jørgensen, Stephen R. Decker, Geoffrey B. Turner, Jaclyn D. DeMartini, Charles E. Wyman, and Claus Felby. Evaluation of high throughput screening methods in picking up differences between cultivars of lignocellulosic biomass for ethanol production. *Biomass and Bioenergy*, 66:261–267, July 2014. 00004.

[17] G. W. Ohlde, K. Becker, D. E. Akin, L. L. Rigsby, and C. E. Lyon. Differences in rumen bacterial degradation of morphological fractions in eight cereal straws and the effect of digestion on different types of tissues and mechanical properties of straw stalks. *Animal Feed Science and Technology*, 36(3):173–186, March 1992. 00016.

[18] Z. L. Tan, H. P. Chen, L. H. He, R. J. Fang, and T. X. Xing. Variation in the nutritional characteristics of wheat straw. *Animal Feed Science and Technology*, 53(3):337–344, July 1995. 00027.

[19] Helena Oakey, Reza Shafiei, Jordi Comadran, Nicola Uzrek, Brian Cullis, Leonardo D. Gomez, Caragh Whitehead, Simon J. McQueen-Mason, Robbie Waugh, and Claire Halpin. Identification of crop cultivars with consistently high lignocellulosic sugar release requires the use of appropriate statistical design and modelling. *Biotechnology for Biofuels*, 6:185, 2013. 00004.

[20] Ritesh Mewalal, Eshchar Mizrachi, Shawn D. Mansfield, and Alexander A. Myburg. Cell Wall-Related Proteins of Unknown Function: Missing Links in Plant Cell Wall Development. *Plant and Cell Physiology*, 55(6):1031–1043, June 2014. 00006.

[21] Stephen R. Decker, Roman Brunecky, Melvin P. Tucker, Michael E. Himmel, and Michael J. Selig. High-Throughput Screening Techniques for Biomass Conversion. *BioEnergy Research*, 2(4):179, December 2009. 00082.

[22] Michael H. Studer, Jaclyn D. DeMartini, Simone Brethauer, Heather L. McKenzie, and Charles E. Wyman. Engineering of a high-throughput screening system to identify cellulosic biomass, pretreatments, and enzyme formulations that enhance sugar release. *Biotechnology and Bioengineering*, 105(2):231–238, February 2010. 00060.

[23] Nicholas Santoro, Shane L. Cantu, Carl-Erik Tornqvist, Tanya G. Falbel, Jenny L. Bolivar, Sara E. Patterson, Markus Pauly, and Jonathan D. Walton. A High-Throughput Platform for Screening Milligram Quantities of Plant Biomass for Lignocellulose Digestibility. *BioEnergy Research*, 3(1):93–102, January 2010. 00045.

[24] N. Dowe and J. McMillan. SSF Experimental Protocols—Lignocellulosic Biomass Hydrolysis and Fermentation. 2008. 00194.

[25] Charles E. Wyman, Bruce E. Dale, Richard T. Elander, Mark Holtzapple, Michael R. Ladisch, and Y. Y. Lee. Comparative sugar recovery data from laboratory scale application of leading pretreatment technologies to corn stover. *Bioresource Technology*, 96(18):2026–2032, 2005. 00482.

[26] Charles E. Wyman, Bruce E. Dale, Richard T. Elander, Mark Holtzapple, Michael R. Ladisch, and Y. Y. Lee. Coordinated development of leading biomass pretreatment technologies. *Bioresource Technology*, 96(18):1959–1966, 2005. 01231.

[27] Cliff E. Foster, Tina M. Martin, and Markus Pauly. Comprehensive Compositional Analysis of Plant Cell Walls (Lignocellulosic biomass) Part I: Lignin. *Journal of Visualized Experiments : JoVE*, (37), March 2010. 00000.

[28] R Core Team. *R: A Language and Environment for Statistical Computing*. R Foundation for Statistical Computing, Vienna, Austria, 2016. 49578.

[29] Felipe de Mendiburu. agricolae: Statistical Procedures for Agricultural Research, June 2016. 00314.

[30] Hadley Wickham. *ggplot2: Elegant Graphics for Data Analysis*. Springer-Verlag New York, 2009. 03217.

[31] John Fox, Sanford Weisberg, Daniel Adler, Douglas Bates, Gabriel Baud-Bovy, Steve Ellison, David Firth, Michael Friendly, Gregor Gorjanc, Spencer Graves, Richard Heiberger, Rafael Laboissiere, Georges Monette, Duncan Murdoch, Henric Nilsson, Derek Ogle, Brian Ripley, William Venables, David Winsemius, Achim Zeileis, and R-Core. car: Companion to Applied Regression, August 2016. 00017.

[32] Larry M. White, Glenn P. Hartman, and Jerald W. Bergman. In Vitro Digestibility, Crude Protein, and Phosphorus Content of Straw of Winter Wheat, Spring Wheat, Barley, and Oat Cultivars in Eastern Montana. *Agronomy Journal*, 73(1):117–121, 1981. 00084.

[33] A. Kleinhofs, A. Kilian, M. A. Saghai Maroof, R. M. Biyashev, P. Hayes, F. Q. Chen, N. Lapitan, A. Fenwick, T. K. Blake, V. Kanazin, E. Ananiev, L. Dahleen, D. Kudrna, J. Bollinger, S. J. Knapp, B. Liu, M. Sorrells, M. Heun, J. D. Franckowiak, D. Hoffman, R. Skadsen, and B. J. Steffenson. A molecular, isozyme and morphological map of the barley (Hordeum vulgare) genome. *Theoretical and Applied Genetics*, 86(6):705–712, July 1993. 00683.

[34] A. Tondelli, E. Francia, D. Barabaschi, A. Aprile, J. S. Skinner, E. J. Stockinger, A. M. Stanca, and N. Pecchioni. Mapping regulatory genes as candidates for cold and drought stress tolerance in barley. *Theoretical and Applied Genetics*, 112(3):445–454, November 2005. 00099.

[35] L. Arru, E. Francia, and N. Pecchioni. Isolate-specific QTLs of resistance to leaf stripe (Pyrenophora graminea) in the 'Steptoe' x 'Morex' spring barley cross. *Theoretical and applied genetics.*, 106(4):668–675, February 2003. 00000.

[36] Timothy J. Close, Prasanna R. Bhat, Stefano Lonardi, Yonghui Wu, Nils Rostoks, Luke Ramsay, Arnis Druka, Nils Stein, Jan T. Svensson, Steve Wanamaker, Serdar Bozdag, Mikeal L. Roose, Matthew J. Moscou, Shiaoman Chao, Rajeev K. Varshney, Péter Szucs, Kazuhiro Sato, Patrick M. Hayes, David E. Matthews, Andris Kleinhofs, Gary J. Muehlbauer, Joseph DeYoung, David F. Marshall, Kavitha Madishetty, Raymond D. Fenton, Pascal Condamine, Andreas Graner, and Robbie Waugh. Development and implementation of high-throughput SNP genotyping in barley. *BMC genomics*, 10:582, 2009. 00390.

[37] Shiaoman Chao, Wenjun Zhang, Jorge Dubcovsky, and Mark Sorrells. Evaluation of Genetic Diversity and Genome-wide Linkage Disequilibrium among U.S. Wheat (L.) Germplasm Representing Different Market Classes. *Crop Science*, 47(3):1018, 2007. 00125.

[38] J. Lindedam, S.B. Andersen, J. DeMartini, S. Bruun, H. Jørgensen, C. Felby, J. Magid, B. Yang, and C.E. Wyman. Cultivar variation and selection potential relevant to the production of cellulosic ethanol from wheat straw. *Biomass and Bioenergy*, 37(0):221–228, February 2012.

[39] G. Caruso, L. D. Gomez, F. Ferriello, A. Andolfi, C. Borgonuovo, A. Evidente, R. Simister, S. J. McQueen-Mason, D. Carputo, L. Frusciante, and M. R. Ercolano. Exploring tomato Solanum pennellii introgression lines for

residual biomass and enzymatic digestibility traits. *BMC Genetics*, 17:56, 2016. 00000.

[40] Fang Chen and Richard A. Dixon. Lignin modification improves fermentable sugar yields for biofuel production. *Nature Biotechnology*, 25(7):759–761, July 2007. 00769.

[41] Rebecca Van Acker, Ruben Vanholme, Véronique Storme, Jennifer C. Mortimer, Paul Dupree, and Wout Boerjan. Lignin biosynthesis perturbations affect secondary cell wall composition and saccharification yield in Arabidopsis thaliana. *Biotechnology for Biofuels*, 6:46, 2013. 00066.

[42] Andrea Bellucci, Anna Maria Torp, Sander Bruun, Jakob Magid, Sven B. Andersen, and Søren K. Rasmussen. Association Mapping in Scandinavian Winter Wheat for Yield, Plant Height, and Traits Important for Second-Generation Bioethanol Production. *Frontiers in Plant Science*, 6, November 2015. 00000.

[43] A. J. Travis, S. D. Murison, D. J. Hirst, K. C. Walker, and A. Chesson. Comparison of the anatomy and degradability of straw from varieties of wheat and barley that differ in susceptibility to lodging. *The Journal of Agricultural Science*, 127(1):1–10, August 1996.

[44] Ye Chen, Ratna R. Sharma-Shivappa, and Chengci Chen. Ensiling agricultural residues for bioethanol production. *Applied Biochemistry and Biotechnology*, 143(1):80–92, October 2007.

[45] Ye Chen, Ratna R. Sharma-Shivappa, Deepak Keshwani, and Chengci Chen. Potential of agricultural residues and hay for bioethanol production. *Applied Biochemistry and Biotechnology*, 142(3):276–290, September 2007.

[46] S. (Polska Akademia Nauk Jezowski. Variation correlation and heritability of characters determining lodging of spring barley (Hordeum vulgare L.). 2. Analysis of relationship between lodging grade and some morphological characters of spring barley varieties. *Polish Journal of Theoretical and Applied Genetics*, 1981. 00009.

[47] JP Tandon and KBL Jain. Relationship between lodging resistance and some morphological characters in barley, 1973. 00008.

[48] J. Brady. Some factors influencing lodging in cereals. *The Journal of Agricultural Science*, 24(02):209–232, 1934. 00048.

[49] C. Saint Pierre, R. Trethowan, and M. Reynolds. Stem solidness and its relationship to water-soluble carbohydrates: association with wheat yield under water deficit. *Functional Plant Biology*, 37(2):166–174, 2010. 00027.

Capítulo 3

HIGH-THROUGHPUT PHENOTYPING OF BIOETHANOL POTENTIAL IN CEREALS BY USING UAV-BASED MULTI-SPECTRAL IMAGERY

Published as:

Francisco J Ostos-Garrido, Ana I de Castro, Jorge Torres-Sánchez, Fernando Pistón, José M Peña. "High-throughput phenotyping of bioethanol potential in cereals by using UAV-based multi-spectral imagery." Front. Plant Sci. - Technical Advances in Plant Science. Under revision

---

3.1. Abstract:

Bioethanol production obtained from cereal straw has aroused great interest in recent years, which is leading to the development of breeding programs to improve the quality of lignocellulosic material in terms of biomass and sugar content. This process requires the analysis of genotype-phenotype relationships, and although genotyping tools are very advanced, the phenotypic tools are not usually capable of satisfying the needs of massive evaluation of potential characters for bioethanol production in field trials. However, the unmanned aerial vehicle (UAV) platforms are demonstrating their capacity for efficient and non-destructive acquisition of crop data with application to high-throughput phenotyping. This work shows the first evaluation of UAV-based multi-spectral images for estimating bioethanol-related variables (total biomass dry weight, sugar release and theoretical ethanol) of several accessions of wheat, barley and triticale (234 cereal plots in total). The full procedure involved several stages: 1) adquisition of multi-temporal UAV images with a six-band camera along different crop phenology stages (94, 104, 119, 130, 143, 161 and 175 days after sowing), 2) generation of ortho-mosaicked images of the full field experiment, 3) image analysis with an object-based (OBIA) algorithm and calculation of vegetation indices (VI), 4) statistical analysis of spectral data and bioethanol-related variables to predict a UAV-based ranking of cereal accessions in terms of theoretical ethanol. The high variability observed in the field trials was captured by the UAV-based system over time. Of the seven VI studied, the Near-infrared-based VIs were more appropriate to estimate crop

biomass, meanwhile the visible-based VIs were suitable for crop sugar release. The temporal factor was very relevant to achieve better estimations. The results obtained from single dates (i.e., temporal scenario 1, TS-1) were always lower than those obtained in TS-2 (i.e., averaging the values of each VI obtained during plant anthesis), mainly for estimating sugar release, and in TS-3 (i.e., averaging the values of each VI obtained during the full crop development), mainly for estimating crop biomass and theoretical ethanol. The Normalized Difference Vegetation Index (NDVI) reported the highest correlation in this study (R^2 of 0.66), which served to provide a ranking of cereal accessions in terms of theoretical ethanol.

3.2. Introduction

Nowadays the panorama in the area of fuel-based energy is complex due to the need of satisfying the progressive increase in demand of energy for an increasing world population and, simultaneously, attending to the concerns about the effect of CO_2 emissions in global Earth temperature [1]. This scenario, together to the technical concept recognized as "peak oil"by International Energy Agency [2], is producing a renewed interest in biomass recovery for energy consumption because the biomass is a renewable feedstock and a carbon neutral source of energy [3]. Two types of biofuels can be distinguished according to the different feedstock types. The first generation liquid biofuel is produced from cereals, sugar crops, and oilseeds, and the second generation liquid biofuel is produced from lignocellulosic feedstock [4]. Between the both types, second-generation biofuel is a more sustainable option because it is not in direct competition with food supply and, consequently, it does not push up food prices. Additionally, it produces lower greenhouse gases emission and better water and land uses [5]. The process of biofuels production could be improved in terms of productivity, efficiency and cost reduction by using two powerful tools named classical breeding and biotechnology, and in both cases, by analyzing the genotype-phenotype relationships. Genotyping tools have been deeply investigated in the last 20 years and have led to a better understanding of plant genome through DNA sequencing and molecular technologies. On the contrary, that has not happened with the phenotyping tools, which have been usually unable to satisfy the greatest number of technical requirements at high perfor-

mance and speed, low price, and nondestructively [6]. However, in recent years, new high-throughput phenotyping platforms are undergoing a rapid evolution that could significantly improve understanding between the association between genes and phenotype [7–9]. These platforms for phenotyping are capable of generating large quantities of data quickly and give the opportunity to evaluate plants in controlled greenhouse conditions and in the actual field conditions. On the one hand, the Plant Accelerator, GROWSCREEN-Rhizo and Phenoscope are three examples of greenhouse-based phenotyping platforms that are being used for plant breeding programs in Australia, Germany and France, respectively [10–12]. On the other hand, several high-throughput platforms had been developed for non-destructive plant data collection under field conditions, as example, tractor-mounted platforms [13, 14], cable-driven platform [15], aerial vehicles [16, 17], and portable or pushed platforms [18–20], among others [6, 9]. In the specific case of cereals, some of these high-throughput sensor-based techniques have been applied, e.g., for assessing salt-tolerance in Triticum [21], drought-tolerance in barley [22] and maize [23], biomass and plant height in barley [24], triticale [25] and sorghum [26], growth status in wheat [27], and seedling emergence and spring stand in winter wheat [28]. However, to our knowledge, there are no works in which image-based technologies were used to make bioethanol potential evaluations on cereals under field conditions. In this specific case, cultivation of cereals with the dual fitness of providing the grains for food and the crop residues for bioethanol production has been the subject of many investigations, in which the main interest lies in obtain organic residues with cell walls more easily degradable by the enzymes, without compromising the grain yield [29, 30]. In recent years, unmanned aerial vehicles (UAVs) are taking relevance as a tool for phenotyping because of some advantages compared to other platforms [31]. UAVs are a low-cost and reliable method for taking remote images by using global positioning and inertial navigation systems, which allows frequent field observations to capture the variation of plant traits over time [32]. Furthermore, the capacities of the UAV to use a wide range of sensors and to operate at low flight altitude provide high-resolution spatial and spectral information of the studied plants. Based on the knowledge of phenotypes related to bioethanol potential and on the capability of the UAVs to collect high-resolution images of the field trials, a UAV-based phenotyping system was developed and tested on a multi-temporal field experiment composed of sixty-six genotypes belonging to several species of cereal crops. Firstly, this work describes

the full protocol to collect the remote images with a multi-spectral camera and to analyze the images by using a customized object-based image analysis (OBIA) algorithm. Then, comparison of multi-temporal UAV-based data and on-ground measurements of the crop trials allowed to determine the correlation between image spectral information in the visible and near-infrared spectrum regions (by focusing to specific vegetation indices) and three primary variables related to bioethanol potential (i.e., total biomass dry weight, sugar release and theoretical ethanol) as affected by species and several temporal scenarios (TS). The final target of the UAV-based phenotyping system was to provide a ranking of accessions in terms of bioethanol potential with value for facilitating the decision making process in the context of plant breeding programs.

3.3. Materials and Methods

Field trial and plant material

A field trial with sixty-six accessions belonging to the species *Hordeum vulgare* L. (barley, 21 accessions), *Triticum aestivum* L. (bread wheat, 24 accessions), *Triticum durum* L. (durum wheat, 11 accessions) and X *Triticosecale* Wittmack (triticale, a hybrid of wheat and rye, 10 accessions) was established at the experimental station of the Institute for Sustainable Agriculture Center in Cordoba, Spain (Table 3.1).

The experiment was sown on 15th November 2013 following a completely randomized block design with three replications. The field trial design was generated with the statistical software **R** version 3.3.1 [33] and its function design.rcbd [34]. Each block counted in 78 plots (66 accessions and 12 control plots) distributed in ten rows, with an inter-plot distance of 30 cm and inter-row distance of 50cm. Each plot included four plants at approximately 15cm apart (Fig 3.1). The crop was under irrigation localized system and the experiment was covered with netting for protecting insect and birds during the growing months.

Specie	ID	Accession name (a)	Accession number
T. aestivum	Anza	Anza *	NA
	BW	BobWhite *	NA
	Peri	Perico *	NA
	TP2	UC1110 **	GSTR 13501
	TP3	OS9A **	PI658243
	TP4	QCB 36 **	PI658244

Specie	ID	Accession name (a)	Accession number
	TP5	Opata 85 **	PI591776
	TP6	Cayuga **	PI595848
	TP7	Caledonia **	PI610188
	TP8	CIGM90.248 **	PI610750
	TP10	P91193 **	GSTR 10001
	TP11	P92201 **	GSTR 10002
	TP16	TAM107-R7 **	GSTR 11601
	TP17	SS550 **	GSTR 12501
	TP21	M6 **	PI83534
	TP22	Kanqueen **	PI401539
	TP24	Avocet **	PI464644
	TP25	Penawawa **	PI495916
	TP27	Renan **	PI564569
	TP28	Excalibur **	PI572701
	TP29	McNeal **	PI574642
	TP30	Thatcher **	CItr 10003
	TP31	Jaypee **	PI592760
	TP32	USG 3209 **	PI617055
	TP33	Caledonia **	PI610188
	TP34	Cayuga **	PI595848
T. durum	TP1	IDO444 **	GSTR 12902
	TP9	UC1113 Yr36 Gpc-B1 **	PI638741
	TP12	Grandin*5/ND614-A **	GSTR 10401
	TP13	NY18/Clark's Cream 40-1 **	GSTR 10402
	TP14	Jupateco 73S **	GSTR 10501
	TP15	CO940610 **	GSTR 10702
	TP18	Amadina **	GSTR 12701
	TP19	Weebill 1 **	GSTR 10502
	TP20	Rugby **	CItr 17284
	TP23	Avalon **	PI446910
	TP26	Rio Blanco **	PI531244
H. vulgare	CP1	Vada **	PI280422
	CP2	Clipper **	PI349366
	CP3	Ko A **	PI383935

Specie	ID	Accession name (a)	Accession number
	CP4	Igri **	PI406263
	CP5	Mokusekko 3 **	PI420938
	CP6	Dicktoo **	CIho 5529
	CP7	L94 **	CIho 11797
	CP8	Fredrickson **	CIho 13647
	CP9	Steptoe **	CIho 15229
	CP10	Morex **	Ciho 15773
	CP11	Lina **	PI584808
	CP12	Apex **	PI600966
	CP13	OWB dominant **	GSHO3450
	CP14	OWB recessive **	GSHO3451
	CP16	Golden Promise **	PI467829
	CP17	Cebada Capa **	PI539113
	CP18	Stander **	PI564743
	CP19	Franklin **	PI373729
	CP20	Franka **	PI574293
	CP21	Azumamugi ***	J698
	CP22	Kanto Nakate Gold ***	J518
X *Triticosecale*	TS43	Rahum **	PI422269
	TS45	Zebra **	PI429031
	TS51	Kramer **	PI476216
	TS53	Currency **	PI483066
	TS58	Wapiti **	PI511870
	TS61	Yoreme Tehuacan 75 **	PI519876
	TS67	Navojoa **	PI520421
	TS75	Drira **	PI520478
	TS78	Juanillo 95 **	PI520488
	TS97	Armadillo 130 **	PI583701

Table 3.1: Plant material used in this work. More information on the genotypes can be found at https://npgsweb.ars-grin.gov/gringlobal/search.aspx.
(a) Plant material availability:
* IAS-CSIC;
** USDA-ARS, National Small Grains Germplasm Research Facility, Aberdeen, ID 83210, USA.;
*** Barley and Wild Plant Resource Center. Institute of Plant Science and Resources. Okayama University, Kurashiki, 710-0046, Japan.

The *T. aestivum* accessions Perico, Anza, and Bobwhite were used as field and laboratory controls. These genotypes are normally used in our trials as we are well aware of their phenological characteristics. The Cayuga and Caledonia accessions were planted in duplicate because we had two replicates with different acquisition dates. Plant material was obtained from the USDA-ARS National Small Grain Collection (http://www.ars.usda.gov/) or from the Barley and Wild Plant Resource Center at Okayama University (http: // Earth, Lab.nig.ac.jp). When available, the accessions used as parental lines in the cartographic populations were selected according to a double criterion: 1) to allow the identification of suitable cartographic populations to study the genetic basis of saccharification, and 2) to have a fair representation of the available variability in each species, since parental lines are normally selected to be as divergent as possible.

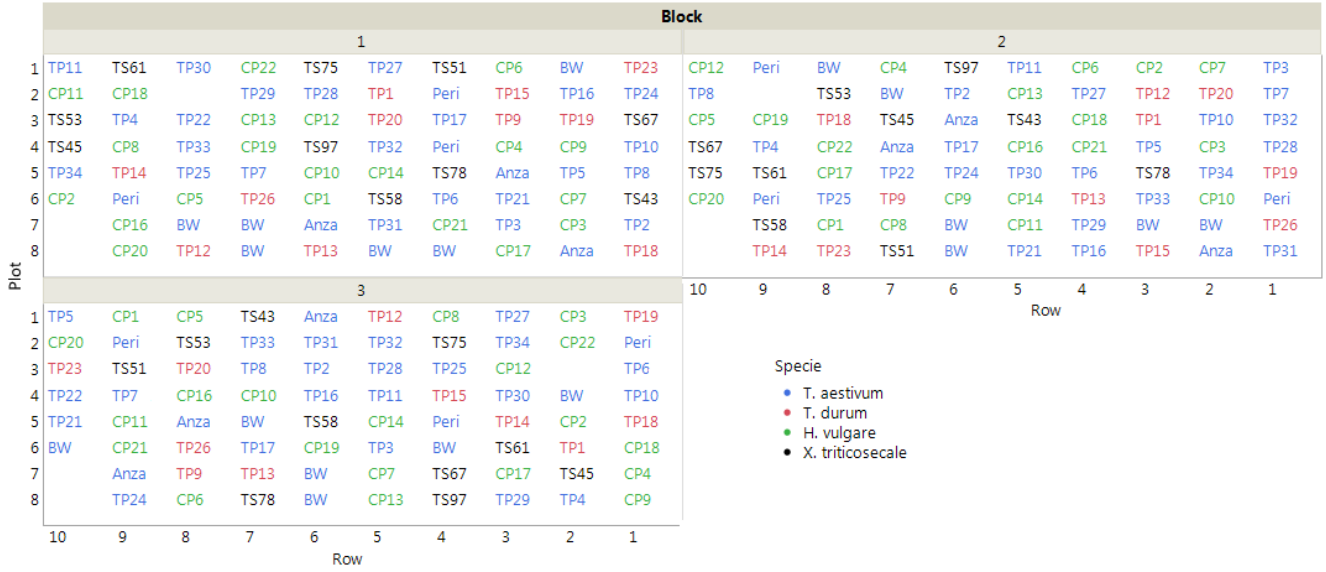

Figure 3.1: The layout of the field trial (plot IDs correspond to the accessions listed in Table 3.1). The empty plots were not considered in the evaluation due to errors committed in plant identification.

UAV-based phenotyping system

A quadrocopter UAV model md4-1000 (microdrones GmbH, Siegen, Germany) was used to collect the multi-temporal set of aerial images (Fig 3.2). The whole system consists of the vehicle, the radio control transmitter, a ground station with the software for mission planning and flight control, a telemetry system, and the camera or sensor embedded in the UAV. In this experiment, a six-band Tetracam camera, model mini-MCA-6 (Tetracam Inc., Chatsworth, CA, USA) was used to collect the multi-spectral images. This camera collected six individual images at B (450*nm*), G (530*nm*), R (670*nm*), R edge (700*nm*) and near-infrared (NIR, 740 and 780*nm*) by using its user configurable bandpass filters (Andover Corporation, Salem, NH, USA) of 10-*nm* full-width at half-maximum. These bandwidth filters were selected across the visible and NIR regions with regard to well-known biophysical indices developed for vegetation monitoring [35].

Figure 3.2: The UAV with the multi-spectral camera flying towards the experimental field on the 7th date (175 DAS)

The UAV system collected the remote images of the experimental field on seven different dates: 1) 17 February (94 days after sowing, DAS), 2) 27 February (104 DAS), 3) 14 March (119 DAS), 4) 25 March (130 DAS), 5) 7 April (143 DAS), 6) 25 April (161 DAS), and 7) 9 May (175 DAS). The UAV route was configured for flight at 3 m/s and at 10 m flight altitude over the ground, and for taking

down-facing photos at an interval of 1s to achieve a side overlap of 60 % and a forward overlap of 90 %. At this flight altitude, the spatial resolution of the multi-spectral images was 5.41 mm/pixel of ground sampling distance. Next, the set of UAV images were processed with the Agisoft PhotoScan Professional software, version 1.2.4 build 2399 (Agisoft LLC, St. Petersburg, Russia) to generate the ortho-mosaicked images of the experimental field at each study date (Fig 3.3).

The ortho-mosaicked images enabled visual identification of each one of the 234 trial plots, which were manually defined over the image and saved as a vector file. Then, a customized algorithm was created with the eCognition Developer software (Trimble GeoS-patial, Munich, Germany) to analyze the images of each studied date by using an object-based approach after image segmentation [36]. The algorithm was specifically programmed to run in a fully automatic manner without the need for user intervention, and with the ability to sequentially discriminate the vegetation fraction of every trial plot over time by applying the Otsu thresholding method described in [37]. Once the crop objects were classified in each plot, the algorithm computed the central coordinates and relative position of every plot within the experiment design (row, order in the row and block), the crop spectral values from the multi-spectral camera and a list of crop-related vegetation indices (VIs), grouped into VIs computed from bands in the visible spectrum region (referred to as visible-based VIs) and VIs that included the NIR band (referred to as NIR-based VIs) Table 3.2. Finally, the customized algorithm automatically exported all the trial plot data as a table file (e.g., CSV or ASCII format) for further descriptive and statistical analysis.

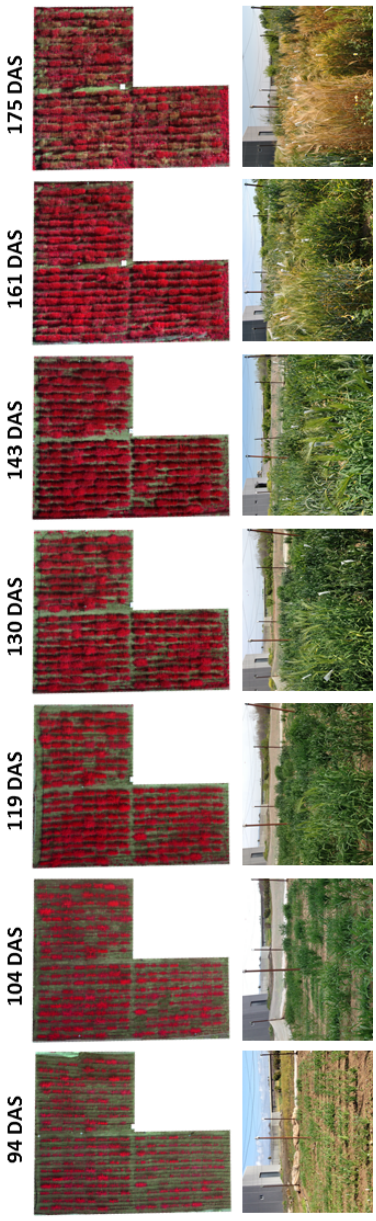

Figure 3.3: UAV-based ortho-mosaicked images in color-infrared of the experimental field over time. DAS: Days After Sowing.

Manual measurements of plant phenotypic data

In order to evaluate the UAV-based assessments, total biomass dry weight (kg/m^2) and sugar release (µl/mg), which are two crop variables particularly related to bioethanol potential from lignocellulosic biomass, were determined in each trail plot after harvest. Biomass was measured as weight for complete plant (spike, stem and leaves) and sugar release was obtained by using a suitable method of saccharification. Assays to determine saccharification involved three main steps: pretreatment, hydrolysis and sugar detection. Firstly, 20 mg of ground straw were loaded into 2 mL screw-cap tubes. In pretreatment solution was used a volume of 1.5 mL of NaOH (6.25 mM) and incubated at 90ºC for 3 h in a water bath, and then cooled on ice. Enzymatic hydrolysis was performed using 0.05µL of enzyme cocktail with a 4:1 ratio of Celluclast - Novozyme 188 (Novozymes, Bagsværd, Denmark) for 1 straw mg dry weight (dw). Hydrolysis was performed during 20 h with constant shaking, at 50 ºC in a 0.5 M sodium citrate buffer at pH 4.5. The determination of sugars released after hydrolysis was carried out using the glucose oxidase/peroxidase (GOPOD) assay kit (Megazyme International Ireland, Bray, Ireland). The assay volumes were reduced to allow the procedure to be performed in 96-well ELISA plates. In every plate we include solution blanks, enzime blancks, glucose standards used in the calibration curve as an internal control for the reaction, and eight technical repetition leaving 76 wells free for the samples. These eight samples were formed by eight different genotypes. The used genotypes were randomly selected except for the controls Anza, Bobwhite and Perico that were chosen because their glucose releases were previously known. Determination was performed using 8µL of the digestion reaction mixture and 240µL of the GOPOD assay reagent followed by incubation at 50ºC during 20 min. The yield of glucose was analyzed using 96 well plates. Absorbance readings were determined at 490 nm in a BioTek ELx800 Absorbance Microplate Reader (BioTek Instruments, Inc., Winooski, VT-USA). After determining total biomass and sugar release, the theoretical ethanol yield was calculated considering the total biomass conversion per surface area unit (ha) according to the National Renewable Energy Laboratory Standards [38], as follows 3.1:

$$\text{Theoretical ethanol(L/ha)} = \frac{\text{Sugar/release (µL/mg)} \cdot 0{,}511 \cdot \text{Biomass (kg/ha)}}{1000} \tag{3.1}$$

In addition, other data were also accounted throughout the experiment: 1) the plant heights on the same days on which the UAV flights were performed, 2) starting and ending dates of plant anthesis, as well as dates of plant and spikes emergences, 3) damages due to pests and diseases, specifically stem rust and barley yellow dwarf (BYD) virus, as well as the ones provoked by birds and rodents.

Data analysis

Data analysis was conducted with the statistical software JMP version 10 software (SAS Institute Inc., Cary, NC, USA). Firstly, variability of plant phenotypic data was studied by using analysis of the variance (ANOVA). Next, capability of the UAV-based phenotyping system to predict bioethanol potential was studied by analyzing the degree of correlation (in terms of coefficient of determination, R2) of the multi-temporal UAV-based VIs with total biomass dry weight, sugar release, and theoretical ethanol. These correlations were determined in several temporal scenarios, as follows: 1) on each single date of the seven UAV flights (TS-1), 2) averaging the values of each VI obtained during plant anthesis (TS-2), and 3) averaging the values of each VI obtained during the full crop development (TS-3). TS-2 was proposed because anthesis is a critical period for cereal grain filling, which could also have an influence on plant biomass accumulation and sugar left in the stems [39, 40] and, hypothetically, increase the spectral differences between the studied accessions. Finally, the VI and TS that reported the highest coefficient of determination was adjusted to a lineal model, which allowed ranking the plant accessions in terms of theoretical ethanol.

3.4. Results

Variability of plant phenotypic data

All cultivars were well adapted to Mediterranean climate conditions, which were favorable for low incidence of pests and diseases during the growing-season in the studied campaign. The studied varieties were hardly affected by stem rust or barley yellow dwarf (BYD) virus, and only occasional bird attacks of moderate importance were accounted. Given the multitude of screened genotypes, many different phenotypes were observed in the study trail plots in terms of plant anthesis, plant heights, total biomass dry weight, sugar release and theoretical ethanol 3.4, which suggested high potential for ranking the observed phenotypes. The earliest plant anthesis started in the *T. durum* TP14 (Jupateco 73S) and the *T. aestivum*

Spectral Region and Vegetantion Index (VI)	*Equation**	Reference
Visible		
Excess Green (ExG)	$2 \cdot G - R_1 - B$	[41]
Green VI (VIgreen)	$\frac{(G - R_1)}{G + R_1}$	[42]
Triangular Chlorophyll Index (TCI)	$1{,}2 \cdot (R_2 - G) - 1{,}5 \cdot (R_1 - G) \cdot \sqrt{\frac{R_2}{R_1}}$	[43]
Visible & NIR		
Normalized Difference VI (NDVI)	$\frac{(NIR_1 - R_2)}{(NIR_1 + R_2)}$	[44]
Green NDVI (GNDVI)	$\frac{(NIR_2 - G)}{(NIR_2 + G)}$	[45]
Modified Chlorophyll Absorption in Reflectance Index (MCARI)	$[(NIR_1 - R2) - 0{,}2 \cdot (NIR_1 - G)] \cdot \frac{NIR_1}{R_2}$	[46]
Modified Simple Ratio (MSR)	$\frac{\frac{NIR_1}{R_2} - 1}{\sqrt{\frac{NIR_1}{R_2}} + 1}$	[47]

* Reflectance (%) at central wavelengths: B = 480nm (blue region); G = 530nm (green region); R_1 = 670nm (red region); R_2 = 700nm (Red-edge region); NIR_1 = 740nm (NIR region); NIR_2 = 780nm (NIR region)

Table 3.2: Crop-based vegetation indices computed in every trial plot.

TP5 (Opata 85) accessions at 110 and 112 DAS, respectively, and the latest plant anthesis started 160 DAS in the *T. durum* TP23 (Avalon), the T. *aestivum* TP34 (Cayuga) and the *T. aestivum* TP27 (Renan) accessions. The early anthesis date of some accessions could be due to a short duration of their vegetative stage (Jamieson et al., 1998), which might have produced a fewer number of leaf primordia that resulted in lower sink capacity and a decrease in biomass accumulation during the pre-anthesis period (Giunta et al., 1999). This was partially observed at the level of cereal species, in which the average dates of anthesis and total biomass of X *Triticosecale* were significantly lower in comparison with the average values of the other three species studied. The plants height was a highly variable factor among genotypes over time. The average plant heights collected on ground along the crop development ranked from minimum values of 38 – 40 cms in the cases of the *H. vulgare* CP20 (Franka), the *T. durum* TP23 (Avalon) and the *T. aestivum* TP27 (Renan) accessions, to maximum values of 92 – 99 cms in the cases of the X *Triticosecale* TS58 (Wapiti) and TS78 (Juanillo 95) and the *T. durum* TP20 (Rugby) accessions. At the level of cereal species, average heights of *T. aestivum* and X *Triticosecale* (62.24 cm and 80.93 cm, respectively) were significantly smaller and higher, respectively, than the other species, while *H. vulgare* and *T. durum* did not show significant differences in average plant heights (65.90 cm and 69.87 cm, respectively). Regarding the bioethanol-related variables, the values of total biomass ranked from 0.26 – 0.29 kg/m^2 measured in the X *Triticosecale* TS67 (Navojoa) and TS45 (Zebra) accessions, respectively, to 1.31 – 1.40 kg/m^2 measured in the *H. vulgare* CP19 (Franklin) and the *T. durum* TP1 (IDO444) accessions, respectively, the values of sugar release ranked from 0.77 µL/mg measured in the *T. durum* TP26 (Cayuga) and BW (Bobwhite) accessions to 1.35 – 1.36 µL/mg measured in the *H. vulgare* CP9 (Steptoe) and CP14 (Oregon wolfe barley recessive) accessions, respectively, and the values of theoretical ethanol ranked from 1.18 m^3/ha obtanied in the X *Triticosecale* TS67 (Navojoa) accession to 7.60 m^3/ha obtained in the *T. durum* TP1 (IDO444) accessions.

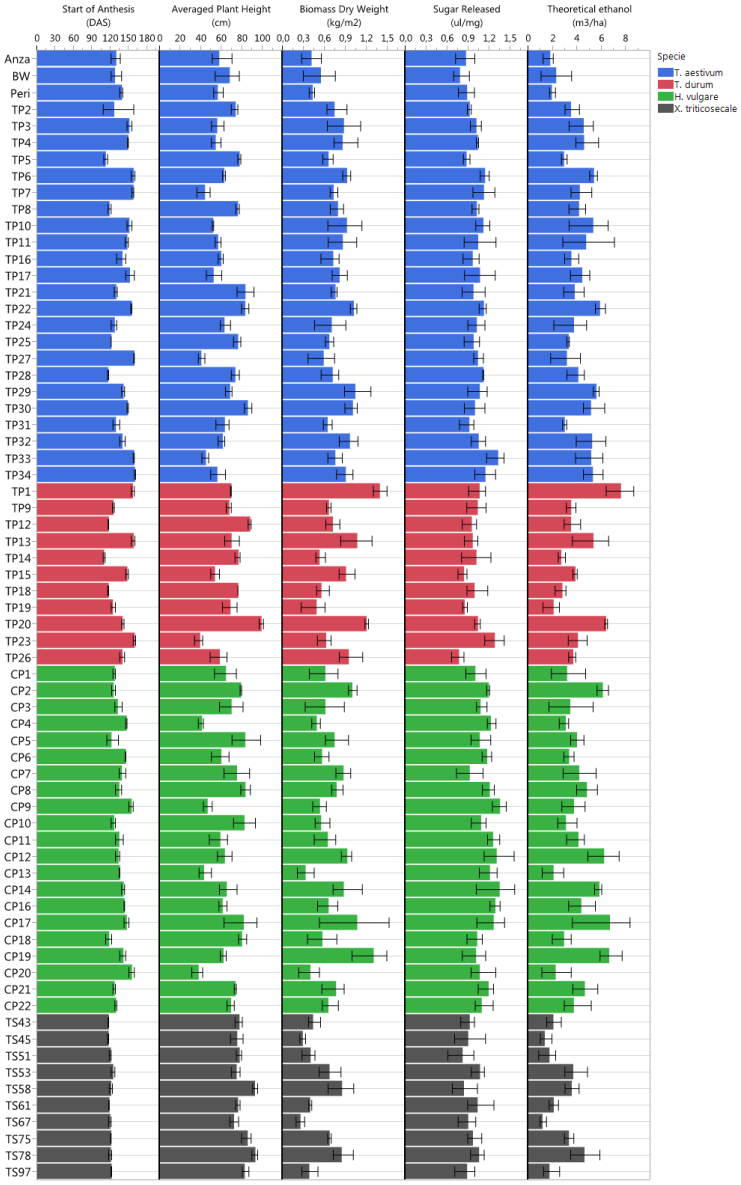

Figure 3.4: Plant phenotyping variability observed in the study trail plots in terms of start of plant anthesis (in Days after Sowing, DAS), plant height, total biomass dry weight, sugar release, and theoretical ethanol.

Variability of vegetation index (VI) values over time

The VI values were automatically retrieved from the multi-spectral images collected at each UAV flight and applying the customized OBIA procedure developed in this investigation. As example, the figure 3.5 shows the progress of the three

VIs (i.e., ExG, NDVI and GNDVI) that produced better results in predicting some of the bioethanol-related variables (see below the table 3.4). The ExG values varied from a minimum of 0.14 of the *T. aestivum* Anza measured at the first date (94 DAS) to a maximum of 0.73 of the *H. vulgare* CP7 (L94) and CP14 (OWB recessive) at the last date (175 DAS). The NDVI values varied from a minimum of 0.36 of the *T. aestivum* BW (BobWhite) measured at the first date (94 DAS) to a maximum of 0.84 of the *H. vulgare* CP8 (Fredrickson) and CP11 (Lina) at the fourth date (130 DAS). The GNDVI values varied from a minimum of 0.38 of the *T. aestivum* BW (BobWhite) measured at the first date (94 DAS) and the *H. vulgare* CP5 (Mokusekko 3) and the X *Triticosecale* TS67 (Navojoa) at the last date (175 DAS) to a maximum value of 0.72 of the *T. aestivum* TP30 (Thatcher) at the 6th date (161 DAS).

A detailed analysis of the variation of each VI over time confirmed that two different spectral patterns were observed (Fig 3.6). On the one hand, the visible-based VIs (i.e. ExG, VIgreen and TCI) generally followed a horizontal trend, characterized by minor variations from date 1 (94 DAS) to date 6 (161 DAS), but with a marked increase in the last date (175 DAS), mostly pronounced in the species *T. aestivum*, *T. durum* and X *Triticosecale*. The spectral profiles of these three species was analogous in the three visible-based VIs studied, although the mean values of the two Triticum species were slightly higher than those of X *Triticosecale* species between the date 2 (104 DAS) and 6 (161 DAS), but all three species showed significantly lower values than those of *H. vulgare* species on all the studied dates. On the other hand, the values of the NIR-based VIs (i.e. NDVI, GNDVI, MSR and MCARI) generally described a bell-shaped curve. Depending on the accession considered, the maximum values were mostly around the 4^{th} (130 DAS), 5^{th} (143 DAS) or 6^{th} (161 DAS) dates, while the values of the previous dates progressed increasingly and those of the following dates declined away from the maximum, some accessions even reaching values in the last date close to those obtained at the earliest dates of the study. In this case, the lowest average values were always for X *Triticosecale* species at all dates studied, while the highest values were observed for *H. vulgare* species up to the 5th date (143 DAS) for GNDVI and MSR and up to the 6th date (161 DAS) for NDVI and MCARI, while from these dates onward, the maximum average values for these four NIR-based VIs were reached for *T. durum* species followed by *T. aestivum* species. This turning point corresponded to cereal anthesis in most species, which suggested us to pay special attention to

the UAV images taken during the anthesis period.

Performance of UAV-based vegetation indices to predict bioethanol-related variables

Simple linear regression analysis showed the degree of correlation (in terms of coefficient of determination, R^2) between the VIs and crop total biomass dry weight, sugar release and theoretical ethanol (Table 3.3), which may indicate the ability of the UAV-based system to predict bioethanol potential of the studied cereals. Of the seven dates studied in our experiment, we observed that correlations were generally higher during anthesis of each accession, hence our proposal to study the three temporal scenarios described in "Data analisys" sub-section. For the interpretation of the results, correlations were considered hereafter as low (R^2 <0.50), moderate (0.50 $\leq$ R^2 <0.60) and high ($R^2 \geq 0.60$).

The NIR-based VIs showed better correlation with crop total biomass dry weight than the visible-based VIs for all dates and TS considered, although no high R^2 values were obtained in any case. On single dates (TS-1), moderate correlations were found only on the 6th date (161 DAS), with R^2 values of 0.50 and 0.51 for NDVI and GNDVI, respectively, while the correlations on the other dates were low. The NDVI and GNDVI reported slightly better results in the TS-2 (i.e., averaged VI values during plant anthesis), with R^2 values of 0.54 and 0.57, respectively, and even better in the TS-3 (i.e., averaged VI values during the full crop development), with R^2 values of 0.58 and 0.59, respectively. Moderate correlations were also obtained with MSR in the TS-2 and TS-3 (with R^2 values of 0.52 and 0.56, respectively), and with MCARI in TS-3 (R^2 of 0.58). Regarding the visible-based VIs, correlations were low in all cases, with maximum values of 0.33 and 0.37 obtained with TCI on the last date (175 DAS) and in TS-3, respectively.

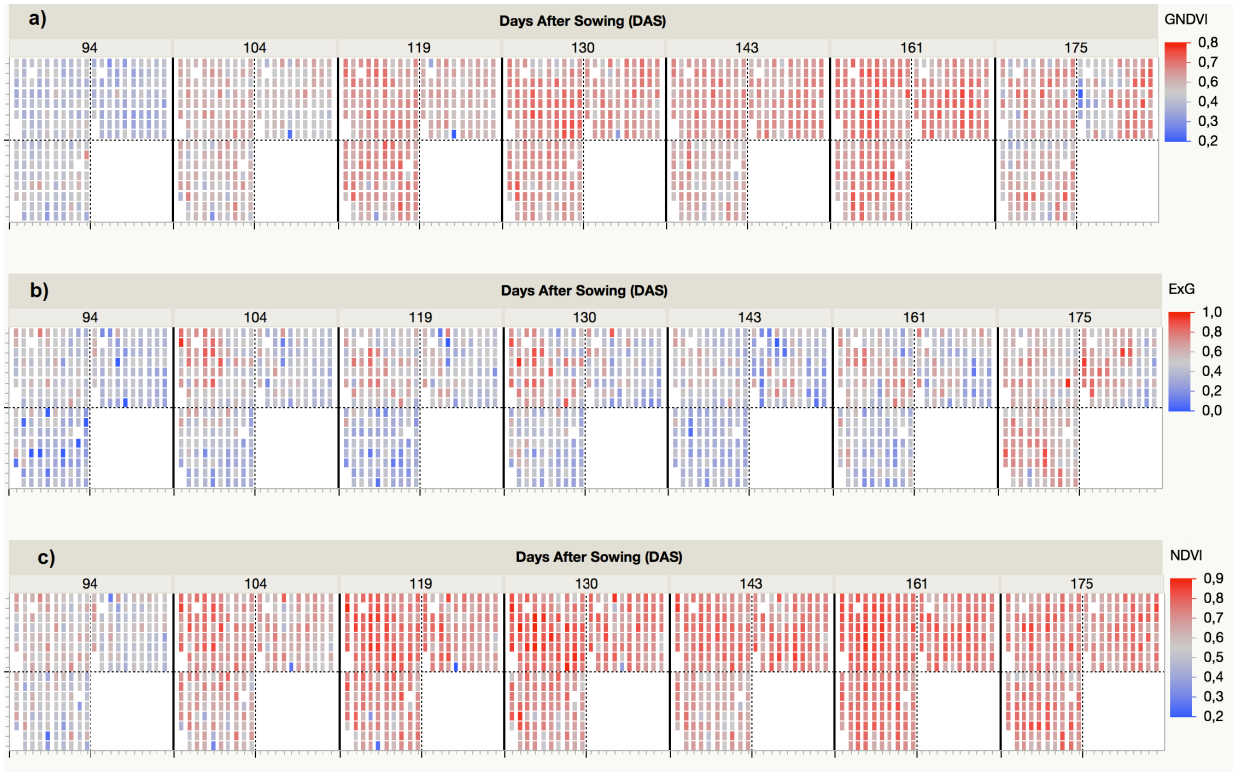

Figure 3.5: Spectral variability of three selected vegetation indices measured by the UAV-based phenotyping system over time: a) ExG, b) NDVI, c) GNDVI.

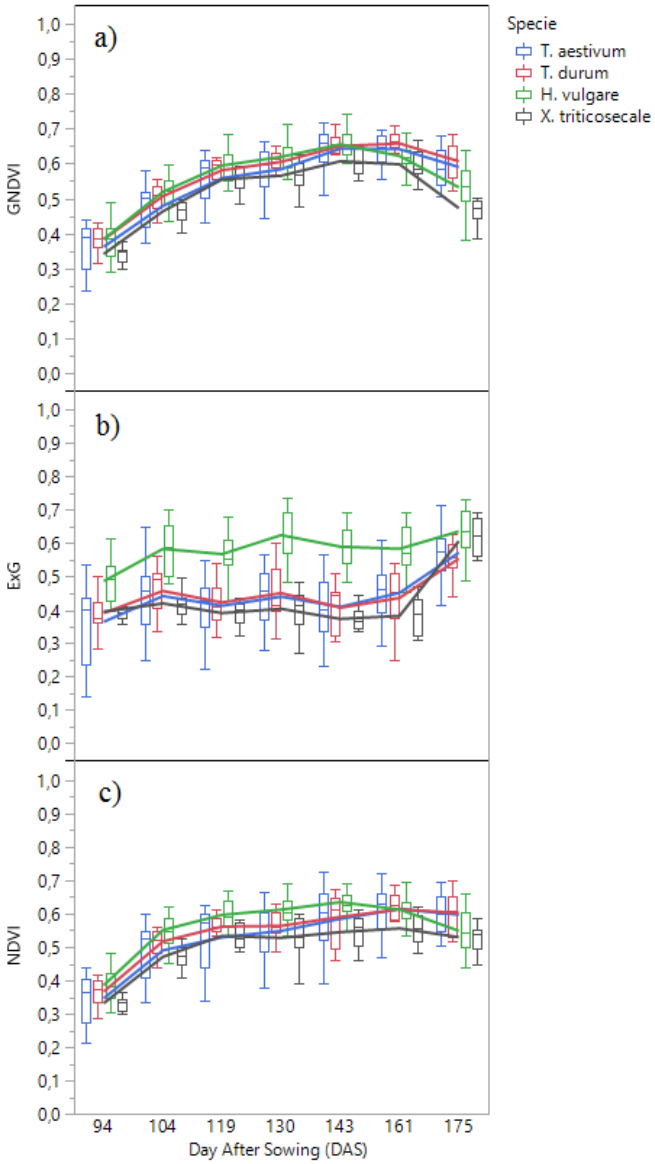

Figure 3.6: Temporal profile of three selected vegetation indices as affected by cereal species: a) ExG, b) NDVI, c) GNDV.

Bioethanol related variable	Single dates, in DAS (TS-1)							Combined dates	
Vegetation Index	94	104	119	130	143	161	175	On anthesis (TS-2)	Full crop development (TS-3)
Total Biomass									
Visible									
- ExG	0.18*	**0.22***	0.16*	0.15*	0.11			0.16*	0.17
- VIgreen	0.19*	**0.23***	0.16*	0.19*	0.14*	0.27*		0.22*	**0.23***
- TCI	0.29*	0.30*	0.25*	0.17*	0.21*	0.15	0.33*	0.19	**0.37***
Visible & NIR									
- NDVI	0.41*	0.41*	0.40*	0.35*	0.45*	0.50*	0.34*	0.54*	**0.58***
- GNDVI	0.40*	0.40*	0.40*	0.39*	0.49*	0.51*	0.35*	0.57*	**0.59***
- MCARI	0.39*	0.39*	0.41*	0.39*	0.47*	0.48*	0.40*	0.41*	**0.58***
- MSR	0.30*	0.32*	0.37*	0.35*	0.40*	0.41*	0.41*	0.52*	**0.56***
Sugar release									
Visible									
- ExG	0.29*	0.43*	0.45*	0.48*	0.47*	0.39*		**0.57***	0.51*
VIgreen	0.28*	0.42*	0.43*	0.46*	0.46*	0.36*		0.52*	**0.48***
- TCI	0.18*	0.44*	0.47*	0.43*	0.39*	0.32*	0.12	**0.52***	0.48*
Visible & NIR									
- NDVI	0.18*	0.41*	0.42*	**0.45***	**0.45***	0.24*		0.34*	**0.44***
- GNDVI	0.17*	0.28*	**0.26***	**0.26***	0.25*			0.20	0.23*
- MCARI	0.16*	0.35*	0.33*	0.37*	**0.45***	0.17*		0.37*	0.39*
- MSR	0.13	0.29*	0.31*	0.32*	**0.45***	0.22*		0.25*	0.39*
Theoretical ethanol									
Visible									
- ExG	0.26*	**0.35***	0.28*	0.27*	0.24*	0.21*		0.32*	0.32*
- VIgreen	0.27*	0.36*	0.28*	0.32*	0.27*	**0.39***		0.37*	0.37*
- TCI	0.36*	0.42*	0.37*	0.27*	0.32*	0.27*	0.33*	0.34*	**0.51***
Visible & NIR									
- NDVI	0.46*	0.51*	0.48*	0.46*	0.54*	0.55*	0.34*	0.62*	**0.66***
- GNDVI	0.43*	0.47*	0.45*	0.45*	0.53*	0.45*	0.28*	0.58*	**0.61***
- MCARI	0.45*	0.50*	0.50*	0.48*	0.54*	0.49*	0.35*	0.53*	**0.65***
- MSR	0.37*	0.42*	0.48*	0.44*	0.52*	0.48*	0.37*	0.57*	**0.65***

Table 3.3: The coefficient of determination (R^2) of the linear relationship between the studied vegetation indices and crop total biomass dry weight, sugar release and theoretical ethanol as affected by the three temporal scenarios (TS) studied. Significant R^2 values at p≤0.001 are marked with an asterisk, while insignificant R^2 values are not shown. White, grey and black cells indicate low (R^2 <0.50), moderate (0.50 R^2 <0.60) and high ($R^2 \leq 0.60$) correlations, respectively. The bold numbers and the underlined numbers enphasize the best result of each VI and each TS, respectively.

However, the results differed when studying the linear relationship of the VIs to sugar release. In this case, the highest correlations were obtained with the visible-based VIs in all the TS considered, with moderate R^2 values ranging from 0.52 (VIgreen and TCI) to 0.57 (ExG) in the TS-2, and with a R^2 value of 0.51 obtanied with ExG in the TS-3. For the rest of the cases, the correlations were low, although the visible-based VIs obtained higher R^2 values than the NIR-based VIs on all the single dates studied, in particular ExG on the 4th (130 DAS) and 5th (143 DAS) dates (R^2 of 0.48 and 0.47, respectively) and TCI on the 2^{nd} (104 DAS) and 3^{th} (119 DAS) dates (R^2 of 0.44 and 0.47, respectively). Regarding the prediction of theoretical ethanol, high correlations were obtained with the four NIR-based VIs in TS-3, with R^2 values between 0.61 (GNDVI) and 0.66 (NDVI). The NDVI also obtained a high correlation with theoretical ethanol in TS-2 (R^2 of 0.62), while the better correlations in the singles dates were obtained with NDVI on the 6^{th} (161 DAS) date (R^2 of 0.55) and with the four NIR-based indices on the 5^{th} (143 DAS) date (R^2 ranged from 0.52 to 0.54). On the contrary, the visible-based indices obtained low correlations in almost all the TS studied, except TCI that obtained a moderate correlation (R^2 of 0.51) with theoretical ethanol in TS-3. At the level of cereal species, ordering and significant values reported for the selected VIs and the three bioethanol-related variables were equal (table 3.4). *T. durum* had significantly higher average values than the other screened species for the factors GNDVI (0.57) and total biomass (0.83 kg/m^2), while *H. vulgare* was significantly higher for the factors ExG (0.59) and sugar release (1.16 µL/mg). Both species obtained significantly higher mean values of NDVI (0.54 and 0.56, respectively) and theoretical ethanol (4.14 m^3/ha and 4.21 m^3/ha, respectively) than *T. aestivum* and X *Triticosecale*. In all the factors, X *Triticosecale* showed significant lowest mean values than the other species, which confirmed the good performance of the selected VIs to predict a ranking of cereal species in terms of bioethanol potential.

	GNDVI (in TS-3) vs. Total Biomass		ExG (in TS-2) vs. Sugar release		NDVI (in TS-3) vs. Theoretical ehtanol	
Cereal species	GNDVI	Biomass (kg/m2)	EXG	Sugar Release (ul/mg)	NDVI	Theoretical Ethanol (m3/ha)
T. aestivum	0.54 b	0.67 b	0.44 b	0.98 b	0.52 b	3.49 b
T. durum	0.57 a	0.83 a	0.43 b	0.98 b	0.54 ab	4.14 a
H. vulgare	0.55 b	0.71 b	0.59 a	1.16 a	0.56 a	4.21 a
X *Triticosecale*	0.51 c	0.52 c	0.38 c	0.94 c	0.49 c	2.54 c

Table 3.4: Mean values and ANOVA of the GNDVI, ExG and NDVI indices selected at the best temporal scenario (TS) for phenotyping of total biomass, sugar release and theoretical ethanol, respectively, at the level of cereal specie.

3.5. Discussion

Several investigations have recently demonstrated the capability of UAVs for collecting phenotypic data on numerous crops and case studies [16, 31, 48]. This study went beyond this by presenting the first experiment with an UAV-based a multi-spectral system for phenotyping several characters of a population of known genotypes of wheat, barley and triticale with the purpose of identify the best accessions for bioethanol production. The field trial showed high variability in plant height, anthesis dates, and bioethanol-related factors such as total dry biomass, sugar release, and theoretical ethanol. These variability was not significantly associated to grain yields [49], which was consistent with previous investigations in barley [50] and wheat [29, 30]. This is a key aspect in breeding programs that aims for selecting plants with better straw quality for bioethanol production deprived of sacrificing grain yield. Since there was phenotypic variability in the experiment, the challenge was to quantify this variability with an efficient and reliable system. The UAV-based phenotyping system first computed spectral variability of plant material (234 cereal plots) over time, and then the system estimated the bioethanol-related variables with acceptable precision by using selected image-based vegetation indices calculated at specific temporal intervals. At this point, it is relevant to highlight the influence of the temporal factor to achieve better estimations. As observed in Table 3.3, the results of TS-1 (i.e., on each single date) were always lower than those obtained in TS-2 (i.e., averaging the values of each VI obtained during plant anthesis) and TS-3 (i.e., averaging the values of each VI obtained during the full crop development). This result suggests that future research on crop phenotyping should include a multi-temporal study, and even in some cases, primarily consider the crop anthesis dates (TS-2). For example, predictions of sugar release in our experiment were more accurate with the visible-based VIs calculated in TS-2 (R^2 from 0.52 to 0.57) than in TS-3 (R^2 from 0.48 to 0.51). A general result was that the NIR-based VIs (i.e., NDVI, GNDVI, MCARI and MSR in this study) were more appropriate to estimate crop biomass, meanwhile the visible-based VIs (i.e., ExG, VIgreen and TCI in this study) were suitable for crop sugar release. Estimations were low on most of the single dates studied (TS-1), although moderate correlations between NDVI and GNDVI with crop biomass were obtained on DAS 161 (R^2 of 0.50 and 0.51, respectively). The difference between both VIs is that NDVI uses NIR-red and GNDVI uses NIR-green spectral bands. Therefore, it seems that the green band, which is sensitive to

small changes in vegetation greenness and canopy, was slightly more correlated to crop biomass. Better biomass estimations were however obtained when GNDVI was calculated during plant anthesis (TS-2, R^2 of 0.57), and even better when NDVI, GNDVI and MCARI were calculated during the full crop development (TS-3, R^2 of 0.58-0.59). In the case of sugar release, ExG calculated during plant anthesis (TS-2) revealed the highest correlation (R^2 of 0.57) of the studied VIs. To our knowledge, there are no previous research that explain the indirect relationship that may exist between any visible-based index and sugar release. [51] and [52] revealed some near- and mid- infrared spectral regions with a significant contribution in the prediction of total sugar release by applying spectroscopy analysis, and partially attributed their results to plant senescence components such as lignin, cellulose and hemicellulose. However, our experiment reported the best estimations prior to crop senescence, which points to components or aspects related to green vegetation. Upward progress of ExG correlations to reach a maximum during crop anthesis may be explained by the influence that changes of crop greenness and plant pigments have on ExG measurements [32, 53]. On crop anthesis, the plants have the greatest amount of carbon in the form of sugars and the maximum number of leaves as easily degradable plant material [29, 30, 54]. ExG correlations decreased after crop anthesis (i.e., from 161 DAS onwards in almost all accessions), just as the plants progressed towards senescent stages caused by the decrease in the proportion of chlorophyll (green pigments) in favor of anthocyanin (red pigments). The primary purpose of phenotyping techniques is to provide a ranking of the studied plants in order to facilitate or accelerate the process of selecting genetic material for the next stages of plant breeding. However, a ranking is not provided in many cases, which reduces the impact of the experiment to only monitoring one or various crop variables. Our UAV-based system aimed to rank the cereal accesions in terms of theoretical ethanol, as a result of the linear combination of total biomass and sugar release (see Eq. 3.1). In this case, NIR-based VIs in TS-3 reported the highest correlations, being NDVI the best indice (R^2 of 0.66), so the linear equation of NDVI served to predict a ranking of accessions for theoretical ethanol (Fig 3.7).

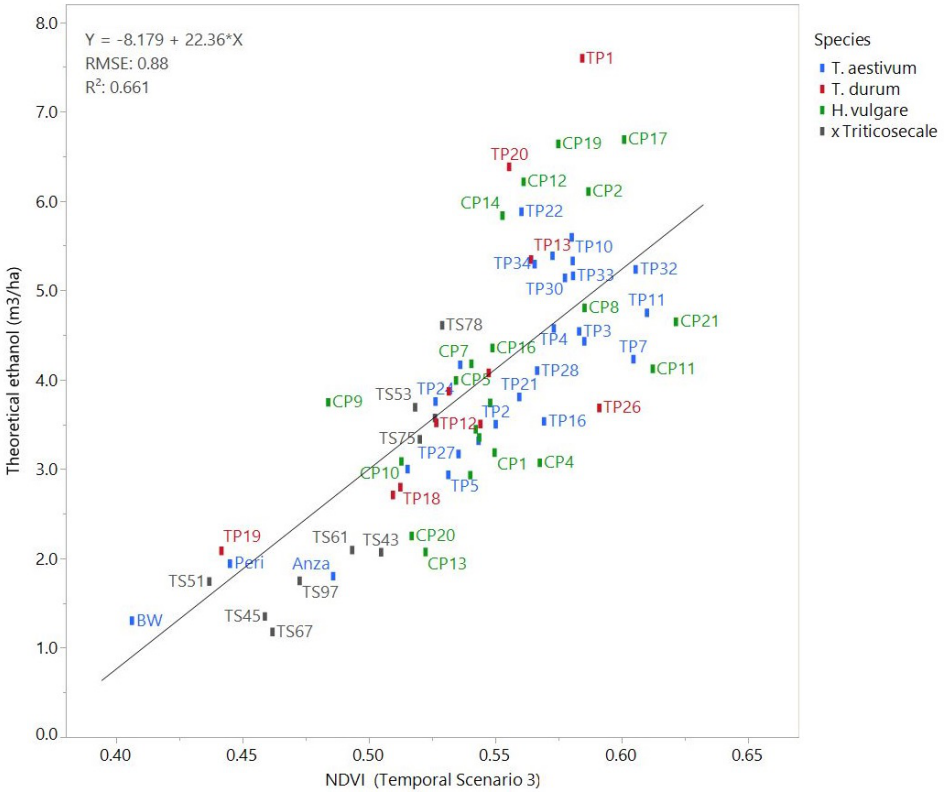

Figure 3.7: Linear regression of NDVI (in TS-3) against crop theoretical ethanol (m^3/ha) showing the rank of cereal accessions.

The range of NDVI values ordered the large variability of cereal accessions with a root mean square error (RMSE) of prediction of 0.88 m^3/ha. This ranking showed the cereal accessions with higher and lower values of theoretical ethanol, and consequently demonstrated the value of the UAV-based system for the early and non-destructive identification of the improved varieties that combine high saccharification potential and high biomass production for a cereal breeding program. The UAV-based system mostly pointed out the *H. vulgare* accessions (e.g., CP21 (Azumamugi), CP17 (Cebada Capa), CP12 (Apex), CP19 (Franklin), among others) as those with the best lignocellulosic source for bioethanol production, followed by the *Triticum* accessions (e.g., TP11 (P92201), TP32 (USG 3209), and TP1 (IDO444)) and, finally, the X *Triticosecale* accessions, which generally agreed with the results of the laboratory analysis of cereal straw (table 3.4). These results were also in line with previous research of [55, 56], which evaluated the production of bioethanol from several straws and hays, and also highlighted barley as

a major source of biomass and a greater potential for bioethanol than the other cereals studied. Some of the contrasting accessions observed in the ranking, e.g. CP9 (Steptoe) x CP10 (Morex) and OWB (CP13 and CP14) populations [57], have been used as parental lines in mapping populations for different characters, including regulatory genes [58], resistance to rust [59], or to develop a genetic link map of SNP by consensus in barley [60], which is an important resource for genetic studies. As a first approximation, our results suggest that some barley mapping populations, e.g. CP13 (OWB dominant) × CP14 (OWB recessive) and CP19 (Franklin) x CP13, could be good candidates to identify the genetic factors underlying the difference in theoretical bioethanol potential and in wall recalcitrance. While genotypic tools have advanced much technologically, phenotypic tools remain the main bottleneck in the decision-making process. However, this innovative UAV-based phenotyping system can enrich the breeding programs for bioethanol production by drastically accelerating the timing to capture and process data of the field trials. In fact, the time required to conduct the entire process, from operating the UAV flight to computing the spectral data, was approximately one hour, while obtaining phenotypic data from 234 cereal plots using conventional laboratory techniques took several days. Therefore, although the UAV-based predictions were moderate in most cases, the saving of time and resources certainly justifies the usefulness of this technology. Additionally, this research reported the phenological dates and specific spectral regions (i.e., vegetation indices) that provide reliable beforehand information to predict biomass and sugar contain of sixty-six cultivars of wheat, barley and triticale, whose large variability constituted a valuable resource for cereal genetic studies.

Referencias

[1] Andreas Uihlein and Liselotte Schebek. Environmental impacts of a lignocellulose feedstock biorefinery system: An assessment. *Biomass and Bioenergy*, 33(5):793–802, May 2009. 00114.

[2] IEA. *World Energy Outlook 2010*. Organisation for Economic Co-operation and Development, Paris, November 2010. 00004.

[3] Leonardo D. Gomez, Jennifer K. Bristow, Emily R. Statham, and Simon J. McQueen-Mason. Analysis of saccharification in Brachypodium distachyon stems under mild conditions of hydrolysis. *Biotechnology for Biofuels*, 1:15, 2008. 00036.

[4] Óscar J. Sánchez and Carlos A. Cardona. Trends in biotechnological production of fuel ethanol from different feedstocks. *Bioresource Technology*, 99(13):5270–5295, September 2008. 00000.

[5] Ralph E. H. Sims, Warren Mabee, Jack N. Saddler, and Michael Taylor. An overview of second generation biofuel technologies. *Bioresource Technology*, 101(6):1570–1580, March 2010. 00953.

[6] José Luis Araus and Jill E. Cairns. Field high-throughput phenotyping: the new crop breeding frontier. *Trends in Plant Science*, 19(1):52–61, 2014. 00191.

[7] Joshua N. Cobb, Genevieve Declerck, Anthony Greenberg, Randy Clark, and Susan McCouch. Next-generation phenotyping: requirements and strategies for enhancing our understanding of genotype-phenotype relationships and its relevance to crop improvement. *TAG. Theoretical and applied genetics. Theoretische und angewandte Genetik*, 126(4):867–887, April 2013. 00139.

[8] Stijn Dhondt, Nathalie Wuyts, and Dirk Inzé. Cell to whole-plant phenotyping: the best is yet to come. *Trends in Plant Science*, 18(8):428–439, August 2013. 00079.

[9] Jeffrey W. White, Pedro Andrade-Sanchez, Michael A. Gore, Kevin F. Bronson, Terry A. Coffelt, Matthew M. Conley, Kenneth A. Feldmann, Andrew N. French, John T. Heun, Douglas J. Hunsaker, Matthew A. Jenks, Bruce A. Kimball, Robert L. Roth, Robert J. Strand, Kelly R. Thorp, Gerard W. Wall, and Guangyao Wang. Field-based phenomics for plant genetics research. *Field Crops Research*, 133:101–112, July 2012. 00156.

[10] Nora Honsdorf, Timothy John March, Bettina Berger, Mark Tester, and Klaus Pillen. High-Throughput Phenotyping to Detect Drought Tolerance QTL in Wild Barley Introgression Lines. *PLoS ONE*, 9(5):e97047, May 2014. 00026.

[11] Kerstin A. Nagel, Alexander Putz, Frank Gilmer, Kathrin Heinz, Andreas Fischbach, Johannes Pfeifer, Marc Faget, Stephan Blossfeld, Michaela Ernst, Chryssa Dimaki, Bernd Kastenholz, Ann-Katrin Kleinert, Anna Galinski, Hanno Scharr, Fabio Fiorani, and Ulrich Schurr. GROWSCREEN-Rhizo is a novel phenotyping robot enabling simultaneous measurements of root and shoot growth for plants grown in soil-filled rhizotrons. *Functional Plant Biology*, 39(11):891–904, 2012. 00088.

[12] Sébastien Tisné, Yann Serrand, Liên Bach, Elodie Gilbault, Rachid Ben Ameur, Hervé Balasse, Roger Voisin, David Bouchez, Mylène Durand-Tardif, Philippe Guerche, Gaël Chareyron, Jérôme Da Rugna, Christine Camilleri, and Olivier Loudet. Phenoscope: an automated large-scale phenotyping platform offering high spatial homogeneity. *The Plant Journal*, 74(3):534–544, May 2013. 00000.

[13] Lucas Busemeyer, Daniel Mentrup, Kim Möller, Erik Wunder, Katharina Alheit, Volker Hahn, Hans Peter Maurer, Jochen C. Reif, Tobias Würschum, Joachim Müller, Florian Rahe, and Arno Ruckelshausen. BreedVision — A Multi-Sensor Platform for Non-Destructive Field-Based Phenotyping in Plant Breeding. *Sensors*, 13(3):2830–2847, February 2013. 00097.

[14] J. M. Montes, F. Technow, B. S. Dhillon, F. Mauch, and A. E. Melchinger. High-throughput non-destructive biomass determination during early plant development in maize under field conditions. *Field Crops Research*, 121(2):268–273, March 2011. 00064.

[15] J. W. White and R. V. Bostelman. Large-area overhead manipulator for access of fields. *ResearchGate*, 1:221–226, January 2011. 00004.

[16] Yeyin Shi, J. Alex Thomasson, Seth C. Murray, N. Ace Pugh, William L. Rooney, Sanaz Shafian, Nithya Rajan, Gregory Rouze, Cristine L. S. Morgan, Haly L. Neely, Aman Rana, Muthu V. Bagavathiannan, James Henrickson, Ezekiel Bowden, John Valasek, Jeff Olsenholler, Michael P. Bishop, Ryan Sheridan, Eric B. Putman, Sorin Popescu, Travis Burks, Dale Cope, Amir Ibrahim, Billy F. McCutchen, David D. Baltensperger, Robert V. Avant Jr, Misty Vidrine, and Chenghai Yang. Unmanned Aerial Vehicles for High-Throughput Phenotyping and Agronomic Research. *PLOS ONE*, 11(7):e0159781, July 2016. 00000.

[17] Maria Tattaris, Matthew P. Reynolds, and Scott C. Chapman. A Direct Comparison of Remote Sensing Approaches for High-Throughput Phenotyping in Plant Breeding. *Crop Science and Horticulture*, page 1131, 2016. 00000.

[18] Geng Bai, Yufeng Ge, Waseem Hussain, P. Stephen Baenziger, and George Graef. A multi-sensor system for high throughput field phenotyping in

soybean and wheat breeding. *Computers and Electronics in Agriculture*, 128:181–192, October 2016.

[19] Jared L. Crain, Yong Wei, Jared Barker, Sean M. Thompson, Phillip D. Alderman, Matthew Reynolds, Naiqian Zhang, and Jesse Poland. Development and Deployment of a Portable Field Phenotyping Platform. *Crop Science*, 56(3):965, 2016. 00002.

[20] Sylvain Jay, Gilles Rabatel, Xavier Hadoux, Daniel Moura, and Nathalie Gorretta. In-field crop row phenotyping from 3d modeling performed using Structure from Motion. *Computers and Electronics in Agriculture*, 110:70–77, January 2015. 00010.

[21] Karthika Rajendran, Mark Tester, and Stuart J. Roy. Quantifying the three main components of salinity tolerance in cereals. *Plant, Cell & Environment*, 32(3):237–249, March 2009. 00169.

[22] Anja Hartmann, Tobias Czauderna, Roberto Hoffmann, Nils Stein, and Falk Schreiber. HTPheno: An image analysis pipeline for high-throughput plant phenotyping. *BMC Bioinformatics*, 12:148, 2011. 00102.

[23] Loïc Winterhalter, Bodo Mistele, Sansern Jampatong, and Urs Schmidhalter. High throughput phenotyping of canopy water mass and canopy temperature in well-watered and drought stressed tropical maize hybrids in the vegetative stage. *European Journal of Agronomy*, 35(1):22–32, June 2011. 00039.

[24] Juliane Bendig, Andreas Bolten, Simon Bennertz, Janis Broscheit, Silas Eichfuss, and Georg Bareth. Estimating Biomass of Barley Using Crop Surface Models (CSMs) Derived from UAV-Based RGB Imaging. *Remote Sensing*, 6(11):10395–10412, October 2014. 00058.

[25] Katharina V. Alheit, Lucas Busemeyer, Wenxin Liu, Hans Peter Maurer, Manje Gowda, Volker Hahn, Sigrid Weissmann, Arno Ruckelshausen, Jochen C. Reif, and Tobias Würschum. Multiple-line cross QTL mapping for biomass yield and plant height in triticale (× Triticosecale Wittmack). *Theoretical and Applied Genetics*, 127(1):251–260, January 2014. 00022.

[26] Kakeru Watanabe, Wei Guo, Keigo Arai, Hideki Takanashi, Hiromi Kajiya-Kanegae, Masaaki Kobayashi, Kentaro Yano, Tsuyoshi Tokunaga, Toru Fujiwara, Nobuhiro Tsutsumi, and Hiroyoshi Iwata. High-Throughput Phenotyping of Sorghum Plant Height Using an Unmanned Aerial Vehicle and Its Application to Genomic Prediction Modeling. *Frontiers in Plant Science*, 8, 2017.

[27] Mengmeng Du and Noboru Noguchi. Monitoring of Wheat Growth Status and Mapping of Wheat Yield's within-Field Spatial Variations Using Color

Images Acquired from UAV-camera System. *Remote Sensing*, 9(3):289, March 2017.

[28] Sindhuja Sankaran, Lav R. Khot, and Arron H. Carter. Field-based crop phenotyping: Multispectral aerial imaging for evaluation of winter wheat emergence and spring stand. *Computers and Electronics in Agriculture*, 118:372–379, October 2015.

[29] Jacob Wagner Jensen, Jakob Magid, Jens Hansen-Møller, Sven Bode Andersen, and Sander Bruun. Genetic variation in degradability of wheat straw and potential for improvement through plant breeding. *Biomass and Bioenergy*, 35(3):1114–1120, March 2011. 00009.

[30] J. Lindedam, S.B. Andersen, J. DeMartini, S. Bruun, H. Jørgensen, C. Felby, J. Magid, B. Yang, and C.E. Wyman. Cultivar variation and selection potential relevant to the production of cellulosic ethanol from wheat straw. *Biomass and Bioenergy*, 37(0):221–228, February 2012.

[31] Guijun Yang, Jiangang Liu, Chunjiang Zhao, Zhenhong Li, Yanbo Huang, Haiyang Yu, Bo Xu, Xiaodong Yang, Dongmei Zhu, Xiaoyan Zhang, Ruyang Zhang, Haikuan Feng, Xiaoqing Zhao, Zhenhai Li, Heli Li, and Hao Yang. Unmanned Aerial Vehicle Remote Sensing for Field-Based Crop Phenotyping: Current Status and Perspectives. *Frontiers in Plant Science*, 8, 2017.

[32] J. Torres-Sánchez, J. M. Peña, A. I. de Castro, and F. López-Granados. Multi-temporal mapping of the vegetation fraction in early-season wheat fields using images from UAV. *Computers and Electronics in Agriculture*, 103:104–113, April 2014.

[33] R Core Team. *R: A Language and Environment for Statistical Computing*. R Foundation for Statistical Computing, Vienna, Austria, 2016. 49578.

[34] Felipe de Mendiburu. agricolae: Statistical Procedures for Agricultural Research, June 2016. 00314.

[35] Joshua Kelcey and Arko Lucieer. Sensor Correction of a 6-Band Multispectral Imaging Sensor for UAV Remote Sensing. *Remote Sensing*, 4(5):1462–1493, May 2012. 00052.

[36] Thomas Blaschke, Geoffrey J. Hay, Maggi Kelly, Stefan Lang, Peter Hofmann, Elisabeth Addink, Raul Queiroz Feitosa, Freek van der Meer, Harald van der Werff, Frieke van Coillie, and Dirk Tiede. Geographic Object-Based Image Analysis – Towards a new paradigm. *ISPRS Journal of Photogrammetry and Remote Sensing*, 87:180–191, January 2014.

[37] J. Torres-Sánchez, F. López-Granados, and J. M. Peña. An automatic object-based method for optimal thresholding in UAV images: Application for vegetation detection in herbaceous crops. *Computers and Electronics in Agriculture*, 114:43–52, June 2015.

[38] N. Dowe and J. McMillan. SSF Experimental Protocols—Lignocellulosic Biomass Hydrolysis and Fermentation. 2008. 00194.

[39] Gero Barmeier and Urs Schmidhalter. High-Throughput Field Phenotyping of Leaves, Leaf Sheaths, Culms and Ears of Spring Barley Cultivars at Anthesis and Dough Ripeness. *Frontiers in Plant Science*, 8, November 2017.

[40] Jianchang Yang and Jianhua Zhang. Grain filling of cereals under soil drying. *New Phytologist*, 169(2):223–236, 2006.

[41] D. M. Woebbecke, G. E. Meyer, K. Von Bargen, and D. A. Mortensen. Color Indices for Weed Identification Under Various Soil, Residue, and Lighting Conditions. *Transactions of the ASAE*, 38(1):259–269, 1995.

[42] Anatoly A. Gitelson, Yoram J. Kaufman, Robert Stark, and Don Rundquist. Novel algorithms for remote estimation of vegetation fraction. *Remote Sensing of Environment*, 80(1):76–87, April 2002.

[43] D. Haboudane, N. Tremblay, J. R. Miller, and P. Vigneault. Remote Estimation of Crop Chlorophyll Content Using Spectral Indices Derived From Hyperspectral Data. *IEEE Transactions on Geoscience and Remote Sensing*, 46(2):423–437, February 2008.

[44] J. W. Rouse. Monitoring vegetation systems in the Great Plains with ERTS. January 1974.

[45] Anatoly A. Gitelson and Mark N. Merzlyak. Signature Analysis of Leaf Reflectance Spectra: Algorithm Development for Remote Sensing of Chlorophyll. *Journal of Plant Physiology*, 148(3):494–500, January 1996.

[46] C. S. T Daughtry, C. L Walthall, M. S Kim, E. Brown de Colstoun, and J. E McMurtrey. Estimating Corn Leaf Chlorophyll Concentration from Leaf and Canopy Reflectance. *Remote Sensing of Environment*, 74(2):229–239, November 2000.

[47] Jing M. Chen. Evaluation of Vegetation Indices and a Modified Simple Ratio for Boreal Applications. *Canadian Journal of Remote Sensing*, 22(3):229–242, September 1996.

[48] Sindhuja Sankaran, Lav R. Khot, Carlos Zúñiga Espinoza, Sanaz Jarolmasjed, Vidyasagar R. Sathuvalli, George J. Vandemark, Phillip N. Miklas, Arron H. Carter, Michael O. Pumphrey, N. Richard Knowles, and Mark J. Pavek. Low-altitude, high-resolution aerial imaging systems for row and field crop phenotyping: A review. *European Journal of Agronomy*, 70:112–123, October 2015. 00012.

[49] Francisco J. Ostos Garrido, Fernando Pistón, Leonardo D. Gómez, and Simon J. McQueen-Mason. Biomass recalcitrance in barley, wheat and triticale straw: Correlation of biomass quality with classic agronomical traits. *PLOS ONE*, 13(11):e0205880, November 2018.

[50] B. S. Capper. Genetic variation in the feeding value of cereal straw. *Animal Feed Science and Technology*, 21(2):127–140, October 1988. 00062.

[51] Georgios Bekiaris, Jane Lindedam, Clément Peltre, Stephen R. Decker, Geoffrey B. Turner, Jakob Magid, and Sander Bruun. Rapid estimation of sugar release from winter wheat straw during bioethanol production using FTIR-photoacoustic spectroscopy. *Biotechnology for Biofuels*, 8(1):85, December 2015.

[52] Jane Lindedam, Sander Bruun, Henning Jørgensen, Claus Felby, and Jakob Magid. Cellulosic ethanol: interactions between cultivar and enzyme loading in wheat straw processing. *Biotechnology for Biofuels*, 3:25, 2010. 00019.

[53] Zhenghong Yu, Zhiguo Cao, Xi Wu, Xiaodong Bai, Yueming Qin, Wen Zhuo, Yang Xiao, Xuefen Zhang, and Hongxi Xue. Automatic image-based detection technology for two critical growth stages of maize: Emergence and three-leaf stage. *Agricultural and Forest Meteorology*, 174-175:65–84, June 2013.

[54] Andrea Bellucci, Anna Maria Torp, Sander Bruun, Jakob Magid, Sven B. Andersen, and Søren K. Rasmussen. Association Mapping in Scandinavian Winter Wheat for Yield, Plant Height, and Traits Important for Second-Generation Bioethanol Production. *Frontiers in Plant Science*, 6, November 2015. 00000.

[55] Fang Chen and Richard A. Dixon. Lignin modification improves fermentable sugar yields for biofuel production. *Nature Biotechnology*, 25(7):759–761, July 2007. 00769.

[56] Ye Chen, Ratna R. Sharma-Shivappa, Deepak Keshwani, and Chengci Chen. Potential of agricultural residues and hay for bioethanol production. *Applied Biochemistry and Biotechnology*, 142(3):276–290, September 2007.

[57] A. Kleinhofs, A. Kilian, M. A. Saghai Maroof, R. M. Biyashev, P. Hayes, F. Q. Chen, N. Lapitan, A. Fenwick, T. K. Blake, V. Kanazin, E. Ananiev, L. Dahleen, D. Kudrna, J. Bollinger, S. J. Knapp, B. Liu, M. Sorrells, M. Heun, J. D. Franckowiak, D. Hoffman, R. Skadsen, and B. J. Steffenson. A molecular, isozyme and morphological map of the barley (Hordeum vulgare) genome. *Theoretical and Applied Genetics*, 86(6):705–712, July 1993. 00683.

[58] A. Tondelli, E. Francia, D. Barabaschi, A. Aprile, J. S. Skinner, E. J. Stockinger, A. M. Stanca, and N. Pecchioni. Mapping regulatory genes as candidates for cold and drought stress tolerance in barley. *Theoretical and Applied Genetics*, 112(3):445–454, November 2005. 00099.

[59] L. Arru, E. Francia, and N. Pecchioni. Isolate-specific QTLs of resistance to leaf stripe (Pyrenophora graminea) in the 'Steptoe' x 'Morex' spring barley cross. *Theoretical and applied genetics.*, 106(4):668–675, February 2003. 00000.

[60] Timothy J. Close, Prasanna R. Bhat, Stefano Lonardi, Yonghui Wu, Nils Rostoks, Luke Ramsay, Arnis Druka, Nils Stein, Jan T. Svensson, Steve Wanamaker, Serdar Bozdag, Mikeal L. Roose, Matthew J. Moscou, Shiaoman Chao, Rajeev K. Varshney, Péter Szucs, Kazuhiro Sato, Patrick M. Hayes, David E. Matthews, Andris Kleinhofs, Gary J. Muehlbauer, Joseph DeYoung, David F. Marshall, Kavitha Madishetty, Raymond D. Fenton, Pascal Condamine, Andreas Graner, and Robbie Waugh. Development and implementation of high-throughput SNP genotyping in barley. *BMC genomics*, 10:582, 2009. 00390.

Capítulo 4

A GLYCOSYL TRANSFERASE FAMILY 43 PROTEIN INVOLVED IN XYLAN BIOSYNTHESIS IS ASSOCIATED WITH STRAW DIGESTIBILITY IN *BRACHYPODIUM DISTACHYON*

Published as:

Whitehead C[*], **Ostos Garrido FJ**[*], Reymond M, Simister R, Distelfeld A, Atienza SG, et al. "A glycosyl transferase family 43 protein involved in xylan biosynthesis is associated with straw digestibility in *Brachypodium distachyon*." *New Phytol*. May 2018. doi : 10.1111/nph.15089.
(New Phytologist IF2017=7.433, Ranking: 4/791, D1 in Plant and animal science)

4.1. Summary:

The recalcitrance of secondary plant cell walls to digestion constrains biomass use for the production of sustainable bioproducts and for animal feed.

We screened a population of Brachypodium recombinant inbred lines (RILs) for cell wall digestibility using commercial cellulases and detected a quantitative trait locus (QTL) associated with this trait.

Examination of the chromosomal region associated with this QTL revealed a candidate gene that encodes a putative glycosyl transferase family (GT) 43 protein, orthologue of IRX14 in Arabidopsis, and hence predicted to be involved in the biosynthesis of xylan. Arabinoxylans form the major matrix polysaccharides in cell walls of grasses, such as Brachypodium. The parental lines of the RIL population carry alternative nonsynonymous polymorphisms in the *Bd*GT43A gene, which were inherited in the RIL progeny in a manner compatible with a causative role in the variation in straw digestibility. In order to validate the implied role of our candidate gene in affecting straw digestibility, we used RNA interference to lower the expression levels of the *Bd*GT43A gene in Brachypodium.

[*]These authors contributed equally to this work.

The biomass of the silenced lines showed higher digestibility supporting a causative role of the *Bd*GT43A gene, suggesting that it might form a good target for improving straw digestibility in crops

---

4.2. Introduction

Global commitments to reducing carbon emissions, combined with concerns over food security are increasing the imperative for producing sustainable low-carbon biofuels based on nonfood biomass, such as cereal straw or energy grasses [1]. Lignocellulosic biomass is largely composed of polysaccharides, which can be depolymerized using biochemical methods to provide sugars for conversion to biofuels via fermentation. However, the recalcitrant nature of lignocellulose to digestion stands as a significant barrier to the cost-effective production of biofuels [1–4]. Biomass recalcitrance also limits the value of crop residues as animal feed. Reducing biomass recalcitrance without having a negative impact on yield is therefore an important target for improving the value of crop residues for feed and biorefinery applications.

The main components of the secondary cell walls in grasses are cellulose (35–45 %), hemicellulose (40–50 %) and lignin (c. 20 %) [1]. Complex arabinoxylans (AX) found in the hemicellulosic fraction of the cell wall form the major component of matrix polysaccharides in grasses and comprised a β,1-4 linked xylopyranose backbone that is decorated with side chains of arabinose, xylose, galactose and glucuronic acid, as well as acetyl groups [5–7].

The synthesis of the xylan backbone was first reported in Arabidopsis and it is thought that the xylan backbone of AX in grasses is synthesized in a similar fashion by a complex of glycosyltransferases (GTs) [8]. The Arabidopsis xylan synthase complex contains three different GT proteins belonging to the GT8, GT43 and GT47 families [9]. It is thought that the GT43 enzymes, IRX9 and 14, together with the GT47 protein, IRX10 are involved in the elongation of the xylan backbone [8]. It has been shown that these three proteins work together in a complex in wheat [10]. However, it proved difficult to identify the specific function of each protein in xylan elongation until 2014 when [11]; confirmed biochemically that IRX10 has

β-1,4-xylan synthase activity. It remains unclear if the GT43 genes have a catalytic role in terms of forming the xylan backbone, but their presence is required for the proper functioning of the complex [12]. The Arabidopsis genome encodes four GT43 genes, namely, IRX9 and IRX14 and their homologs IRX9L and IRX14L, which are functionally nonredundant in the formation of the xylan backbone [13]. However, in rice, 10 GT43 genes have been identified, *Os*GT43A–J [14]. In 2013, Chiniquy et al. [15] reported that three genes, *Os*GT43C, *Os*GT43F and *Os*GT43J, found in rice are putative orthologues to the Arabidopsis GT43 family genes IRX9, IRX9L and IRX14, respectively. Lee et al. (2014) [14] studied four rice GT43 genes and discovered that *Os*GT43A and *Os*GT43E are orthologues for IRX9 and confirmed that *Os*GT43J is an orthologue of IRX14. They also suggested that *Os*GT43H was not an orthologue of either IRX9 or IRX14.

Grass AX contains more complex side chain decorations than that of xylans in dicot plants. Grass AX is dominated by α-1,2- and α-1,3-linked arabinosyl side chains, whereas dicots predominantly contain glycuronosyl and 4-O-methylglucuronosyl residues as side chains [16, 17]. It was recently shown that these arabinosyl side chains are added to the backbone by the action of GT61 proteins. The XAT1 and XAT2 genes belong to clade A of the large GT61 family of genes in Arabidopsis and are reported to have α-1,3-arabinosyltransferase activity. Some of the arabinosyl side chains are further decorated with a xylose unit added at position O-2 by a β-1,2-xylosyltranserase, which is also thought to belong to the GT61 family [18]. In rice, the GT61 gene XAX1 appears to be responsible for this addition, with loss of function resulting in lower concentrations of xylose and ferulic acid in the AX, accompanied by increased biomass digestibility [17]. Some arabinosyl residues are further decorated with ferulic acid (FA, *c*. 4 %) or *p*-coumaric acid (*p*CA *c*. 3 %) [19, 20]. The FA esters can be oxidatively coupled to form dimers as well as trimers, producing AX crosslinks within the cell wall [16, 21]. FA can also form links between AX and lignin [22, 23]. This crosslinking through FA has important functions, such as controlling the ability of the cell wall to extend, protection against pathogen attack, and inhibition of cell wall degradation by microorganisms and ruminants as well as cellulase digestion [23]. Xylosyl residues in xylan that are not decorated with sugars are often acetylated in the C2 or C3 positions, and in Arabidopsis the patterns of xylan substitution have been shown to contribute to xylan conformation and its interactions with cellulose [7], and altering xylan acetylation leads to changes in stem digestibility [24].

Genetic engineering to improve biomass digestibility requires knowledge of the genetic factors that determine recalcitrance. Methods used for reducing biomass recalcitrance in grasses have involved reverse genetic approaches such as overexpression or RNA interference (RNAi) techniques of possible genes or transcription factors that play a role in cell wall biosynthesis [25]. Quantitative trait analysis in recombinant inbred populations provides a powerful tool for identifying such genetic determinants based on linkage disequilibrium. Such studies can identify so-called quantitative trait loci (QTLs), which are regions of the genome harbouring polymorphisms that cause quantitative variation in the trait of interest. QTL studies have been used to investigate animal feed digestibility to determine the major factors affecting this trait in maize [26–28]. In the work presented here, we used a population of recombinant inbred lines (RILs) of the model grass *Brachypodium dystachyon* (Brachypodium) to look for QTLs for digestibility by measuring the saccharification potential of stems (susceptibility to digestion with commercial cellulases). Our data revealed a single QTL associated with saccharification and found that the most plausible candidate gene responsible for the variation in stem digestibility in this population encodes a putative GT43 protein. The putative role of this gene was supported by RNAi gene silencing to produce plants with reduced expression levels, which exhibited increased saccharification accompanied by modest changes in xylan content in their cell walls.

4.3. Materials and methods

Plant material and growth conditions

A *Brachypodium distachyon* (Brachypodium) RIL population Bd3-1 x Bd21 [29] was sown for QTL analysis in three randomized replicates (blocks 1–3) containing 12 plants per line within each replicate. The seeds were vernalized in the dark at 4°C for 3 wk before being transferred to the glasshouse where they grew under a long-day, short-night regime (16 : 8 h, light : dark) with temperatures ranging from 18 to 20°C. After 3 wk the plants were staked to help support the stems. Watering was stopped when the plants began to senesce and once they were completely dry the main stems were harvested. Brachypodium Bd21 and transgenic seeds were vernalized in the dark at 4°C for 1 wk before being transferred to the glasshouse and where they grew under the same conditions as the RIL population.

Experimental design and statistical analysis

All analyses were conducted with the statistical software R v.3.2.3 [30]. The experimental design was completely randomized replicated in three blocks. Data were adjusted to a lineal model with the function lm and factors effects were checked by an analysis of variance with the function ANOVA. The normality and heteroscedasticity assumptions were tested by plotting the residuals vs the predicted values and Q-Q plots. The differences between lines were assessed using post hoc multiple-comparison test (function glht, package multcomp) [31].

Saccharification analysis

Saccharification analysis was performed on Brachypodium stem material which was prepared by removing the top and bottom internodes as well as all nodes. The main stem was selected and cut into 2 cm fragments and placed into 2 ml tubes together with two ball bearings and milled within the tube. The samples were formatted in 96-well plates to contain four technical replicates of 4 mg each. The formatted 96-well plates underwent saccharification analysis using a liquid handling platform which pretreated the samples with 0.5N NaOH at 90°C for 30min, followed by enzymatic hydrolysis at 50°C, pH 4.5 for 8 h. The enzyme cocktail contained commercially available Celluclast and Novozyme 188 (Novozymes A/S, Bagsvaerd, Denmark) at a ratio of 4:1. The reducing sugars released during hydrolysis were detected using a colorimetric assay involving 3-methyl-2-benzothiazolinone hydrozone (MTBH) [32, 33].

Quantitative trait detection

The saccharification data together with the genotype data [29](Cui et al., 2012) from the RIL Bd3-1 9 Bd21 population underwent QTL analysis following the method described in [34]. A correction coefficient was applied to the saccharification data before QTL analysis to take into account any environmental effects caused by well position and sample weight. The command data=convert2riself(mydata) was used to include the algorithm for the investigation of a RIL population during the QTL analysis using the R/QTL program. Standard interval mapping was performed using a genome-wide scan for the identification of loci. The significant threshold was determined using a 1000-replicate permutation test and was displayed as a logarithm of the odds (LOD) 5 % score. The QTL peak was selected as it exceeded this threshold. The QTL effect was obtained from an effect plot. The fit

of the model was determined using the function fitqtl and 128 imputations with a 1 cM grid, which calculated the genetic variance of the QTL identified.

Broad-sense heritability (H^2) was calculated from the value of the means squares of the RILs [34, 35] as follows:

$$H^2 = \frac{V_G}{V_T} = \frac{V_G}{(V_G + V_E)} \tag{4.1}$$

where V_G is the genotype variance, V_E is the environmental variance and V_T is the total variance of the trait of interest.

Identification of candidate genes

GBROWSER (http://mips.helmholtz-muenchen.de/gbrowse/plant/cgi-bin/gbrowse/brachy/) was used to investigate, *in silico*, the genomic region between the two markers flanking the QTL peak for possible candidate genes. The region on either side of marker BD1676.1 (physical position: 25 970 456 bp, according to the reference genome of Bd 21) on chromosome 5 was explored, therefore from marker BD4088.6 (physical position: 25889793bp) to marker BD3488.1 (physical position: 2678751 bp).

Phylogenetic tree

Protein sequences from *Arabidopsis thaliana*, *Nicotiana attenuate*, *Nicotianna tabacum*, *Oryza sativa* and *B. distachyon* were collated for the IRX subfamilies 9 and 14 from the National Center for Biotechnology Information and Phytozyme12 databases. All the sequences were uploaded into MEGA6.0 [36] and aligned using CLUSTALW. The phylogenetic analysis was conducted using the neighbour joining method with 2000 bootstrap replicates [37].

Polymorphism detection in the candidate gene sequence

One hundred milligrams of green stems were harvested from 4-wk-old plants of both parental lines BD21 and Bd3-1. Samples were flash-frozen in liquid nitrogen before RNA extraction using the Qiagen RNeasy Mini kit (Qiagen). The quality and quantity of RNA were checked on a 1 % agarose gel as well as a NanoDrop spectrophotometer (ThermoScientific, Loughborough, UK). The samples were diluted to 2µg in 10µl. The RNA was incubated for 5min at 65°C together with 1µl of 10mM dNTPs and 1µl oligo dT. cDNA was generated using the SuperScript

II reverse transcriptase kit (Thermofisher, Stafford, UK) once the samples were at room temperature.

The target gene, Bradi5g24290.1, was amplified from the cDNA using the primers designed according to the specification of the cloning kit. The following primer sequences were used: GT43-F: 5' -CAC CAT GAA GCT CCC GCT-3' ; GT43-R: 5' -CTA GTG ACC ATC TTC AGT ATT TAC TAC G-3'. The PCR products were cloned using the StrataClone Blunt PCR cloning kit and sequenced. BIOEDIT v.7.2.5 software was used to determine the presence of any single nucleotide polymorphism (SNPs) by comparing the sequences of the cloned parents to each other as well as to the mRNA sequence of Bradi5g25290.1 (NCBI accession: XM-010242235 https://www.ncbi.nlm.nih.gov/nuccore/XM_010242235).

Sorting Intolerant From Tolerant (SIFT) analysis was conducted to determine effects on protein function due to the amino acid substitutions detected (http://sift.jcvi.org/www/SIFT_seq_submit2.html).

Artificial microRNA construction

Artificial microRNA sequences were designed using the Web MicroRNA Designer platform (http://wmd3.weigelworld.org) and were based on the JGI Brachypodium genome annotation [38]. Constructs were engineered from the pBract214 plasmid to replace the targeting regions of the native Brachypodium microRNA precursor (Supporting Information Fig 4.9; Table 4.2). MicroRNA targets were PCR-amplified according to [39] and cloned into the pCR®8/GW/TOPO® TA Cloning Kit.

Plant transformation

Transformation was carried out according to [40] where seeds were collected from 6- to 7-wk-old plants and the gluma was removed. Surface sterilization of the seeds was conducted with a 1.3 % NaClO solution containing 0.01 % Triton-X100 for 4 min. The embryos were dissected and placed on callus initiation medium. The calli were propagated for 7 wk with two subsequent subcultures at 4 and 6 wk following dissection. The 7-wk- old calli were immersed in an *A. tumefaciens* suspension for 5 min and dried on filter paper. The agrobacterium strain AGL1 was used together with the pBract 204 vectors which contain the hpt gene conferring hygromycin resistance under a 35s promoter at the left border (LB) and a gus gene encoding b-glucuronidase under the control of the maize ubiquitin promoter at the right border

(RB). The calli were then cocultivated on dry filter paper for 3 d in the dark at 22°C. Following cocultivation, the calli were moved to selective plates containing 40 mgl^{-1} hygromycin and 200 mgl^{-1} timentin and were left for 4 wk in the dark at 28°C. Following selection, they were moved to LS media for regeneration at 28°C under constant light and then onto MS media for root establishment. Finally, the plantlets were transplanted to soil and grown as previously described.

Quantitative real-time PCR

RNA was isolated from Brachypodium stems using TRIzol reagent (Invitrogen). An amount of RNA (0.4 µg) was subjected to a reverse transcription step using the high-capacity cDNA archive kit (RevoScript RT PreMix Kit). Expression of the gene targeted for silencing was quantified by comparative quantitative real-time PCR (qRT-PCR), where 4 µl of cDNA was added to 7 µl of dH_2O, 12.5 µl of 2X SYBR Green Master Mix (Applied Biosystems, Foster City, CA, USA) and 0.75 µl of 10 mM of each primer (Table 4.3). Three duplicate reactions were used for each sample, and each set included template controls containing water. The qRT-PCR amplifications were conducted using an ABI Prism 7000 Sequence Detection System (Applied Biosystems, Foster City, CA, USA) under the following conditions: 10 min initial denaturation at 94°C and 40 cycles (94°C for 15 s; 60°C for 60 s) with a single fluorescent reading (SYBR Green I chemistry) at the end of each cycle. The qRT-PCR data were normalized against the housekeeping genes ubiquitin-conjugating enzyme 18 (UBC18) and S-adenosylmethionine decarboxylase (SamDC).

Cell wall polysaccharide composition analysis

Alcohol insoluble residue (AIR) was prepared as described by [41] with modifications. A total of 100 mg of ground stem material was incubated in phenol for 30 min at room temperature while shaking, followed by centrifugation at 3000 g for 10 min at 4°C. The supernatant was removed and the pellet was washed with the following solutions: twice with chloroform: methanol (1:1, v/v), twice with 80 % (v/v) methanol, and once with 100 % methanol. The pellets were left to dry overnight at room temperature. The samples were destarched by amylase treatment and 20 mg were suspended in 2 ml of 10 mM potassium phosphate buffer (pH 6.5), 1 mM $CaCl_2$ and 0.05 % NaN_3. This suspension was heated at 95°C and the starch was allowed to gelatinize for 30 s before 1 U ml^{-1} thermostable

α-amylase (Megazyme, Leinster, Ireland). The suspension was incubated at 85°C for 15 min then cooled to 25°C before 10 U ml^{-1} amyloglucosidase and 1 U ml^{-1} pullulanase (Megazyme) were added. This solution was incubated for 16 h at 25°C with continuous shaking at 500 rpm. The suspension was centrifuged for 10 min at 6000 g and the supernatant was removed. The pellet was washed with 2 ml 10 mM potassium phosphate (pH 6.5), 1 mM $CaCl_2$, 0.05 % NaN_3, centrifuged at 6000 g and the supernatant was discarded.

Cell wall fractionation and determination of xylan molecular weight

Sequential extraction of xylan was performed by agitating 20 mg AIR in 2 ml 0.05 M trans-1,2-cyclohexanediaminetetraacetic acid (CDTA) (pH 6.5) for 24 h at room temperature. The suspension was centrifuged (14 000 g, 4°C for 10 min) and the pellet washed once with deionized water. The supernatants were combined as the CDTA-soluble fraction. The samples were subsequently extracted under oxygen-free conditions using 0.05 M Na_2CO_3 containing 0.01 M $NaBH_4$ for 24 h at 4°C to form the Na_2CO_3-soluble fraction, 1 M KOH containing 0.01 M $NaBH_4$ for 24 h at 4°C to form the 1 M KOH-soluble fraction and 4 M KOH containing 0.01 M $NaBH_4$ for 24 h at 4°C to form the 4 M KOH-soluble fraction. All fractions were filtered through a GF/C glass fibre filter (Whatman). The Na_2CO_3 and KOH fractions were also chilled on ice and adjusted to pH 5 with glacial acetic acid. All cell wall fractions were then dialysed extensively against deionized water for 24 h and then lyophilized. The fractionation was repeated three times on three sets of plants grown independently and the mean of these three independent replicas was calculated. Analysis of the molecular weight of the xylan was conducted using a size-exclusion chromatography (SEC) method [42]. The 1 and 4 KOH fractions were separated by SEC and analysed with multi-angle light-scattering detector and a refractive index detector system. Fractions of both wild-type and silenced lines were treated with xylanase and analysed in the same way. The data were analysed using the ASTRA V software and the molecular weights were estimated using the Zimm fit method with degree 1. The sample refractive index increment (dn/dc) used was 0.145.

Monosaccharide profiling

Noncellulosic monosaccharide analysis was performed using high-performance anion exchange chromatography (HPAEC) (Carbopac PA-10; Dionex, Camberley,

UK). AIR samples of 3 mg were hydrolysed with 1 ml of 2 M trifluoroacetic acid (TFA) for 4 h at 100°C, cooled to room temperature and evaporated completely. The pellet was rinsed twice with 200 µl isopropanol and resuspended in 100 µl deionized water. Samples were filtered with 0.45 µm polytetrafluoroethylene filters and separated by HPAEC as described in [43]. The separated monosaccharides were quantified using an external calibration containing seven monosaccharide standards at 100 µM (arabinose, fucose, galactose, glucose, mannose, rham-nose, and xylose) that were subjected to acid hydrolysis in parallel with the samples.

p-Coumaric and FA measurements

Ferulic acid in the cell was quantified according to [41]. One millilitre of 1 M NaOH was added to 10 mg AIR and incubated under argon at 25°C in the dark for 24 h. After the addition of 2 M TFA, phenolics were partitioned twice in 1 ml butan-1-ol. The residue after evaporation was dissolved in 200 µl 50 % methanol and filtered using 1 ml Strata-X polymeric solid phase extraction columns (Phenomenex, Macclesfield, UK). The extract was analysed using high-performance liquid chromatography on an activated reverse-phase C18 5 µm (4.6 x 250 mm) XBridge column (Waters Inc., Wilmslow, UK) in 100 % methanol-5 % acetic acid, with a 20–70 % methanol gradient over 25 min at a flow rate of 2 ml min^{-1}. FA was detected and quantified with a SpectraSYSTEM® UV6000LP photodiode array detector (Thermo Scientific) and the UV-visible spectra were collected at 240–400 nm and analysed against an FA standard.

4.4. Results

Screening a Brachypodium RIL population for saccharification potential reveals a single significant QTL

A Brachypodium F6 RIL population derived from a Bd21 x Bd3-1 cross [29] was kindly supplied by David Garvin (University of Minnesota) and grown to maturity in a glasshouse in three independent blocks to provide straw for digestibility assays. The parental lines are significantly different from one another in terms of germination frequency and height, excluding the inflorescence, but showed similar total biomass yield (Fig S4.10). Internodes from the stems of the plants were milled and subject to digestion with a commercial cellulase cocktail following a mild alkaline pretreatment as described previously [32, 33]. These analyses showed that straw from the parental lines (Fig 4.1a) had significant differences in

digestibility. Bd21 straw showed higher saccharification potential (37 nmol sugar released mg^{-1} h^{-1}) than Bd3-1 (31 nmol mg^{-1} h^{-1}). This difference in digestibility was shown to be statistically significant (two-sample *t*-test, $P = 0.01$).

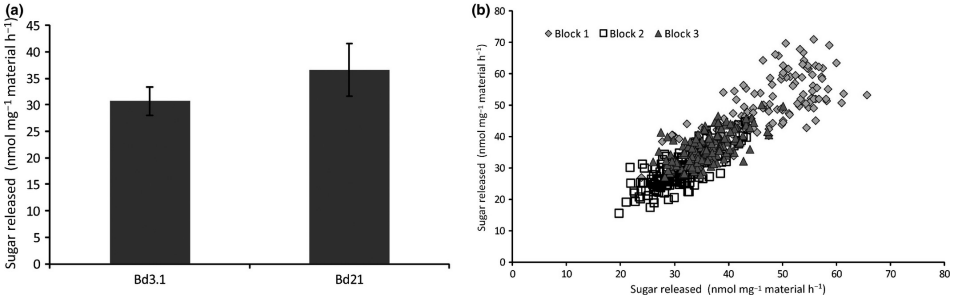

Figure 4.1: Saccharification analysis of Brachypodium stems. (a) Saccharification in straw from parental lines Bd3-1 and Bd21. The ground material was digested with a commercial cellulase for 8 h at 50°C following a 0.5 N NaOH pretreatment of 30 min at 90°C. The results are the means +/- SD of 48 replicates. (b) Distribution of the saccharification data from straw of three randomized replicate plots of the Brachypodium recombinant inbred line (RIL) population Bd21 9 Bd3-1. The ground material was digested with a commercial cellulase for 8 h at 50°C following a 0.5N NaOH pretreatment of 30 min at 90°C. The results are the means of the three plots containing 12 plants per line, which were analysed twice.

The RIL population was analysed in three independent blocks and the results showed that the distribution of saccharification values within blocks 2 and 3 were similar, whereas block 1 showed a different distribution from these two (Fig 4.1b). The plants grown in block 2 released on average the least amount of sugar (29.83 nmol mg^{-1} h^{-1}) and block 1 released the most sugar (46.67 nmol mg^{-1} h^{-1}), with block 3 releasing 35 nmol mg^{-1} h^{-1} on average.

QTL analysis was conducted using the saccharification data together with SNP data for the RIL population generated by [29]. QTL analysis conducted using R/QTL [34] identified a single QTL that exceeded the LOD 5 % threshold of 3.3 on chromosome 5 linked to marker BD1676_1 (Fig 4.2a).

It was calculated that this QTL accounts for 11.83 % of the total variance observed for saccharification, allowing its classification as a major QTL [44, 45]. The QTL resulted in an effect of -1.391 nmol sugar released mg^{-1} h^{-1} when comparing RIL bearing alleles from parental line AA with those bearing alleles from parental line BB (Fig 4.2b); it also had a broad-sense heritability (H^2) of 0.45.

The QTL linked to marker BD1676_1 was confirmed by selecting specific lines from the RIL population for further saccharification analysis. These lines were

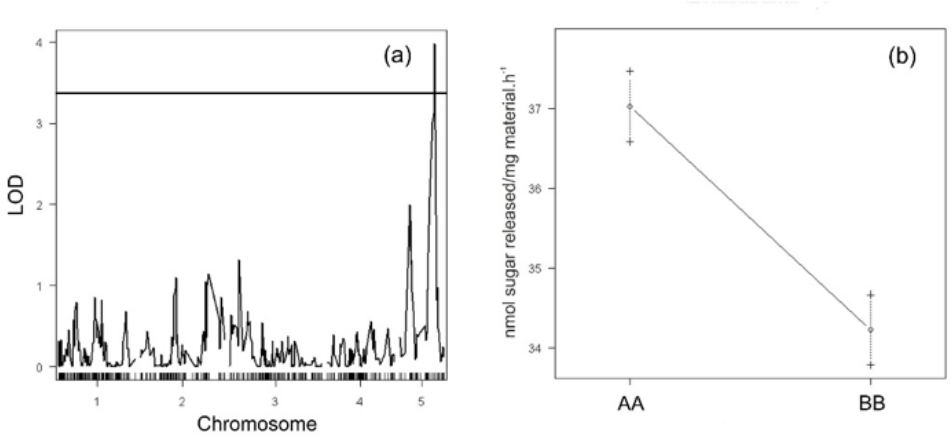

Figure 4.2: Quantitative trait locus (QTL) analysis of the recombinant inbred line (RIL) population. (a) Saccharification data from the RIL population showing a single peak, linked to straw digestibility, located on chromosome 5 (logarithm of the odds (LOD) 5 % = 3.03). (b) Effect of the alleles on digestibility for the QTL linked to marker BD1676_1. Data are means *pm*SD.

selected based on having either alleles from Bd21 or Bd3-1 at marker BD1676_1. For this analysis, 24 lines were grown randomly in six replicates and analysed for digestibility using the same protocol as for the main population. The results revealed a significant difference (one-way ANOVA, P = 0.023) in saccharification between straw from lines carrying the alleles from AA (38.26nmol sugar released mg^{-1} h^{-1}) and the ones carrying the alleles from BB (36.13 nmol mg^{-1} h^{-1}), giving independent support for the presence of the detected QTL for saccharification on this genomic region on chromosome 5.

The QTL region contains a candidate family 43 glucosyltranferase gene

The genomic region around marker BD1676_1 (physical position 25 970 456 bp) was scrutinized between markers BD4088_6 (physical position 25 889 793 bp) and BD34881 (physical position 2647 871 bp) to identify candidate genes that could be responsible for variations in straw digestibility. A total of 104 genes are located in the examined region of the Brachypodium genome sequence v3.1 from the Phytozome12 database) (Table S4.4). Six candidate genes were selected for further in silico analysis based on known cell wall roles. The six genes included three WAK receptor-like protein kinase subfamily B genes (*Bradi5g24180.2*, *Bradi5g24190.1* and *Bradi5g24310.1*) [46], a UDP-galactosyltransferase (*Bradi5g24280.1*) [47], a xylosyltransferase GT43 family gene (*Bradi5g24290.1*) [48] and a UDP-arabinopyranose mutase, GT75, gene (*Bradi5g24850.1*) [10].

In silico gene expression data were analysed for each of these candidates across different libraries corresponding to different organs and developmental stages available from (2017) https://phytozome.jgi.doe.gov (Table 4.1). The expression levels for the *WAK*s and galactosyltransferase genes were low, particularly in stem libraries, while transcripts for the GT43 and GT75 genes are abundantly expressed in inflorescence stems, supporting a role in stem cell wall development. The profile of SNPs of GT43 and GT75 was examined to look for allelic differences between the genomic sequences of Bd21 and Bd3-1 that might be related to the differences in saccharification observed. The genomic data showed the presence of a nonsynonymous SNP for GT43 and none for GT75 in the genome sequences of the parental lines (http://jbrowser.brachypodium.org). Based on these data we decided to focus our attention on the GT43 gene.

The GT43 gene, *Bradi5g24290.1*, was cloned from each parental line and sequenced to confirm the presence of SNPs that might account for the observed allelic variation in digestibility. Two SNPs were identified; the first was at a position of 111 bp from the start of the coding region and consisted of a change from a cytosine (C) to an adenine (A), which leads to no change in the encoded protein sequence. By contrast, the second SNP at position 238 altered a guanine (G) to an A, resulting in a missense variation leading to a change from an alanine at position 80 in the protein to a threonine in the sequence carried in the Bd3-1 parental line Fig 4.3.

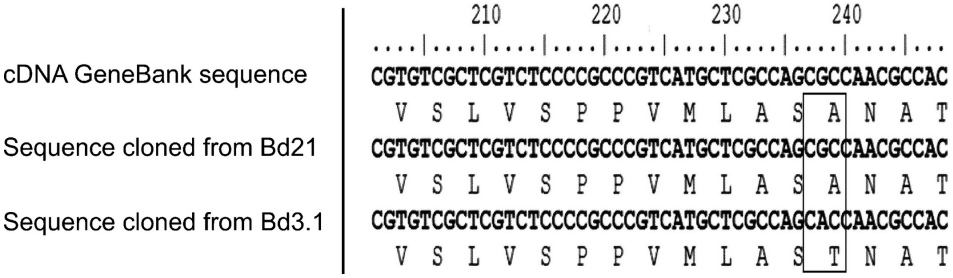

Figure 4.3: Sequence alignment of *Bradi5g290.1* cloned from the parental lines, Bd21 and Bd3-1 compared with wild-type mRNA sequence (accession no. XM_010242235, https://www.ncbi.nlm.nih.gov/nuccore/XM_010242235) from the National Center for Biotechnology Information database indicating a missense polymorphism.

This change in amino acid occurs in a conserved region of the protein, and SIFT analysis indicates that a threonine is not tolerated at this position, as a score below 1.0 was returned in all databases analysed (Table S4.5) [49]. Therefore,

it is possible that this variation within the sequence of the gene could have an allelic effect on protein function that might impact on biomass digestibility and explain the presence of the detected QTL. The Arabidopsis GT43 gene family involved in xylan synthesis consists of four members comprising two functionally nonredundant groups, IRX9 and its homologue IRX9L, as well as IRX14 and its homologue IRX14L [13].

	Candidate genes with cell wall functions											
	5g24180.2 (WAKb)		5g24190.1 (WAKb)		5g24310.1 (WAKb)		5g24280.1 (Galactosyltransferase)		5g24290.1 (GT43)		5g24850.1 (GT75)	
Expression libraries at different developmental stages	FPKM	Locus DE	FPKM	Locus DE	FPKM	Locus DE	FPKM	Locus DE	FPKM	Locus DE	FPKM	Locus DE
Flag leaf 47d 18lgt 6dk	0.181	NS	0.16	*	0.713	NS	0.19	NS	2.859	*	47.744	*
Flower 47d 18lgt 6dk	0.325	**	1.125	NS	0.655	NS	1.116	NS	31.991	**	151.81	**
Leaf mature 47d 18lgt 6dk	0.501	**	0.606	NS	0.983	NS	0.085	NS	3.451	NS	53.802	*
Leaf young 23d 18lgt 6dk	0.192	NS	0.701	NS	0.821	NS	0.181	NS	1.559	*	39.207	*
Shoot 24d 18lgt 6dk	0.166	NS	0.954	NS	0.836	NS	0.044	NS	4.058	NS	78.597	NS
Stem base 47d 18lgt 6dk	0.184	NS	1.874	NS	0.776	NS	0.052	NS	9.252	NS	165.28	**
Stem tip 47d 18lgt 6dk	0.158	NS	1.446	NS	0.785	NS	0.042	NS	14.591	**	136.98	**
Stem 47d 18lgt 6dk	0.096	*	1.074		0.77	NS	0.085	NS	25.954	**	162.18	**

Table 4.1: The expression levels of candidate genes in the chromosome 5 region Candidate genes with cell wall functions. Data collected from selected *Brachypodium distachyon* v.3.1 expression libraries within the Phytozome database (`https://phytozome.jgi.doe.gov`). FPKM, fragments per kilobase of transcript per million mapped reads; Locus DE, for the gene, the expression level in this library is more than 1 SD above/below the average across all libraries; ns, not significant; *, significantly lower; **, significantly higher.

The Brachypodium genome contains 10 GT43 genes, the same number as reported in rice [14]. The Brachypodium genes fall into clear orthologous groups along with those of rice, as determined by protein sequence phylogenetic analysis Fig 4.4. The *Bradi5g24290.1* gene falls within the same clade as IRX14 genes from both Arabidopsis and rice, indicating that it is an IRX14 orthologue.

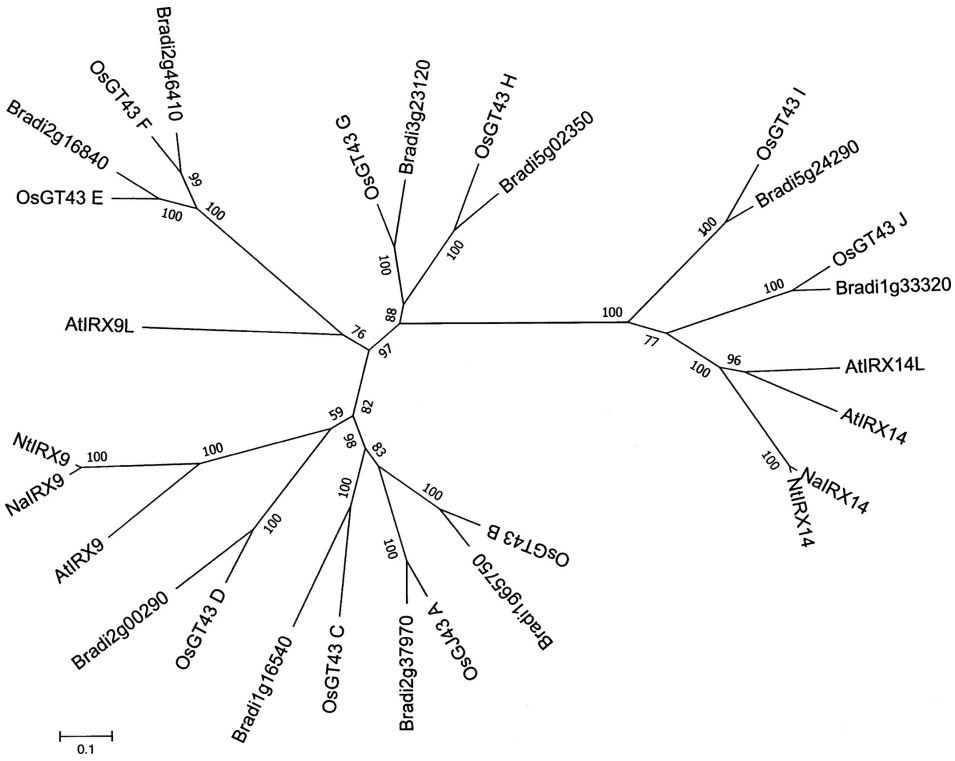

Figure 4.4: Phylogenetic analysis of the IRX9 and IRX14 proteins from Arabidopsis, tobacco, rice and Brachypodium. The sequence alignment was conducted using CLUSTALW and the phylogenetic analysis was done using the neighbour-joining method in MEGA 6.0. The bootstrap scores are from 2000 replicates and are shown on the nodes.

RNAi gene suppression of the candidate BdGT43A leads to altered cell wall composition and increased saccharification

Transgenic RNAi gene-silenced lines targeting *Bradi5g24290.1* were generated (Fig S4.10; Table S4.3) and analysed to explore the effect of the knockdown of the candidate gene on cell wall com- position, structure, and saccharification. The expression of the *Bd*GT43A gene was analysed in all transformants and four lines with expression levels of the gene reduced by c. 70 % in stem tissue were characterized (Fig 4.5a). Saccharification analysis using the same conditions as

in the RIL population screening was conducted and the released glucose for the silenced lines was measured against nontransformed Bd21 as the wild-type (Fig 4.5b). An increase in saccharification compared with the wild-type was observed in all four silenced lines, although only lines RNAi3 and RNAi4 showed a significant difference (Tukey's honest sig- nificant difference test). Interestingly, the transgenic plants showed no visible phenotype compared with the wild-type.

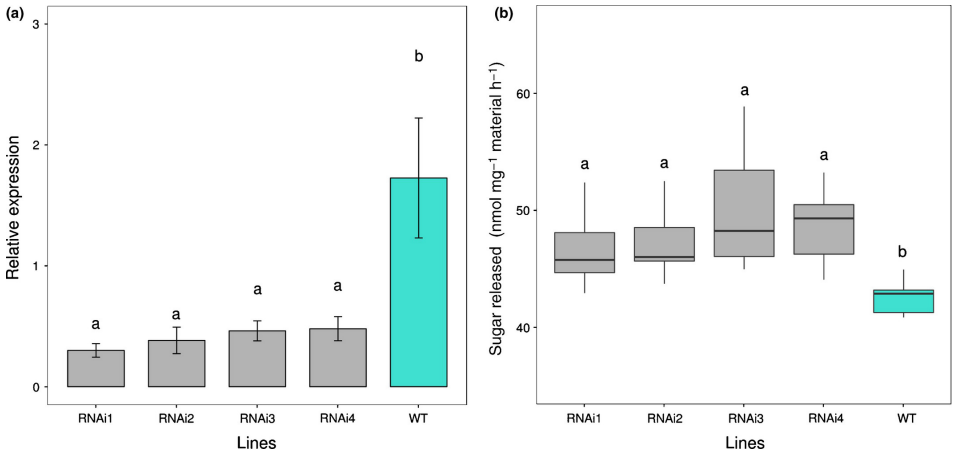

Figure 4.5: Analysis of the RNAinterference (RNAi) transgenic straw. (a) Transcript abundance indicated by the bar plot of the means for each level of independent variable of ANOVA showing ±SE. Tukey's honest significant difference (HSD) test indicates that those sharing the same letter are not significantly different. (b) Saccharification in silenced lines shown as boxplots to highlight the mean (line), 25^{th}–75^{th} percentile (box) and 10^{th}–90^{th} percentile (whiskers) of the glucose released for each genotype. Tukey's HSD test indicates that those sharing the same letter are not significantly different.

The cell walls of the transgenic plants and segregating wild-types were further analysed to understand the underlying cause of the differences in saccharification. Stems from the transgenic and wild-type plants were sequentially extracted with CDTA, Na_2CO_3, 1 M KOH and 4 M KOH to analyse the monosaccharide profile of matrix polysaccharide-enriched fractions. The 1 M KOH cell wall fraction from mutant lines showed a statistically significant lower amount of xylose (Fig 4.6a) and arabinose (Fig 4.6b) compared with wild-type plants.

It was previously reported that *irx14* mutants in Arabidopsis showed a decrease in stem xylose content and that this was accompanied by shorter xylan backbones [8]. The average chain length of xylans in the Brachypodium-silenced lines was investigated using size exclusion chromatographic analysis, but no significant differences were observed, although the abundance of xylans in the 1 M KOH

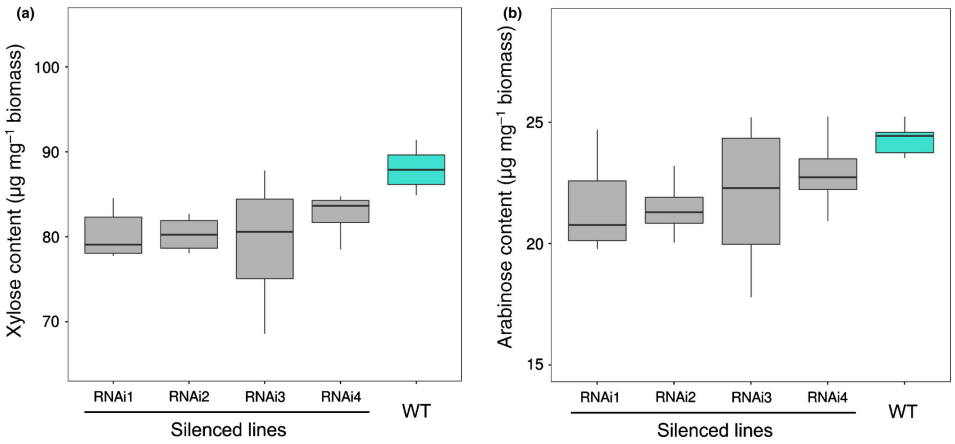

Figure 4.6: Amount of xylose (a) and arabinose (b) in the 1 M KOH cell wall fraction of silenced lines. The boxplots indicate the mean (line), 25^{th}–75^{th} percentile (box) and 10^{th}–90^{th} percentile (whiskers) for each genotype.

fraction from silenced lines is lower (Fig 4.7).

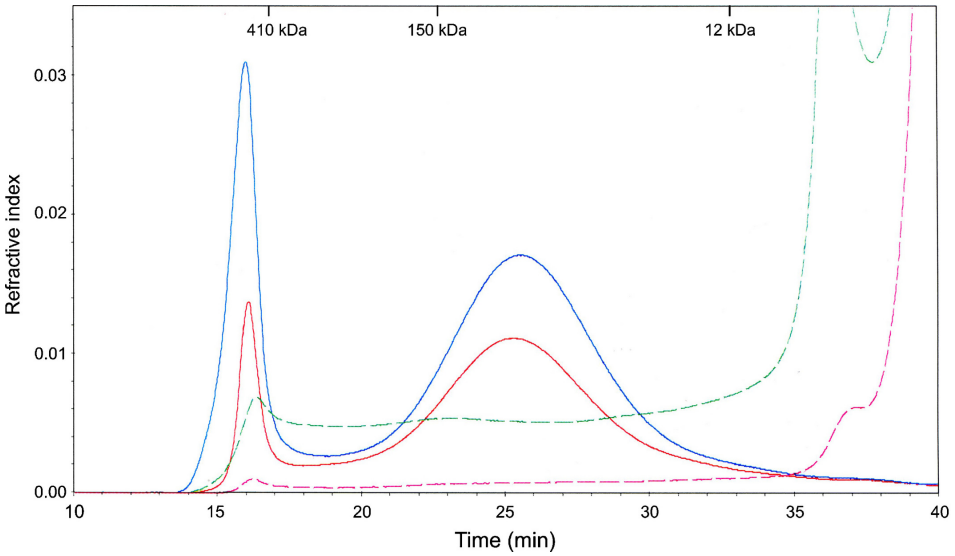

Figure 4.7: SECMALLS analysis to determine xylan chain length in the 1 M KOH fraction of cell walls from silenced lines. Blue line, wild type (WT) extracts; green dashed line, WT fraction treated with xylanase (control); red line, silenced lines; magenta dashed line, silenced control. Data shown are for the RNAi2, which is representative of the results obtained for all silenced lines. A 100 *upmu*l sample injection was used and data were analysed using AstraV software together with the Zimm Fit method to estimate the molecular weight. The sample refractive index increment was 0.145.

The amount of FA and pCA linked to arabinose residues in AX has been associated with the saccharification potential in grasses [23]. As the lines silenced for the

BdGT43A gene show a small but significant reduction in arabinose, the FA and pCA content of the cell wall was analysed in stems of both transgenic and wild-type plants. Transgenic lines showed a small but significant decrease in FA and an increase in pCA (Fig 4.8a,b) when compared with the wild-type.

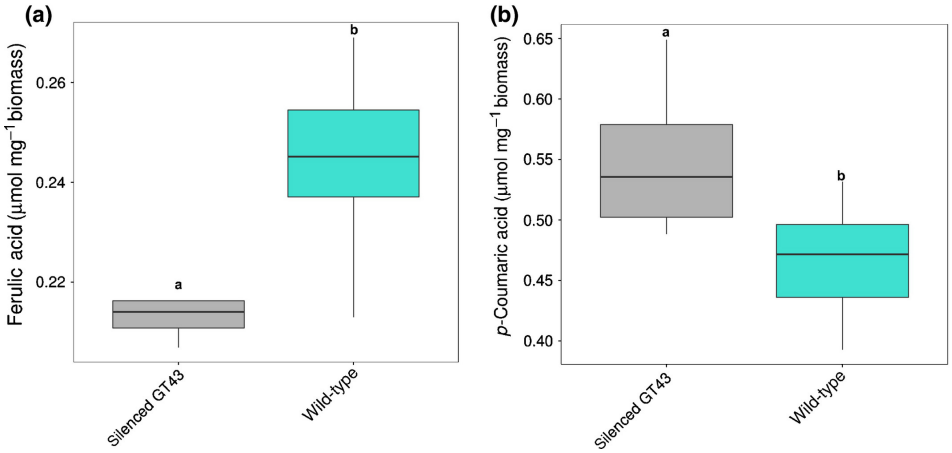

Figure 4.8: Amount of (a) ferulic acid and (b) p-coumaric acid in wild-type and the RNAi1 silenced line. The boxplots indicate the mean (line), 25^{th}–75^{th} percentile (box) and 10^{th}–90^{th} percentile (whiskers) for each genotype.

4.5. Discussion

Screening of the Brachpodium RIL population generated from a Bd3-1 9 Bd21 cross for straw saccharification revealed a single significant QTL for this characteristic on chromosome 5 (Fig 4.2). Analysis of the QTL interval on chromosome 5 revealed several candidate genes with known functions in the cell wall, the most plausible of which encodes a *GT43* gene orthologue of *AtIRX14* (Fig **??**), which is involved in the biosynthesis of the xylan backbone in Arabidopsis [13]. We tested if the BdGT43A gene is implicated in this process, by generating transgenic plants expressing RNAi gene suppression constructs, which showed an increase in straw saccharification compared with wild-type plants (Fig 4.5). Compositional analysis of cell wall matrix polysaccharides revealed decreased concentrations of xylose, arabinose and FA in the transgenic lines, suggesting that altered arabinoxylan composition was probably responsible for the increased digestibility of the straw.

The Brachypodium RIL population Bd3-1 9 Bd21 has been successfully used previously in the identification of the barley stripe mosaic virus resistant gene *bsr1* [29], QTLs for grass–pathogen interactions [50] and in understanding water-

use efficiency [51]. The parental lines in this population showed a significant difference in saccharification potential (Fig 4.1), allowing us to identify a single QTL for straw digestibility. A number of previous studies have identified QTLs for straw digestibility in rice [52, 53], maize [54], barley [55], sorghum [56] and *Miscanthus* [57]. None of these previous studies succeeded in identifying and validating the causative genes and SNPs.

A QTL for saccharification was detected on chromosome 5 (Fig 4.2). This QTL accounted for 11.83 % of the total variance observed for saccharification within the population, which classifies it as a major QTL [44, 45]. The heritability value for saccharification was 0.45, which is a slightly lower than that reported for saccharification as 0.53 in *Miscanthus* [57]. Saccharification is a trait determined by a large number of environmental factors. Indeed, various lignocellulosic traits in maize including neutral detergent fibre (NDF), acid detergent lignin (ADL) and acid detergent fibre (ADF), have higher values (0.92, 0.74 and 0.92, respectively) [58]. In this study we have identified a single QTL related to saccharification potential. In *Miscanthus*, using the same method, seven QTLs were identified [57]. There are a number of possible reasons for this low detection rate. First, the population size was relatively small and therefore only major QTLs could be detected [35]. Second, although the parental lines have a significant difference in digestibility, the value of this difference is relatively small [59]. In a recent study in rice we also detected a single QTL for saccharification, and observed that the parental lines, although not deviating enough from the median of the population, produced a progeny showing a much higher variation due to new combinations of interacting loci [60].

GT43 genes have been characterized in plants as causing an *irregular xylem (irx)* phenotype initially described in Arabidopsis as secondary cell wall mutants, some of them associated with decreased xylan content [61]. The *Bradi5g24290.1* gene family members have been suggested as putative β-1,4-xylan-synthases by [16]. *Bradi5g24290.1* RNAi gene-silenced lines showed expression levels that were c. 75 % below the wild-type, and stem saccharification was higher than in the wild-type. This increase in saccharification observed in the transgenic lines strongly supported the selection of *Bd*GT43A as the gene responsible for the QTL observed in chromosome 5, and was accompanied by a decrease in stem cell wall xylose content, evident in a 1 M KOH extracted fraction.

We could find little or no significant difference in the cell wall composition of our inbred lines carrying the alternate allelic forms. However, transgenic plants in which the expression of *Bd*GT43A was suppressed showed a stronger saccharification phenotype than the RILs. In addition to decreased xylose content, the *Bradi5g24290.1*-silenced lines showed a significant decrease in arabinose in the 1 M KOH cell wall fraction, most likely reflecting an overall decrease in AX.

In grasses, α-(1-3)-linked arabinofuranosyl substitutions can be esterified with FA or pCA. FA can form crosslinks with other AX chains or with lignin [62, 63]. The rice *GT61* gene, *XAX1*, has been shown to have decreased FA as well as xylose when expression is disrupted, and this is accompanied by an increase in stem digestibility [17]. *XAX1* appears to introduce xylosyl side chains associated with arabinosyl residues that carry FA esters, and the *xax1* mutant exhibits decreased concentrations of FA in its AX; a similar phenotype is reported in the Brachypodium *sac1* mutant, which may be an orthologue of the rice *XAX1* gene [1]. It is unclear what is involved in this change in FA content, but it has been proposed that this is produced because the FA is only added to the arabinose side chain once the xylosyl residues are in position [17].

Overexpression of the rice acyltransferase *OsAT10*, involved in the addition of hydroxycinnamates to arabinoxylans, leads to a decrease in FA and an increase in pCA, exposing a possible common regulation of both phenolics [23], and results in higher stem digestibility. A similar effect is observed in our *Bd*GT43A-silenced lines, where a decrease in the AX content is associated with lower FA content. Our results reaffirm the importance of AX in determining lignocellulose digestibility in grasses. Interestingly, we compared the saccharification of stems from Arabidopsis *irx14* mutants with their wild-type equivalents, but found no increased saccharification (Fig S4.11), although these mutants have significantly lower xylan content than wild-type Arabidopsis [61]. Arabidopsis xylans lack the extensive arabinosylation seen in grass xylans, as well as the associated FA esters. This suggests that it is the lower concentrations of FA seen in the *Bradi5g24290.1* gene suppression lines that are responsible for the increased saccharification of their stems.

4.6. Supporting Information

Additional Supporting Information may be found online in the Supporting Information tab for this article: Fig. S1 Sequence and map of the silencing construct.

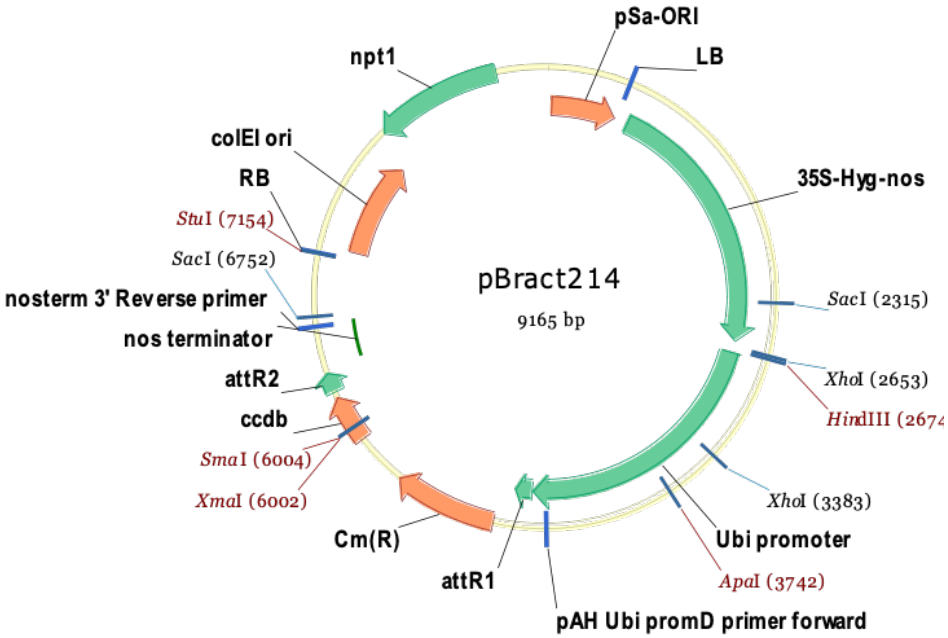

Figure 4.9: Sequence and map of the silencing construct.

```
      1 TTTTTATCCC CGGAAGCCTG TGGATAGAGG GTAGTTATCC ACGTGAAACC GCTAATGCCC
     61 CGCAAAGCCT TGATTCACGG GGCTTTCCGG CCCGCTCCAA AAACTATCCA CGTGAAATCG
    121 CTAATCAGGG TACGTGAAAT CGCTAATCGG AGTACGTGAA ATCGCTAATA AGGTCACGTG
    181 AAATCGCTAA TCAAAAAGGC ACGTGAGAAC GCTAATAGCC CTTTCAGATC AACAGCTTGC
    241 AAACACCCCT CGCTCCGGCA AGTAGTTACA GCAAGTAGTA TGTTCAATTA GCTTTTCAAT
    301 TATGAATATA TATATCAATT ATTGGTCGCC CTTGGCTTGT GGACAATGCG CTACGCGCAC
    361 CGGCTCCGCC CGTGGACAAC CGCAAGCGGT TGCCCACCGT CGAGCGCCAG CGCCTTTGCC
    421 CACAACCCGG CGGCCGGCCG CAACAGATCG TTTTATAAAT TTTTTTTTTT GAAAAAGAAA
                                                            LB
                                                            ~
    481 AAGCCCGAAA GGCGGCAACC TCTCGGGCTT CTGGATTTCC GATCCCCGGA ATTAGATCTT
         LB
~~~~~~~~~~~~~~~~~~~~~~~~~
    541 GGCAGGATAT ATTGTGGTGT AACGTATCAC AAGTTTGTAC AAAAAAGCAG GCTCCGCGGC
    601 CGCCCCCTTC ACCTAGACTC GACGCGTCCT AGAGATCCGT CAACATGGTG GAGCACGACA
    661 CTCTCGTCTA CTCCAAGAAT ATCAAAGATA CAGTCTCAGA AGACCAAAGG GCTATTGAGA
    721 CTTTTCAACA AAGGGTAATA TCGGGAAACC TCCTCGGATT CCATTGCCCA GCTATCTGTC
    781 ACTTCATCAA AAGGACAGTA GAAAAGGAAG GTGGCACCTA CAAATGCCAT CATTGCGATA
    841 AAGGAAAGGC TATCGTTCAA GATGCCTCTG CCGACAGTGG TCCCAAAGAT GGACCCCCAC
    901 CCACGAGGAG CATCGTGGAA AAAGAAGACG TTCCAACCAC GTCTTCAAAG CAAGTGGATT
```

```
 961 GATGTGATAT CTCCACTGAC GTAAGGGATG ACGCACAATC CCACTATCCT TCGCAAGACC
1021 CTTCCTCTAT ATAAGGAAGT TCATTTCATT TGGAGAGGAC GACCCCGATA TGAAAAAGCC
1081 TGAACTCACC GCGACGTCTG TCGAGAAGTT TCTGATCGAA AAGTTCGACA GCGTCTCCGA
1141 CCTGATGCAG CTCTCGGAGG GCGAAGAATC TCGTGCTTTC AGCTTCGATG TAGGAGGGCG
1201 TGGATATGTC CTGCGGGTAA ATAGCTGCGC CGATGGTTTC TACAAAGATC GTTATGTTTA
1261 TCGGCACTTT GCATCGGCCG CGCTCCCGAT TCCGGAAGTG CTTGACATTG GGGAATTCAG
1321 CGAGAGCCTG ACCTATTGCA TCTCCCGCCG TGCACAGGGT GTCACGTTGC AAGACCTGCC
1381 TGAAACCGAA CTGCCCGCTG TTCTGCAGGT AAATTTCTAG TTTTTCTCCT TCATTTTCTT
1441 GGTTAGGACC CTTTTCTCTT TTTATTTTTT TGAGCTTTGA TCTTTCTTTA AACTGATCTA
1501 TTTTTTAATT GATTGGTTAT GGTGTAAATA TTACATAGCT TTAACTGATA ATCTGATTAC
1561 TTTATTTCGT GTGTCTATGA TGATGATGAT AACTGCAGCC GGTCGCGGAG GCCATGGATG
1621 CGATCGCTGC GGCCGATCTT AGCCAGACGA GCGGGTTCGG CCCATTCGGA CCGCAAGGAA
1681 TCGGTCAATA CACTACATGG CGTGATTTCA TATGCGCGAT TGCTGATCCC CATGTGTATC
1741 ACTGGCAAAC TGTGATGGAC GACACCGTCA GTGCGTCCGT CGCGCAGGCT CTCGATGAGC
1801 TGATGCTTTG GGCCGAGGAC TGCCCCGAAG TCCGGCACCT CGTGCACGCG GATTTCGGCT
1861 CCAACAATGT CCTGACGGAC AATGGCCGCA TAACAGCGGT CATTGACTGG AGCGAGGCGA
1921 TGTTCGGGGA TTCCCAATAC GAGGTCGCCA ACATCTTCTT CTGGAGGCCG TGGTTGGCTT
1981 GTATGGAGCA GCAGACGCGC TACTTCGAGC GGAGGCATCC GGAGCTTGCA GGATCGCCGC
2041 GGCTCCGGGC GTATATGCTC CGCATTGGTC TTGACCAACT CTATCAGAGC TTGGTTGACG
2101 GCAATTTCGA TGATGCAGCT TGGGCGCAGG GTCGATGCGA CGCAATCGTC CGATCCGGAG
2161 CCGGGACTGT CGGGCGTACA CAAATCGCCC GCAGAAGCGC GGCCGTCTGG ACCGATGGCT
2221 GTGTAGAAGT ACTCGCCGAT AGTGGAAACC GACGCCCCAG CACTCGTCCG AGGGCAAAGG
                          SacI
                         ~~~~~~~
2281 AATAGAGTAG ATGCCGACCG GGATCCGGAG AGCTCGAATT TCCCCGATCG TTCAAACATT
2341 TGGCAATAAA GTTTCTTAAG ATTGAATCCT GTTGCCGGTC TTGCGATGAT TATCATATAA
2401 TTTCTGTTGA ATTACGTTAA GCATGTAATA ATTAACATGT AATGCATGAC GTTATTTATG
2461 AGATGGGTTT TTATGATTAG AGTCCCGCAA TTATACATTT AATACGCGAT AGAAAACAAA
2521 ATATAGCGCG CAAACTAGGA TAAATTATCG CGCGCGGTGT CATCTATGTT ACTAGATCGG
2581 GAATTCATCG ATGATATCAG ATCAAGGGTG GGCGCGCCGA ACCAGCTTTC TTGTACAAAG
        XhoI                 HindIII
       ~~~~~~               ~~~~~~
2641 TGGTGATCCC CCTCGAGGTC GACGGTATCG ATAAGCTTGA TATCGAATTC CGTGCAGCGT
2701 GACCCGGTCG TGCCCCTCTC TAGAGATAAT GAGCATTGCA TGTCTAAGTT ATAAAAAATT
2761 ACCACATATT TTTTTTGTCA CACTTGTTTG AAGTGCAGTT TATCTATCTT TATACATATA
2821 TTTAAACTTT ACTCTACGAA TAATATAATC TATAGTACTA CAATAATATC AGTGTTTTAG
2881 AGAATCATAT AAATGAACAG TTAGACATGG TCTAAAGGAC AATTGAGTAT TTTGACAACA
2941 GGACTCTACA GTTTTATCTT TTTAGTGTGC ATGTGTTCTC CTTTTTTTTT GCAAATAGCT
3001 TCACCTATAT AATACTTCAT CCATTTTATT AGTACATCCA TTTAGGGTTT AGGGTTAATG
3061 GTTTTTATAG ACTAATTTTT TTAGTACATC TATTTTATTC TATTTTAGCC TCTAAATTAA
3121 GAAAACTAAA ACTCTATTTT AGTTTTTTTA TTTAATAATT TAGATATAAA ATAGAATAAA
3181 ATAAAGTGAC TAAAAATTAA ACAAATACCC TTTAAGAAAT TAAAAAAACT AAGGAAACAT
3241 TTTTCTTGTT TCGAGTAGAT AATGCCAGCC TGTTAAACGC CGTCGACGAG TCTAACGGAC
3301 ACCAACCAGC GAACCAGCAG CGTCGCGTCG GGCCAAGCGA AGCAGACGGC ACGGCATCTC
                  XhoI
                 ~~~~~~
3361 TGTCGCTGCC TCTGGACCCC TCTCGAGAGT TCCGCTCCAC CGTTGGACTT GCTCCGCTGT
3421 CGGCATCCAG AAATTGCGTG TCGGACGGCA GACGTGAGCC GGCACGGCAG GCGGCCTCCT
3481 CCTCCTCTCA CGGCACCGGC AGCTACGGGG GATTCCTTTC CCACCGCTCC TTCGCTTTCC
3541 CTTCCTCGCC CGCCGTAATA AATAGACACC CCCTCCACAC CCTCTTTCCC CAACCTCGTG
```

```
    3601 TTGTTCGGAG CGCACACACA CACAACCAGA TCTCCCCCAA ATCCACCCGT CGGCACCTCC
    3661 GCTTCAAGGT ACGCCGCTCG TCCTCCCCCC CCCCCCCTCT CTACCTTCTC TAGATCGGCG
                 ApaI
                ~~~~~~~
    3721 TTCCGGTCCA TGGTTAGGGC CCGGTAGTTC TACTTCTGTT CATGTTTGTG TTAGATCCGT
    3781 GTTTGTGTTA GATCCGTGCT GCTAGCGTTC GTACACGGAT GCGACCTGTA CGTCAGACAC
    3841 GTTCTGATTG CTAACTTGCC AGTGTTTCTC TTTGGGGAAT CCTGGGATGG CTCTAGCCGT
    3901 TCCGCAGACG GGATCGATTT CATGATTTTT TTTTGTTTCG TTGCATAGGG TTTGGTTTGC
    3961 CCTTTTCCTT TATTTCAATA TATGCCGTGC ACTTGTTTGT CGGGTCATCT TTTCATGCTT
    4021 TTTTTTGTCT TGGTTGTGAT GATGTGGTCT GGTTGGGCGG TCGTTCTAGA TCGGAGTAGA
    4081 ATTAATTCTG TTTCAAACTA CCTGGTGGAT TTATTAATTT TGGATCTGTA TGTGTGTGCC
    4141 ATACATATTC ATAGTTACGA ATTGAAGATG ATGGATGGAA ATATCGATCT AGGATAGGTA
    4201 TACATGTTGA TGCGGGTTTT ACTGATGCAT ATACAGAGAT GCTTTTTGTT CGCTTGGTTG
    4261 TGATGATGTG GTGTGGTTGG GCGGTCGTTC ATTCGTTCTA GATCGGAGTA GAATACTGTT
    4321 TCAAACTACC TGGTGTATTT ATTAATTTTG GAACTGTATG TGTGTGTCAT ACATCTTCAT
    4381 AGTTACGAGT TTAAGATGGA TGGAAATATC GATCTAGGAT AGGTATACAT GTTGATGTGG
    4441 GTTTTACTGA TGCATATACA TGATGGCATA TGCAGCATCT ATTCATATGC TCTAACCTTG
    4501 AGTACCTATC TATTATAATA AACAAGTATG TTTTATAATT ATTTTGATCT TGATATACTT
        pAH Ubi_promD primer forward
        ~~~~~~~~~~~~~~~~~~~~~~~~~
    4561 GGATGATGGC ATATGCAGCA GCTATATGTG GATTTTTTTA GCCCTGCCTT CATACGCTAT
    4621 TTATTTGCTT GGTACTGTTT CTTTTGTCGA TGCTCACCCT GTTGTTTGGT GTTACTTCGC
    4681 CCATCACAAG TTTGTACAAA AAAGCTGAAC GAGAAACGTA AAATGATATA AATATCAATA
    4741 TATTAAATTA GATTTTGCAT AAAAAACAGA CTACATAATA CTGTAAAACA CAACATATCC
    4801 AGTCACTATG GCGGCCGCAT TAGGCACCCC AGGCTTTACA CTTTATGCTT CCGGCTCGTA
    4861 TAATGTGTGG ATTTTGAGTT AGGATCCGTC GAGATTTTCA GGAGCTAAGG AAGCTAAAAT
    4921 GGAGAAAAAA ATCACTGGAT ATACCACCGT TGATATATCC CAATGGCATC GTAAAGAACA
    4981 TTTTGAGGCA TTTCAGTCAG TTGCTCAATG TACCTATAAC CAGACCGTTC AGCTGGATAT
    5041 TACGGCCTTT TTAAAGACCG TAAAGAAAAA TAAGCACAAG TTTTATCCGG CCTTTATTCA
    5101 CATTCTTGCC CGCCTGATGA ATGCTCATCC GGAATTCCGT ATGGCAATGA AAGACGGTGA
    5161 GCTGGTGATA TGGGATAGTG TTCACCCTTG TTACACCGTT TTCCATGAGC AAACTGAAAC
    5221 GTTTTCATCG CTCTGGAGTG AATACCACGA CGATTTCCGG CAGTTTCTAC ACATATATTC
    5281 GCAAGATGTG GCGTGTTACG GTGAAAACCT GGCCTATTTC CCTAAAGGGT TTATTGAGAA
    5341 TATGTTTTTC GTCTCAGCCA ATCCCTGGGT GAGTTTCACC AGTTTTGATT TAAACGTGGC
    5401 CAATATGGAC AACTTCTTCG CCCCCGTTTT CACCATGGGC AAATATTATA CGCAAGGCGA
    5461 CAAGGTGCTG ATGCCGCTGG CGATTCAGGT TCATCATGCC GTTTGTGATG GCTTCCATGT
    5521 CGGCAGAATG CTTAATGAAT TACAACAGTA CTGCGATGAG TGGCAGGGCG GGGCGTAAAC
    5581 GCGTGGATCC GGCTTACTAA AAGCCAGATA ACAGTATGCG TATTTGCGCG CTGATTTTTG
    5641 CGGTATAAGA ATATATACTG ATATGTATAC CCGAAGTATG TCAAAAAGAG GTATGCTATG
    5701 AAGCAGCGTA TTACAGTGAC AGTTGACAGC GACAGCTATC AGTTGCTCAA GGCATATATG
    5761 ATGTCAATAT CTCCGGTCTG GTAAGCACAA CCATGCAGAA TGAAGCCCGT CGTCTGCGTG
    5821 CCGAACGCTG GAAAGCGGAA AATCAGGAAG GGATGGCTGA GGTCGCCCGG TTTATTGAAA
    5881 TGAACGGCTC TTTTGCTGAC GAGAACAGGG GCTGGTGAAA TGCAGTTTAA GGTTTACACC
    5941 TATAAAAGAG AGAGCCGTTA TCGTCTGTTT GTGGATGTAC AGAGTGATAT TATTGACACG
 XmaI
~~~~~~
 SmaI
~~~~~~
    6001 CCCGGGCGAC GGATGGTGAT CCCCCTGGCC AGTGCACGTC TGCTGTCAGA TAAAGTCTCC
    6061 CGTGAACTTT ACCCGGTGGT GCATATCGGG GATGAAAGCT GGCGCATGAT GACCACCGAT
```

```
6121 ATGGCCAGTG TGCCGGTCTC CGTTATCGGG GAAGAAGTGG CTGATCTCAG CCACCGCGAA
6181 AATGACATCA AAAACGCCAT TAACCTGATG TTCTGGGGAA TATAAATGTC AGGCTCCCTT
6241 ATACACAGCC AGTCTGCAGG TCGACCATAG TGACTGGATA TGTTGTGTTT TACAGTATTA
6301 TGTAGTCTGT TTTTTATGCA AAATCTAATT TAATATATTG ATATTTATAT CATTTTACGT
6361 TTCTCGTTCA GCTTTCTTGT ACAAAGTGGT GATGGGGGAT CCACTAGTTC TAGAATTCGA
6421 TTGAGTCAAG CAGGATCGTT CAAACATTTG GCAATAAAGT TTCTTAAGAT TGAATCCTGT
6481 TGCCGGTCTT GCGATGATTA TCATATAATT TCTGTTGAAT TACGTTAAGC ATGTAATAAT
6541 TAACATGTAA TGCATGACGT TATTTATGAG ATGGGTTTTT ATGATTAGAG TCCCGCAATT
6601 ATACATTTAA TACGCGATAG AAAACAAAAT ATAGCGCGCA AACTAGGATA AATTATCGCG
                     nosterm_3' Reverse primer
                     ~~~~~~~~~~~~~~~~~~~~~~~~
6661 CGCGGTGTCA TCTATGTTAC TAGATCGACC GGCATGCAAG CTGATATCAA TCACTAGTGA
                      SacI
                     ~~~~~~~
6721 ATTCTAGAGC GGCCGCCACC GCGGTGGAGC TCCAGCTTTT GTTCCCTTTA GTGAGGGTTA
6781 ATTGCGCGCT TGGCGTAATC ATGGTCATAG CTGTTTCCTG TGTGAAATTG TTATCCGCTC
6841 ACAATTCCAC ACAACATACG AGCCGGAAGC ATAAAGTGTA AAGCCTGGGG TGCCTAATGA
6901 GTGAGCTAAC TCACATTAAT TGCGTTGCGC TCACTGCCCG CTTTCCAGTC GGGAAACCTG
6961 TCGTGCCAGC TGCATTAATG AATCGGCCAA CGCGCGGGGA GAGGCGGTTT GCGTATTGGG
7021 CGCTCTTCCG CTTCCTCGCT CACTGACTCG CTGCGCTCGG TCGTTCGGCT GCGGCGAGCG
7081 GTATCAGCTC ACTCAAAGGC GGTAATACGG TTATCCACAG AATCAGGGGA TAACGCAGGA
                     RB
            ~~~~~~~~~~~~~~~~~~~~~~~~~~~~
       StuI
      ~~~~~~
7141 AAGAACATGA AGGCCTTGAC AGGATATATT GGCGGGTAAA CTAAGTCGCT GTATGTGTTT
7201 GTTTGAGATC TCATGTGAGC AAAAGGCCAG CAAAAGGCCA GGAACCGTAA AAAGGCCGCG
7261 TTGCTGGCGT TTTTCCATAG GCTCCGCCCC CCTGACGAGC ATCACAAAAA TCGACGCTCA
7321 AGTCAGAGGT GGCGAAACCC GACAGGACTA TAAAGATACC AGGCGTTTCC CCCTGGAAGC
7381 TCCCTCGTGC GCTCTCCTGT TCCGACCCTG CCGCTTACCG GATACCTGTC CGCCTTTCTC
7441 CCTTCGGGAA GCGTGGCGCT TTCTCATAGC TCACGCTGTA GGTATCTCAG TTCGGTGTAG
7501 GTCGTTCGCT CCAAGCTGGG CTGTGTGCAC GAACCCCCCG TTCAGCCCGA CCGCTGCGCC
7561 TTATCCGGTA ACTATCGTCT TGAGTCCAAC CCGGTAAGAC ACGACTTATC GCCACTGGCA
7621 GCAGCCACTG GTAACAGGAT TAGCAGAGCG AGGTATGTAG GCGGTGCTAC AGAGTTCTTG
7681 AAGTGGTGGC CTAACTACGG CTACACTAGA AGAACAGTAT TTGGTATCTG CGCTCTGCTG
7741 AAGCCAGTTA CCTTCGGAAG AAGAGTTGGT AGCTCTTGAT CCGGCAAACA AACCACCGCT
7801 GGTAGCGGTG GTTTTTTTGT TTGCAAGCAG CAGATTACGC GCAGAAAAAA AGGATCTCAA
7861 GAAGATCCTT TGATCTTTTC TACGGGGTCT GACGCTCAGT GGAACGAAAA CTCACGTTAA
7921 GGGATTTTGG TCATGAGATT ATCAAAAAGG ATCTTCACCT AGATCCTTTT AAATTAAAAA
7981 TGAAGTTTTA AATCAATCTA AAGTATATAT GTGTAACATT GGTCTAGTGA TTAGAAAAAC
8041 TCATCGAGCA TCAAATGAAA CTGCAATTTA TTCATATCAG GATTATCAAT ACCATATTTT
8101 TGAAAAAGCC GTTTCTGTAA TGAAGGAGAA AACTCACCGA GGCAGTTCCA TAGGATGGCA
8161 AGATCCTGGT ATCGGTCTGC GATTCCGACT CGTCCAACAT CAATACAACC TATTAATTTC
8221 CCCTCGTCAA AAATAAGGTT ATCAAGTGAG AAATCACCAT GAGTGACGAC TGAATCCGGT
8281 GAGAATGGCA AAAGTTTATG CATTTCTTTC CAGACTTGTT CAACAGGCCA GCCATTACGC
8341 TCGTCATCAA AATCACTCGC ATCAACCAAA CCGTTATTCA TTCGTGATTG CGCCTGAGCG
8401 AGACGAAATA CGCGATCGCT GTTAAAAGGA CAATTACAAA CAGGAATCGA ATGCAACCGG
8461 CGCAGGAACA CTGCCAGCGC ATCAACAATA TTTTCACCTG AATCAGGATA TTCTTCTAAT
8521 ACCTGGAATG CTGTTTTCCC TGGGATCGCA GTGGTGAGTA ACCATGCATC ATCAGGAGTA
8581 CGGATAAAAT GCTTGATGGT CGGAAGAGGC ATAAATTCCG TCAGCCAGTT TAGTCTGACC
```

Oligo Name	Sequence 5’ to 3’
miR-XS24290A-I	agTCTTCAGTATTTACTACGCTGcaggagattcagtttga
miR-XS24290A-II	tgCAGCGTAGTAAATACTGAAGActgctgctgctacagcc
miR*-XS24290A-III	ctCAGCGAAGTTAATACTGAAGAttcctgctgctaggctg
miR*-XS24290A-IV	aaTCTTCAGTATTAACTTCGCTGagagaggcaaaagtgaa
miR-XS24290B-I	agTTCAAATTTCCATACATGCGGcaggagattcagtttga
miR-XS24290B-II	tgCCGCATGTATGGAAATTTGAActgctgctgctacagcc
miR*-XS24290B-III	ctCCGCAAGTAAGGAAATTTGAAttcctgctgctaggctg
miR*-XS24290B-IV	aaTTCAAATTTCCTTACTTGCGGagagaggcaaaagtgaa
G-4368	CTGCAAGGCGATTAAGTTGGGTAAC
G-4369	GCGGATAACAATTTCACACAGGAAACAG

Table 4.2: Primers used during construction of the RNAi lines.

```
8641 ATCTCATCTG TAACAACATT GGCAACGCTA CCTTTGCCAT GTTTCAGAAA CAACTCTGGC
8701 GCATCGGGCT TCCCATACAA TCGGTAGATT GTCGCACCTG ATTGCCCGAC ATTATCGCGA
8761 GCCCATTTAT ACCCATATAA ATCAGCATCC ATGTTGGAAT TTAATCGCGG CCTTGAGCAA
8821 GACGTTTCCC GTTGAATATG GCTCATAACA CCCCTTGTAT TACTGTTTAT GTAAGCAGAC
8881 AGTTTTATTG TTCATGATGA TATATTTTTA TCTTGTGCAA TGTAACATCA GAGATTTTGA
8941 GACACAACGT GGCTTTGTTG AATAAATCGA ACTTTTGCTG AGTTGAAGGA TCAGATCACG
9001 CATCTTCCCG ACAACGCAGA CCGTTCCGTG GCAAAGCAAA AGTTCAAAAT CACCAACTGG
9061 TCCACCTACA ACAAAGCTCT CATCAACCGT GGCTCCCTCA CTTTCTGGCT GGATGATGGG
9121 GCGATTCAGG CGATCCCCAT CCAACAGCCC GCCGTCGAGC GGGCT
```

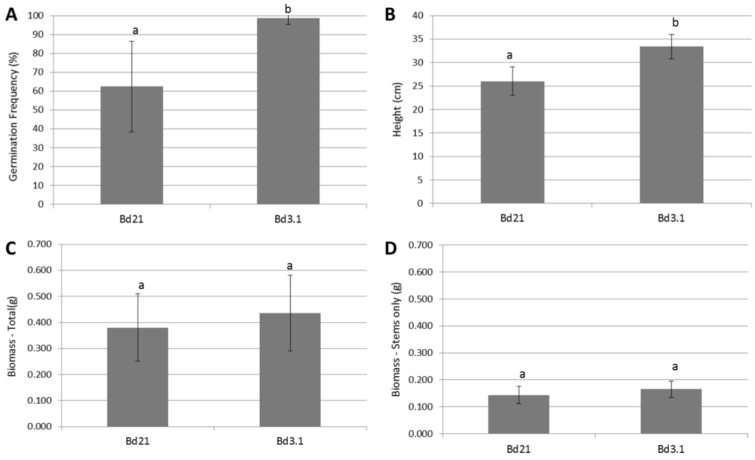

Figure 4.10: Comparison of the Brachypodium parental lines Bd21 and Bd3-1 in terms of (A) germination frequency (B) height, excluding inflorescence (C) total biomass and (D) stem only biomass. The results indicate the mean and ±SD and Anova indicates that those sharing the same letter are not significantly different.

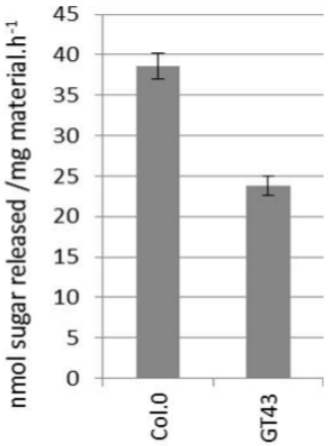

Figure 4.11: Saccharification analysis of Arabidopsis Col.0 and T- DNA line GT43. The results indicate the mean and *pm*SD.

Oligo Name	Direction	Size (bp)	Sequence 5' to 3'
SamDC	Forward	190	TGCTAATCTGCTCCAATGGC
	Reverse		GACGCAGCTGACCACCTAGA
UBC18	Forward	193	GGAGGCACCTCAGGTCATTT
	Reverse		ATAGCGGTCATTGTCTTGCG
Ubi10	Forward	237	TCCACACTCCACTTGGTGCT
	Reverse		GAGGGTGGACTCCTTTTGGA
BraXS90-RT-1	Forward	167	CACGCCCTCAGGGAGATACG
	Reverse		AACGACTCCTTGGTGCCTTC
BraXS90-RT-2	Forward	163	AGTCAAATTCCCGCATGAATGG
	Reverse		TCGGTGGAGGCTTCACAAAG

Table 4.3: Primers used during qPCR of the RNAi lines.

Gene Name	Function	Pfam	Panther
Bradi5g 24160.1	Motor activity, ATPase activity, Rab GTPase binding		GOLGIN-84
24160.2	Motor activity, ATPase activity, Rab GTPase binding		GOLGIN-84
24170.1	Secondary active sulfate transmembrane transporter activity, chloride channel activity, anion exchanger activity	Sulfate transporter family	Sulfate transporter
24170.2	Secondary active sulfate transmembrane transporter activity, chloride channel activity, anion exchanger activity	Sulfate transporter family	Sulfate transporter
24180.1	WAK receptor-like protein kinase, expressed, subfamily WAKb	Protein kinase domain	
24190.1	WAK receptor-like protein kinase, expressed, subfamily WAKb	Protein kinase domain	
24200.1	Putative Gene	Peroxidase	
24207.1	Putative Gene	Alpha-N-acetylglucosaminidase (NAGLU)	Alpha-N-acetylglucosaminidase

Gene Name	Function	Pfam	Panther
24220.1	Transcription corepressor activity, phosphoglycerate dehydrogenase activity		2-Hydroxyacid dehydrogenase
24227.1	Putative Gene	Asparaginase	Protease T2 asparaginase
24240.1	Putative Gene	Sec1 family	Vesicle protein sorting-associated
24250.1	Single-standed DNA specific 3'-5' exodeoxyribonuclease activity	Exonuclease	Exonuclease-related
24257.1	Putative Gene	DUF2930	
24267.1	Putative Gene	Dedicator of cytokinesis	dedicator of cytokinesis (DOCK)
24280.1	UDP-galactosyltransferase activity	UDP-glucoronosyl and UDP-glucosyl transferase	UDP-glucuronosyltransferase related
24290.1	Putative xylosyltransferase, CAZy family GT43	Glycosyltransferase family 43	Beta-1,3-glucuronyltransferase-related

Gene Name	Function	Pfam	Panther
24300.1	Serine-type carboxypeptidase activity	Serine carboxypeptidase	Serine carbosypeptidase II (carboxypeptidase D)
24310.1	WAK receptor-like protein kinase, expressed, subfamily WAKb	Protein kinase domain	
24320.1	Putative Gene		
24330.1	Putative Gene		
34340.1	Putative Gene		
34350.1	Putative Gene		
24360.1	Putative Gene	AP2 domain	Protein kinase
24370.1	NADPH-hemoprotein reductase activity, iron ion binding, FAD binding, nitric-oxide synthase activity		NADPH-cytochrome P450 reductase
24380.1	Putative Gene	AUX/IAA family	
24387.1	Putative Gene	Sodium/calcium exchanger protein	
24397.1	Putative Gene	Transmembrane proteins 14C	
24410.1	Putative Gene	Tify domain	
24410.2	Putative Gene	Tify domain	

Gene Name	Function	Pfam	Panther
24420.1	Aminoacyl-tRNA hydrolase activity	Peptidyl-tRNA hydrolase PTH2	Peptidyl-tRNA hydrolase 2
24430.1	Endonuclease activity	S1/P1 nuclease	
24430.2	Endonuclease activity	S1/P1 nuclease	
24440.1	Putative Gene		
24450.1	Protein kinase family protein, putative, expressed, subfamily RLCK-VI	Protein tyrosine kinase	
24460.1	Putative Gene	Calmodulin binding protein-like	
24460.2	Putative Gene	Calmodulin binding protein-like	
24460.3	Putative Gene	Calmodulin binding protein-like	
24470.1	Metalloendopeptidase activity	Mov34/MPN/PAD-1 family	JUN activation domain binding protein
24480.1	Protein kinase family protein, putative, subfamily, SD-2a	Protein kinase domain	
24490.1	F-Box	F-Box	
24490.2	F-Box	F-Box	

Gene Name	Function	Pfam	Panther
24490.3	F-Box	F-Box	
24500.1	Serine-type endopeptidase activity		Subtilinsin/Kexin-related serine protease
24510.1	Putative Gene		
24520.1	Serine-type endopeptidase activity	Peptidase inhibitor I9	Subtilinsin/Kexin-related serine protease
24530.1	Protein serine/threonine phosphatase activity	Protein phosphatase 2C	Protein phosphatase 2c
24536.1	Putative Gene		
24542.1	Putative Gene	Cupin superfamily protein	MINA53 (MYC induced nuclear antigen
24550.1	Glutamate-ammonia ligase activity, ATP binding	Glutamine synthetase	Glutamine synthetase
24550.2	Glutamate-ammonia ligase activity, ATP binding	Glutamine synthetase	Glutamine synthetase
24560.1	Putative Gene		

Gene Name	Function	Pfam	Panther
24570.1	Protein kinase family protein, putative, subfamily, RLCK-OS1	Protein kinase domain	
24580.1	Putative Gene	Nucleolar protein, Nop52	NNP-1 protein (novel nuclear protein 1, NOP52
24590.1	ATP binding	ATPase family associated with various cellular activities (AAA)	
24600.1	Putative Gene		
24610.2	Glucose-6-phosphate 1-epimerase activity	Aldose 1-epimerase	Apospory-associated protein c-related
24610.3	Glucose-6-phosphate 1-epimerase activity	Aldose 1-epimerase	Apospory-associated protein c-related
24610.4	Glucose-6-phosphate 1-epimerase activity	Aldose 1-epimerase	Apospory-associated protein c-related
24620.1	Putative Gene		

Gene Name	Function	Pfam	Panther
24630.1	ATP binding	Lipase (class 3)	Alpha/beta hydrolase related
24640.1	Protein farnesyltransferase activity	Polyprenyl synthetase	Farnesylprophosphate synthetase
24640.2	Protein farnesyltransferase activity	Polyprenyl synthetase	Farnesylprophosphate synthetase
24650.1	Putative Gene	Peroxidase	
24660.1	Putative Gene	Universal stress protein family	
24670.1	Putative Gene	SBP domain	
24680.1	Putative Gene	Ribosomal protein L7Ae/L30e/S12e/Gadd45 family	60S Ribosomal protein 10A-related
24690.1	Autoinhibited H+ P-type ATPase subfamily P3 cluster 2 from PMID:12805592. Similar to AtAHA1 plasma membrane H+ transporter		
24700.1	Putative Gene	AP2 domain	

Gene Name	Function	Pfam	Panther
24710.1	Putative Gene	AP2 domain	
24720.1	Putative Gene	AP2 domain	
24730.1	Protein kinase activity		
24730.2	Protein kinase activity		
24737.1	Putative Gene	Protein tyrosine kinase	
24750.1	Protein kinase family protein, putative, expressed, subfamily RLCK-Os4	Protein tyrosine kinase	
24760.1	Protein kinase family protein, putative, expressed, subfamily RLCK-Os4	Protein tyrosine kinase	
24770.1	Putative Gene		
24780.1	Serine-type endopeptidase activity		Subtilisin/Kexin-related Serine protease
24790.1	BTB	BTB/POZ domain	
24800.1	Neutral amino acid transmembrane transporter activity, L-amino acid transmembrane transporter activity	Transmembrane amino acid transporter protein	Amino acid transporter
24810.1	Neutral amino acid transmembrane transporter activity, L-amino acid transmembrane transporter activity	Transmembrane amino acid transporter protein	Amino acid transporter

Gene Name	Function	Pfam	Panther
24820.1	Endoribonuclease activity	eRF1 domain	PELOTA
24830.1	Putative Gene		
24836.1	Putative Gene	ABC1 family	ABC transporter-related
24842.1	Putative Gene		
24850.1	Similar to UDP-arabinopyranose mutase. Reversibly glycosylated polypeptide. CAZy family GT75	Reversibly glycosylated polypeptiede	
24860.1	Putative Gene		
24870.1	STE_MEKK_ste11_MAP3K.24 - STE kinases include homologs to sterile 7, sterile 11 and sterile 20 from yeast, expressed, subfamily	Protein kinase domain	
24870.2	STE_MEKK_ste11_MAP3K.24 - STE kinases include homologs to sterile 7, sterile 11 and sterile 20 from yeast, expressed, subfamily	Protein kinase domain	

Gene Name	Function	Pfam	Panther
24870.3	STE_MEKK_ste11_MAP3K.24 - STE kinases include homologs to sterile 7, sterile 11 and sterile 20 from yeast, expressed, subfamily	Protein kinase domain	
24880.1	Putative Gene	Heavy-metal-associated domain	Copper transport protein ATOX1-related
24890.1	Inositol pentakisphosphate 2-kinase activity, ATP binding	Inositol-pentakisphosphate 2-kinase	Inositol polyphosphate kinase 1
24900.1	Putative Gene		
24900.3	Putative Gene		
24910.1	Putative Gene		
24917.1	Putative Gene	Eukaryotic DNA topoisomerase I	DNA topoisomerase Type 1
24930.1	Putative Gene		Molybdopterin biosynthesis protein

Gene Name	Function	Pfam	Panther
24930.3	Putative Gene		Molybdopterin biosynthesis protein
24930.4	Putative Gene		Molybdopterin biosynthesis protein
24937.1	Putative Gene		
24950.1	Transcription coactivator activity	MED7 protein	
24950.3	Transcription coactivator activity	MED7 protein	
24960.1	26S, subfamily 19S	Mov34/MPN/PAD-1 family	EIF3F-related
24967.1	Putative Gene	BSD domain	
24980.1	Putative Gene		40S Ribosomal protein S9

Table 4.4: Genes identified on chromosome 5 around the QTL linked to marker BD1676_1.

Database	Predicted amino acid not tolerated	Number of sequences compared	Sequences represented	Predicted amino acid tolerated
SwissPort	ywvtsrqpnmlkihgfedc	15	0.06	a
TreMBL	whyfimqrndelckvtp	54	0.16	gsa
UniRef90	whyfmiqrndelckvtpg	61	0.1	sa
NCBI	whyfimqrndelkcvtp	72	0.15	gsa

Table 4.5: SIFT analysis of the changes produced by the SNP in *Bradi5g24290.1*.

Referencias

[1] Poppy E. Marriott, Leonardo D. Gómez, and Simon J. McQueen-Mason. Unlocking the potential of lignocellulosic biomass through plant science. *New Phytologist*, 209(4):1366–1381, March 2016. 00007.

[2] Leonardo D. Gomez, Jennifer K. Bristow, Emily R. Statham, and Simon J. McQueen-Mason. Analysis of saccharification in Brachypodium distachyon stems under mild conditions of hydrolysis. *Biotechnology for Biofuels*, 1:15, 2008. 00036.

[3] S. Kent Hoekman. Biofuels in the U.S. – Challenges and Opportunities. *Renewable Energy*, 34(1):14–22, January 2009.

[4] S. N. Naik, Vaibhav V. Goud, Prasant K. Rout, and Ajay K. Dalai. Production of first and second generation biofuels: A comprehensive review. *Renewable and Sustainable Energy Reviews*, 14(2):578–597, February 2010.

[5] William S York and Malcolm A O'Neill. Biochemical control of xylan biosynthesis — which end is up? *Current Opinion in Plant Biology*, 11(3):258–265, June 2008. 00130.

[6] Henrik Vibe Scheller and Peter Ulvskov. Hemicelluloses. *Annual Review of Plant Biology*, 61(1):263–289, 2010.

[7] Marta Busse-Wicher, Thiago C F Gomes, Theodora Tryfona, Nino Nikolovski, Katherine Stott, Nicholas J Grantham, David N Bolam, Munir S Skaf, and Paul Dupree. The pattern of xylan acetylation suggests xylan may interact with cellulose microfibrils as a twofold helical screw in the secondary plant cell wall of Arabidopsis thaliana. *The Plant Journal*, 79(3):492–506, August 2014.

[8] David M. Brown, Florence Goubet, Vicky W. Wong, Royston Goodacre, Elaine Stephens, Paul Dupree, and Simon R. Turner. Comparison of five xylan synthesis mutants reveals new insight into the mechanisms of xylan synthesis. *The Plant Journal*, 52(6):1154–1168, December 2007. 00199.

[9] Emilie A Rennie and Henrik Vibe Scheller. Xylan biosynthesis. *Current Opinion in Biotechnology*, 26:100–107, April 2014. 00099.

[10] Wei Zeng, Nan Jiang, Ramya Nadella, Tara L. Killen, Vijayanand Nadella, and Ahmed Faik. A Glucurono(arabino)xylan Synthase Complex from Wheat Contains Members of the GT43, GT47, and GT75 Families and Functions Cooperatively. *Plant Physiology*, 154(1):78–97, September 2010.

[11] Breeanna R. Urbanowicz, Maria J. Peña, Heather A. Moniz, Kelley W. Moremen, and William S. York. Two Arabidopsis proteins synthesize acetylated xylan in vitro. *The Plant Journal*, 80(2):197–206, 2014.

[12] Yanfang Ren, Sara Fasmer Hansen, Berit Ebert, Jane Lau, and Henrik Vibe Scheller. Site-Directed Mutagenesis of IRX9, IRX9l and IRX14 Proteins Involved in Xylan Biosynthesis: Glycosyltransferase Activity Is Not Required for IRX9 Function in Arabidopsis. *PLOS ONE*, 9(8):e105014, 2014.

[13] Ai-Min Wu, Emma Hörnblad, Aline Voxeur, Lorenz Gerber, Christophe Rihouey, Patrice Lerouge, and Alan Marchant. Analysis of the Arabidopsis IRX9/IRX9-L and IRX14/IRX14-L pairs of glycosyltransferase genes reveals critical contributions to biosynthesis of the hemicellulose glucuronoxylan. *Plant Physiology*, 153(2):542–554, June 2010. 00107.

[14] Chanhui Lee, Quincy Teng, Ruiqin Zhong, Youxi Yuan, and Zheng-Hua Ye. Functional roles of rice glycosyltransferase family GT43 in xylan biosynthesis. *Plant Signaling & Behavior*, 9, February 2014.

[15] Dawn Chiniquy, Patanjali Varanasi, Taeyun Oh, Jesper Harholt, Jacob Katnelson, Seema Singh, Manfred Auer, Blake Simmons, Paul D. Adams, Henrik V. Scheller, and Pamela C. Ronald. Three novel rice genes closely related to the Arabidopsis IRX9, IRX9l, and IRX14 genes and their roles in xylan biosynthesis. *Plant Biotechnology*, 4:83, 2013. 00018.

[16] Rowan A. C. Mitchell, Paul Dupree, and Peter R. Shewry. A Novel Bioinformatics Approach Identifies Candidate Genes for the Synthesis and Feruloylation of Arabinoxylan. *Plant Physiology*, 144(1):43–53, May 2007.

[17] Dawn Chiniquy, Vaishali Sharma, Alex Schultink, Edward E. Baidoo, Carsten Rautengarten, Kun Cheng, Andrew Carroll, Peter Ulvskov, Jesper Harholt, Jay D. Keasling, Markus Pauly, Henrik V. Scheller, and Pamela C. Ronald. XAX1 from glycosyltransferase family 61 mediates xylosyltransfer to rice xylan. *Proceedings of the National Academy of Sciences of the United States of America*, 109(42):17117–17122, October 2012.

[18] Nadine Anders, Mark D. Wilkinson, Alison Lovegrove, Jacqueline Freeman, Theodora Tryfona, Till K. Pellny, Thilo Weimar, Jennifer C. Mortimer, Katherine Stott, John M. Baker, Michael Defoin-Platel, Peter R. Shewry, Paul Dupree, and Rowan A. C. Mitchell. Glycosyl transferases in family 61 mediate arabinofuranosyl transfer onto xylan in grasses. *Proceedings of the National Academy of Sciences*, 109(3):989–993, January 2012. 00088.

[19] R D Hatfield, J R Wilson, and D R Mertens. Composition of cell walls isolated from cell types of grain sorghum stems. *Journal of the Science of Food and Agriculture*, 79(6):891–899, May 1999. 00079.

[20] Luc Saulnier and Jean-François Thibault. Ferulic acid and diferulic acids as components of sugar-beet pectins and maize bran heteroxylans. *Journal of the Science of Food and Agriculture*, 79(3):396–402, March 1999.

[21] Marcia M. de O. Buanafina, Tim Langdon, Barbara Hauck, Sue Dalton, and Phillip Morris. Expression of a fungal ferulic acid esterase increases cell wall digestibility of tall fescue (Festuca arundinacea). *Plant Biotechnology Journal*, 6(3):264–280, April 2008. 00057.

[22] John Ralph, Mirko Bunzel, Jane M. Marita, Ronald D. Hatfield, Fachuang Lu, Hoon Kim, Paul F. Schatz, John H. Grabber, and Hans Steinhart. Peroxidase-dependent cross-linking reactions of p-hydroxycinnamates in plant cell walls. *Phytochemistry Reviews*, 3(1-2):79–96, January 2004. 00200.

[23] Laura E. Bartley, Matthew L. Peck, Sung-Ryul Kim, Berit Ebert, Chithra Manisseri, Dawn M. Chiniquy, Robert Sykes, Lingfang Gao, Carsten Rautengarten, Miguel E. Vega-Sánchez, Peter I. Benke, Patrick E. Canlas, Peijian Cao, Susan Brewer, Fan Lin, Whitney L. Smith, Xiaohan Zhang, Jay D. Keasling, Rolf E. Jentoff, Steven B. Foster, Jizhong Zhou, Angela Ziebell, Gynheung An, Henrik V. Scheller, and Pamela C. Ronald. Overexpression of a BAHD Acyltransferase, OsAt10, Alters Rice Cell Wall Hydroxycinnamic Acid Content and Saccharification. *Plant Physiology*, 161(4):1615–1633, April 2013. 00050.

[24] Prashant Mohan-Anupama Pawar, Marta Derba-Maceluch, Sun-Li Chong, Leonardo D. Gómez, Eva Miedes, Alicja Banasiak, Christine Ratke, Cyril Gaertner, Grégory Mouille, Simon J. McQueen-Mason, Antonio Molina, Anita Sellstedt, Maija Tenkanen, and Ewa J. Mellerowicz. Expression of fungal acetyl xylan esterase in Arabidopsis thaliana improves saccharification of stem lignocellulose. *Plant Biotechnology Journal*, 14(1):387–397, January 2016.

[25] Rakesh Bhatia, Joe A. Gallagher, Leonardo D. Gomez, and Maurice Bosch. Genetic engineering of grass cell wall polysaccharides for biorefining. *Plant Biotechnology Journal*, 15(9):1071–1092, September 2017.

[26] A. J. Cardinal, M. Lee, and K. J. Moore. Genetic mapping and analysis of quantitative trait loci affecting fiber and lignin content in maize. *TAG. Theoretical and applied genetics. Theoretische und angewandte Genetik*, 106(5):866–874, March 2003.

[27] Audrey Courtial, Valerie Mechin, Matthieu Reymond, Jacqueline Grima-Pettenati, and Yves Barrière. Colocalizations between several QTLs for cell wall degradability and composition in the F288 x F271 early maize RIL progeny raise the question of the nature of the possible underlying

determinants and breeding targets for biofuel capacity. *BioEnergy Research*, 7(1):142–156, 2014.

[28] Yves Barrière, Audrey Courtial, Marçal Soler, and Jacqueline Grima-Pettenati. Toward the identification of genes underlying maize QTLs for lignin content, focusing on colocalizations with lignin biosynthetic genes and their regulatory MYB and NAC transcription factors. *Molecular Breeding*, 35(3):87, March 2015.

[29] Yu Cui, Mi Yeon Lee, Naxin Huo, Jennifer Bragg, Lijie Yan, Cheng Yuan, Cui Li, Sara J. Holditch, Jingzhong Xie, Ming-Cheng Luo, Dawei Li, Jialin Yu, Joel Martin, Wendy Schackwitz, Yong Qiang Gu, John P. Vogel, Andrew O. Jackson, Zhiyong Liu, and David F. Garvin. Fine Mapping of the Bsr1 Barley Stripe Mosaic Virus Resistance Gene in the Model Grass Brachypodium distachyon. *PLOS ONE*, 7(6):e38333, June 2012.

[30] R Core Team. *R: A Language and Environment for Statistical Computing*. R Foundation for Statistical Computing, Vienna, Austria, 2016. 49578.

[31] Torsten Hothorn, Frank Bretz, and Peter Westfall. Simultaneous inference in general parametric models. *Biometrical Journal. Biometrische Zeitschrift*, 50(3):346–363, June 2008.

[32] Leonardo D. Gomez, Caragh Whitehead, Abdellah Barakate, Claire Halpin, and Simon J. McQueen-Mason. Automated saccharification assay for determination of digestibility in plant materials. *Biotechnology for Biofuels*, 3(1):23, October 2010.

[33] Leonardo D. Gomez, Caragh Whitehead, Philip Roberts, and Simon J. McQueen-Mason. High-throughput Saccharification Assay for Lignocellulosic Materials. *Journal of Visualized Experiments : JoVE*, (53), July 2011.

[34] Karl Broman and Saunak Sen. *A Guide to QTL Mapping with R/qtl*. Statistics for Biology and Health. Springer-Verlag, New York, 2009.

[35] G. D. Parker, K. J. Chalmers, A. J. Rathjen, and P. Langridge. Mapping loci associated with flour colour in wheat (Triticum aestivum L.). *Theoretical and Applied Genetics*, 97(1-2):238–245, July 1998.

[36] Koichiro Tamura, Glen Stecher, Daniel Peterson, Alan Filipski, and Sudhir Kumar. MEGA6: Molecular Evolutionary Genetics Analysis version 6.0. *Molecular Biology and Evolution*, 30(12):2725–2729, December 2013.

[37] David A. Morrison. Phylogenetic Trees Made Easy: A How-to Manual, third edition.—Barry G. Hall. 2008. Sinauer Associates, Sunderland, Massachusetts. xiv + 230 pp. ISBN 978-0-87893-310-5. $US39.95 £24.99 (paperback). *Systematic Biology*, 57(4):658–660, August 2008.

[38] The International Brachypodium Initiative. Genome sequencing and analysis of the model grass *Brachypodium distachyon*. *Nature*, 463(7282):763–768, February 2010.

[39] Norman Warthmann, Hao Chen, Stephan Ossowski, Detlef Weigel, and Philippe Hervé. Highly Specific Gene Silencing by Artificial miRNAs in Rice. *PLoS ONE*, 3(3), March 2008. 00237.

[40] John Vogel. Unique aspects of the grass cell wall. *Current Opinion in Plant Biology*, 11(3):301–307, June 2008. 00284.

[41] K. J. Biggs and S. C. Fry. Phenolic cross-linking in the plant cell wall. *In Physiology of cell expansion during plant growth. American Society of Plant Physiologists., , eds d. j. cosgrove and d. p. knievel edition.*, 1987. 00000.

[42] David M. Brown, Zhinong Zhang, Elaine Stephens, Paul Dupree, and Simon R. Turner. Characterization of IRX10 and IRX10-like reveals an essential role in glucuronoxylan biosynthesis in Arabidopsis. *The Plant Journal: For Cell and Molecular Biology*, 57(4):732–746, February 2009.

[43] Louise Jones, Jennifer L. Milne, David Ashford, and Simon J. McQueen-Mason. Cell wall arabinan is essential for guard cell function. *Proceedings of the National Academy of Sciences*, 100(20):11783–11788, September 2003.

[44] Jean-Louis Prioul, Sandrine Pelleschi, Mamoune Séne, Claudine Thévenot, Mathilde Causse, Dominique de Vienne, and Agnès Leonardi. From QTLs for enzyme activity to candidate genes in maize. *Journal of Experimental Botany*, 50(337):1281–1288, 1999.

[45] B. C. Y. Collard, M. Z. Z. Jahufer, J. B. Brouwer, and E. C. K. Pang. An introduction to markers, quantitative trait loci (QTL) mapping and marker-assisted selection for crop improvement: The basic concepts. *Euphytica*, 142(1):169–196, January 2005.

[46] B. D. Kohorn. WAKs; cell wall associated kinases. *Current Opinion in Cell Biology*, 13(5):529–533, October 2001.

[47] M. E. Edwards, C. A. Dickson, S. Chengappa, C. Sidebottom, M. J. Gidley, and J. S. Reid. Molecular characterisation of a membrane-bound galactosyltransferase of plant cell wall matrix polysaccharide biosynthesis. *The Plant Journal: For Cell and Molecular Biology*, 19(6):691–697, September 1999.

[48] Chanhui Lee, Ruiqin Zhong, and Zheng-Hua Ye. Arabidopsis family GT43 members are xylan xylosyltransferases required for the elongation of the xylan backbone. *Plant & Cell Physiology*, 53(1):135–143, January 2012.

[49] Ngak-Leng Sim, Prateek Kumar, Jing Hu, Steven Henikoff, Georg Schneider, and Pauline C. Ng. SIFT web server: predicting effects of amino acid substitutions on proteins. *Nucleic Acids Research*, 40(Web Server issue):W452–457, July 2012.

[50] Mirko Barbieri, Thierry C. Marcel, Rients E. Niks, Enrico Francia, Marianna Pasquariello, Valentina Mazzamurro, David F. Garvin, and Nicola Pecchioni. QTLs for resistance to the false brome rust Puccinia brachypodii in the model grass Brachypodium distachyon L. *Genome*, 55(2):152–163, February 2012.

[51] David L. Des Marais, Samsad Razzaque, Kyle M. Hernandez, David F. Garvin, and Thomas E. Juenger. Quantitative trait loci associated with natural diversity in water-use efficiency and response to soil drying in Brachypodium distachyon. *Plant Science*, 251:2–11, October 2016.

[52] Chen-fei Dong, Qing-sheng Cai, Cai-lin Wang, Jiro Harada, Keisuke Nemoto, and Yi-xin Shen. QTL Analysis for Traits Associated with Feeding Value of Straw in Rice (Oryza sativa L.). *Rice Science*, 15(3):195–200, September 2008.

[53] Chuan-Fu Liu and Run-Cang Sun. Chapter 5 - Cellulose. In *Cereal Straw as a Resource for Sustainable Biomaterials and Biofuels*, pages 131–167. Elsevier, Amsterdam, 2010. 00000.

[54] Yves Barrière, Valérie Méchin, Bruno Lefevre, and Stéphane Maltese. QTLs for agronomic and cell wall traits in a maize RIL progeny derived from a cross between an old Minnesota13 line and a modern Iodent line. *Theoretical and Applied Genetics*, 125(3):531–549, March 2012. 00014.

[55] S. Grando, M. Baum, S. Ceccarelli, A. Goodchild, F. Jaby El-Haramein, A. Jahoor, and G. Backes. QTLs for straw quality characteristics identified in recombinant inbred lines of a Hordeum vulgare x H. spontaneum cross in a Mediterranean environment. *TAG. Theoretical and applied genetics. Theoretische und angewandte Genetik*, 110(4):688–695, February 2005.

[56] Yi-Hong Wang, Aniruddha Acharya, A. Millie Burrell, Robert R. Klein, Patricia E. Klein, and Karl H. Hasenstein. Mapping and candidate genes associated with saccharification yield in sorghum. *Genome*, 56(11):659–665, October 2013. 00010.

[57] Tim van der Weijde, Claire L. Alvim Kamei, Edouard I. Severing, Andres F. Torres, Leonardo D. Gomez, Oene Dolstra, Chris A. Maliepaard, Simon J. McQueen-Mason, Richard G. F. Visser, and Luisa M. Trindade. Genetic complexity of miscanthus cell wall composition and biomass quality for biofuels. *BMC Genomics*, 18(1):406, May 2017.

[58] M. D. Krakowsky, M. Lee, and J. G. Coors. Quantitative trait loci for cell wall components in recombinant inbred lines of maize (Zea mays L.) II: leaf sheath tissue. *TAG. Theoretical and applied genetics. Theoretische und angewandte Genetik*, 112(4):717–726, February 2006.

[59] Yifang Tan, Mei Sun, Yongzhong Xing, Jinping Hua, X L. Sun, Q F. Zhang, and Harold Corke. Mapping quantitative trait loci for milling quality, protein content and color characteristics of rice using a recombinant inbred line population derived from an elite rice hybrid. *Theoretical and Applied Genetics*, 103:1037–1045, November 2001.

[60] Bohan Liu, Leonardo D. Gómez, Cangmei Hua, Lili Sun, Imran Ali, Linli Huang, Chunyan Yu, Rachael Simister, Clare Steele-King, Yinbo Gan, and Simon J. McQueen-Mason. Linkage Mapping of Stem Saccharification Digestibility in Rice. *PLOS ONE*, 11(7):e0159117, July 2016.

[61] David M. Brown, Leo A. H. Zeef, Joanne Ellis, Royston Goodacre, and Simon R. Turner. Identification of novel genes in Arabidopsis involved in secondary cell wall formation using expression profiling and reverse genetics. *The Plant Cell*, 17(8):2281–2295, August 2005.

[62] Runcang Sun, J. Mark Lawther, and W. B. Banks. Isolation and physicochemical characterisation of xylose-rich pectic polysaccharide from wheat straw. *Progress in Biotechnology*, 14:637–643, January 1996. 00006.

[63] RunCang Sun, X. F. Sun, and J. Tomkinson. Hemicelluloses and Their Derivatives. In *Hemicelluloses: Science and Technology*, volume 864 of *ACS Symposium Series*, pages 2–22. American Chemical Society, October 2003. 00111.

Capítulo 5

DISCUSIÓN FINAL

Actualmente se están llevando a cabo multitud de investigaciones para la producción de un bioetanol lignocelulósico que sea económicamente viable y sostenible. Este objetivo se puede abordar, por ejemplo, mejorando el rendimiento de procesos como pueden ser en el pretratamiento, que como hemos visto anteriormente tanta influencia tiene en la posterior hidrólisis enzimática, en la misma hidrólisis enzimática mediante el uso de enzimas más eficientes y menos costosas de obtener, o como en el trabajo que nos ocupa, haciendo uso de la mejora genética así como de la genética inversa para la obtención de plantas con paredes celulares menos recalcitrantes y que por tanto sean más fácilmente digestibles por las enzimas celulolíticas. La mayoría de los trabajos para incrementar la digestibilidad lignocelulósica mediante una menor recalcitrancia de la pared celular, han optado por aproximaciones de genética inversa, es decir, han modificado la pared celular mediante alteraciones genéticas en las rutas de biosíntesis de ésta [1–4]. Sin embargo, muchos de los trabajos que han obtenido plantas con incrementos de sacarificación también han ido acompañados de modificaciones fenotípicas indeseables como enanismo, debilidad del tallo y alteración del desarrollo normal de la planta.

En este trabajo se llevó a cabo la identificación de la variabilidad natural para la producción de bioetanol sobre un material vegetal de partida compuesto por 66 genotipos de cuatro especies distintas: cebada (*Hordeum vulgare* L.), trigo duro (*T. durum*), trigo blando (*T. aestivum*) y triticale (X *Triticosecale*). Se analizaron estos 66 genotipos mediante dos métodos de sacarificación: un primer método de sacarificación puesto a punto en nuestro laboratorio perteneciente al Instituto de Agricultura Sostenible (IAS), y un segundo método usado durante la estancia breve de la que disfruté en el “Centre for Novel Agricultural Products” (CNAP) en la ciudad York (UK), que nos sirvió como control con el que pudiésemos contrastar nuestros resultados. Ambos métodos estuvieron correlacionados moderadamente (R^2=0,5688), siendo mejor que la correlación observada entre métodos de sacarificación de alto rendimiento en el trabajo de Lindedam et al. [5] (R^2=0,2139). Las diferencias encontradas entre nuestros métodos se podrían deber entre otras

cosas, a que el método usado en el IAS solo determinaba glucosa liberada y el método del CNAP determinaba todos los azúcares liberados en la sacarificación. Ambos métodos fueron capaces de detectar diferencias entre especies, así como entre los genotipos de cada especie. La variabilidad y los coeficientes de variación (CV) entre genotipos fueron muy similares, aunque siempre fueron algo mayores en el método del IAS, lo que se puede explicar porque con este método solo se podía analizar una placa ELISA de 96 pocillos frente las 6 que se analizaban simultáneamente con el método del CNAP. Además, éste último era un método en el que el experimentador intervenía en menor medida que en el método del IAS, ya que se trataba de un método robotizado de alto rendimiento. Otros autores han descrito resultados similares resultados de CV y variabilidad para la degradabilidad de pared celular de diferentes cultivares [6–8] que los que hemos encontrado en nuestro trabajo.

En el análisis de la varianza para el grado de sacarificación, el factor especie fue significativamente distinto por ambos métodos. Pudimos observar como el análisis de comparación de medias para el grado de sacarificación situó a la cebada por encima del trigo y triticale, que estuvieron al mismo nivel. Los genotipos de cebada y trigo fueron seleccionados por tratarse de líneas parentales de poblaciones de mapeo y por estar disponibles en los bancos de germoplasma. El análisis estadístico para el grado de sacarificación reveló también diferencias significativas para el factor genotipo, a partir de la cuales pudimos construir un ranking para el grado de sacarificación de los genotipos de cada especie (Tabla 2.2. Estas poblaciones de mapeo constituyen importantes fuentes de información en estudios genéticos. El desarrollo de poblaciones de mapeo a partir de unos parentales concretos, como por ejemplo Steptoe x Morex, u Oregon Wolf Barleys (OWB) [9] han servido para desarrollar secuencias de consenso SNP en los mapas genéticos de cebada, que ha su vez han dado lugar a trabajos de investigación exitosos de mapeo sobre genes de regulación [10] o resistencias a roya [11].

En este trabajo se han observado potenciales de sacarificación contrastantes en las líneas parentales Steptoe x Morex, Vada x Steptoe, OWB Dominant x Steptoe, OWB Dominant x OWB Recesive y Lina x L94 (Fig 2.2). Sin embargo, si queremos tomar una decisión más robusta, solo las poblaciones OWB y Steptoe x Morex deberían tenerse en cuenta para futuros mapeos, ya que con el método del CNAP no se encontraron diferencias significativas ($p<0,05$) entre los otros parentales.

Distintas correlaciones significativas que se encontraron entre el fenotipo y la liberación de azúcares en biomasa analizada. La más importante de estas correlaciones fue la observada entre el contenido de lignina y el grado de sacarificación, que presentó una correlación significativa para todos los genotipos ensayados en este trabajo con un valor r = -0,55. Lindedam et al. [12] obtuvieron valores similares de correlación entre estos factores en distintos genotipos de trigo. Sin embargo, si en lugar de comparar los resultados de todos los genotipos nos centramos en los más interesantes desde el punto de vista de la cantidad de biomasa producida, vemos que al tomar los 10 genotipos que más biomasa producían (Fig 2.3B), la correlación entre lignina y la sacarificación es mayor (r = -0.82). Este resultado es comparable a los obtenidos en tomate por Caruso et al. [13], en líneas de alfalfa transgénica por Chen et al. [14], y en *Arabidopsis thaliana* por Van Acker et al. [15].

También se encontraron correlaciones significativas interesantes para las plantas con una mayor producción de biomasa, entre el factor altura de la planta y sacarificación (r = -0,79), y entre altura de la planta y contenido en lignina (r = 0,65). Esta relación entre altura y recalcitrancia de pared que se podría atribuir a la lignificación que sufren los tallos más altos para ser más resistentes con la consecuente reducción de su potencial de bioetanol. Es posible que la correlación negativa entre altura de la planta y liberación de azúcares pudiese ser explicada porque las plantas altas tuviesen una menor fracción de hoja que plantas más bajas. Resultados similares han sido descritos por otros autores en los trabajos [6, 16]. Este resultado de correlación no aparece si tomamos todos los genotipos en conjunto, lo que podría ser explicado por factores como la ratio hoja/tallo (que no ha sido tenida en cuenta en este trabajo), o por el efecto sobre la degradabilidad de pared que pudiesen haber causado la obtención de cultivares semienanos o resistentes a enfermedades a través de programas de mejora desarrollados desde los años 40-50 hasta nuestros días [17], y que de alguna manera han tamponado el efecto de altura sobre la degradabilidad de pared.

El grosor de la pared (ILPave y PePave) del tallo en distintos internudos arrojó valores significativos de correlación (Fig 2.3A), de sentido negativo con la degradabilidad, el etanol teórico y el número de nudos, y de tendencia positiva con el contenido de lignina. Se podría entender que una planta con un mayor número de internudos y una misma altura, tiene internudos más cortos y con una pared más delgada que pueden soportar los mismos momentos flectores y torsores que un

internudo más largo y grueso. En este trabajo hemos visto como la paja de cebada tiene un menor contenido de lignina que el trigo y el triticale, contrastando así con un mayor grado de sacarificación y menor grosor de pared (Fig 2.1E). Resultados parecidos fueron observados en cebada, trigo y triticale por Chen et al., aunque solo en un genotipo de cada especie [18, 19]. Esta investigación ha tratado de de obtener resultados para una gran cantidad de genotipos para cada especie. A partir de los resultados obtenidos en ella hemos podido observar como plantas con la misma altura y poco grosor de tallo tienen entrenudos más cortos, lo que implica un mayor número de nudos, siendo estas plantas menos susceptibles al encamado. Estas correlaciones entre resistencia a encamado, grosor de pared del tallo y número de nudos han sido previamente descritas [20–22]. Los índies ILPave y PePave no estuvieron correlacionados con la altura de la planta ni rendimiento del grano, por lo que permitían la reproducción de ese carácter sin comprometer el alto rendimiento del grano. Además, podríamos afirmar que el rendimiento de grano y la sacarificación no estuvieron correlacionados (Fig 2.3A), lo que establece un grado de independencia entre estos dos rasgos.

La mejora genética clásica requiere de una relación eficaz entre fenotipado y genotipado, y a pesar de que las herramientas de genotipado han evolucionado mucho, el fenotipado no lo ha hecho a la par y no disponemos de métodos que permitan evaluar masivamente caracteres complejos del desarrollo de las plantas en condiciones de campo, como es el caso que nos ocupa en el que queremos determinar el potencial en bioetanol de la biomasa de distintos cultivos [23].

Para fenotipar durante el desarrollo del cultivo en campo hemos recurrido a un muestreo manual que coincidió simultáneamente con el empleo de una plataforma UAV (unmanned aerial vehicle) equipada con equipos de toma de imagen VIS/NIR, que ya han demostrado su eficacia en el fenotipado a través de la adquisición masiva de imágenes [24–26]. El ensayo de campo fue sobrevolado para la toma de imágenes en siete fechas distintas a lo largo del desarrollo del cultivo. Los resultados medidos manualmente a lo largo del desarrollo de la planta mostraron una gran variabilidad en las distintas medidas estimadas como fue la altura de la planta, fechas de antesis, producción de grano por unidad de superficie, biomasa total, liberación de azúcar, y etanol teórico. Además, toda esta variabilidad no estuvo asociada al potencial de producción de grano, siendo este un aspecto clave en programas de mejora que estuviesen destinados a mejorar la calidad de la paja del cereal para producción de bioetanol sin afectar a la producción de grano.

Resultados similares han sido reportados en cultivos de trigo y cebada [6, 12, 27].

A la luz de los resultados obtenidos en la estimación de las variables de potencial de bioetanol, biomasa y etanol teórico, podemos ver como las fechas individuales (TS-1) fueron menos informativas que la integral de la curva generada por el conjunto de las fechas hasta la antesis o hasta la senescencia (TS-2 y TS-3). Dependiendo de la variable estimada parece que es más adecuado el uso de un escenario frente a otro, por ejemplo, las predicciones de azúcares liberados en la sacarificación tienen un mejor coeficiente de determinación con los datos tomados en el escenario multi-temporal TS-2 que en el TS-3. Sin embargo, la estimación del etanol teórico es más precisa cuando se toma el escenario TS-3. Por otro lado, en el análisis de los resultados obtenidos en azúcar liberado en la sacarificación, biomasa producida, así como etanol teórico frente a los índices medidos por el UAV a lo largo del desarrollo del cultivo, se encontró que aquellos índices que estaban basados en NIR (infrarrojo cercano) fueron más apropiados para estimar biomasa, mientras que los índices en la banda del visible fueron mejores para la estimación de azúcares liberados. Se observó que la mayoría de las estimaciones en fechas individuales eran bajas, aunque algunas de ellas llegaron a ser moderadas entre la biomasa del cultivo y los índices NDVI y GNDVI para el TS-1 con 161 DAS ("Days after sown", días desde la siembra). Aun así, la mejor estimación obtenida para biomasa se obtuvo para TS-2 (R^2 de 0,57).

En el caso de la liberación de glucosa, es la integral del índice EXG tomado en todas las fechas hasta la antesis (TS-2) la que revela un mayor coeficiente de determinación (R^2 de 0,57). Hasta donde sabemos, no hay ninguna investigación previa que establezca ninguna relación entre este índice de la banda del visible y la liberación de glucosa. En la tabla 3 del capítulo 4, podemos observar un ascenso a lo largo de las fechas individuales hasta la antesis para el índice EXG en la estimación de la glucosa liberada, por lo que podríamos pensar que parece estar relacionado con la cantidad de pigmento verde que tienen las plantas [28, 29]. Los cloroplastos de las hojas de las plantas son los orgánulos donde se produce la fijación de carbono a partir del CO_2 atmosférico. A lo largo del desarrollo de la planta se va fijando carbono que conformará la totalidad de la estructura de la planta. Según los trabajos de [6, 12, 16], la fracción de hoja en trigo es más fácilmente digerible que el tallo, por lo que pensamos que quizá el EXG estima moderadamente bien el potencial de liberación de glucosa porque está muy relacionado con la cantidad de hoja de la planta ya que lo que mide este índice es cantidad de pigmento verde.

La cantidad de pigmento después de la antesis decrece. El índice EXG decrece después de la fecha de antesis, hecho que podemos atribuir a que se produce un descenso en la cantidad de clorofila (pigmento verde) en favor de las antocianinas (pigmento rojo).

Por último, el factor de etanol teórico como combinación lineal de la cantidad de azúcares liberados y la cantidad de biomasa producida por genotipo (ver ecuación 3.1), parece que podría ser un factor para tener en cuenta a la hora hacer selección. En este caso el índice NDVI en el escenario TS-3 fue el que mostró un mejor nivel de predicción del factor de interés, siendo el coeficiente de determinación de R^2=0,66. Se han encontrado que varios parentales que muestran resultados contrastantes para el valor de etanol teórico, coincidiendo algunos de ellos con los propuesto en el capítulo 2 por su carácter contrastante para el factor liberación de glucosa, como son OWB dominant x OWB recesive, y Steptoe x Morex, y otra combinación no coincidente como OWB dominant x Franklin.

Si nos aproximamos con pretensión de comprender el origen de la variabilidad en la biomasa lignocelulósica para el factor potencial en bioetanol, tenemos que conocer la composición química y estructural de esta biomasa compuesta por las paredes celulares vegetales. Que, para empezar, las paredes celulares son distintas en función del tipo de planta de la que proceden (Tabla 1.1). Consultando la bibliografía referente a la composición y estructura de biomasa lignocelulósica proveniente de las gramíneas vemos que se trata de un tema que está relativamente bien descrito, sin embargo, hay ciertas características que aún no han sido desveladas y de las que se desconoce en gran parte cómo funcionan los mecanismos de organización estructural, biosíntesis, funcionalidad, etc. La pared celular de gramíneas está compuesta principalmente por celulosa (32-47 %), hemicelulosas (19-27 %) y lignina (5-24 %) [30]. Los glucoronoarabinoxilanos (GAX) son el principal componente de las hemicelulosas en gramíneas, están constituidos por un esqueleto de xilosa decorado por cadenas de arabinosa y ácido glucorónico [31]. La pared celular de las gramíneas contiene, además, altos contenidos de hidroxicinaminas tales como el ácido ferúlico (FA) y el ácido p-coumárico (pCA). El FA parece jugar un papel similar al de las proteínas estructurales que entrelazan xiloglucanos en las paredes celulares de dicotiledóneas. Este entrelazado formado los FA posee importantes funciones tales como el control de la extensibilidad de pared [32, 33], la protección contra patógenos [34], así como la inhibición de la degradabilidad de las paredes celulares por microorganismos en rumiantes [35].

La matriz formada por los polímeros no celulósicos y el FA impide físicamente porque tiene una porosidad que excluye a la mayoría de las enzimas globulares. De esta forma, la asociación entre GAX, lignina y FA hace que las paredes sean altamente recalcitrantes a la digestión enzimática [35–38].

El análisis de mutantes mediante genética directa e inversa es una de las formas más efectivas de estudiar, identificar y caracterizar la función génica [39]. Aquellas mutaciones que eliminan la expresión de un gen y muestran un fenotipo, proporcionan una relación de causalidad directa entre la secuencia del gen y su función. Sin embargo, el análisis de mutantes se ve limitado tanto por la redundancia genética como por la plasticidad intrínseca del ensamblaje de la pared celular [40]. Con frecuencia, los genes no mutagenizados de la misma familia compensan a los mutados, enmascarando el efecto que pudiesen tener sobre el fenotipo. Una estrategia alternativa para subsanar este inconveniente es la interferencia de ARN (ARNi) que permite dirigir el silenciamiento de varios genes de la misma y/o diferente familia simultáneamente [41]. La interferencia del ARN es un proceso postranscripcional desencadenado por la introducción de RNA de doble cadena el cual inicia un silenciamiento génico específico de secuencia [42, 43]. Esta técnica de supresión de la actividad genética tiene evidentes ventajas con respecto a otras técnicas de mutación clásica cuando se trata de silenciamiento de varios genes de la misma o diferente familia [39, 44, 45].

Por otro lado, no disponemos de mucha información acerca de los genes implicados en la biosíntesis de los GAX y la incorporación del FA en las paredes celulares. Mitchel et al. [46] propusieron varias familias génicas que posiblemente estén implicadas en la síntesis de GAX y en el proceso de ferulación.

Es destacable el uso de *Arabidopsis* como planta modelo en muchos de estos trabajos, siendo un inconveniente dado que las paredes celulares de ésta son muy diferentes respecto a las gramíneas. Los resultados obtenidos en *Arabidopsis* por tanto pueden no ser siempre trasladables a estos cultivos. Sin embargo, no ocurre lo mismo cuando la que usamos como planta modelo es *B. distachyon*. Al tratarse de una gramínea, esta especie tiene unas paredes celulares muy similares a la biomasa de los cultivos propuestos como potenciales productores de bioetanol, así como una correlación importante en cuanto a la organización genética de los principales candidatos en gramíneas. *B. distachyon* tiene además otras importantes ventajas como son su facilidad de cultivo, un genoma pequeño con una pequeña

parte repetitiva y la de estar secuenciado completamente [47].

El silenciamiento se hizo sobre *B. distahcyon* mediante microRNA. Este trabajo se llevó a cabo en la universidad de Tal Aviv, que ya tenía puesto a punto la generación de transgénicos sobre Brachypodium. Afortunadamente se observó que los homólogos en Brachypodium respecto a los propuestos en arroz están bien conservados.

De todos los transgénicos, el que mostró un mejor efecto de contraste por el silenciamiento contra la planta no modificada (WT) para factores de composición y estructura de pared celular, así como el grado de sacarificación, fue el silenciado para el gen *Bradi5g24290*. El análisis de expresión relativa de este gen en los cuatro eventos analizados se vio reducido frente al WT en torno a un 70 % para el tejido procedente del tallo de la planta. El análisis composicional de la matriz de pared celular en tallo reveló concentraciones significativamente menores para xilosa, arabinosa (figura 4.6B, capítulo 4) así como ácido ferúlico (FA) en las líneas silenciadas frente la los silvestres, por lo que podemos sugerir que esta alteración de la composición de arabinoxilanos probablemente sea también la causa del mayor grado de sacarificación de este material. Sin embargo, en la comparación de las líneas analizadas en los RILs no se pudo encontrar una diferencia significativa en la composición celular, tan solo una tendencia.

En el laboratorio del CNAP se llevó a cabo (por Caragh Whitehead) la labor de escrutar una población RIL generada a partir de Bd3-1 x Bd21 en busca de QTL que explicasen las diferencias encontradas en sacarificación. El análisis de QTL en el cromosoma 5 mostró varios genes candidatos que probablemente codifiquen un gen GT43 ortólogo de AtlRX14, que parece ser el responsable de la síntesis de esqueleto de xilano en la pared celular de Arabidopsis [48]

Otros trabajos han revelado como en gramíneas se producen efectos sobre la sacarificación al analizar colecciones de mutantes para xax1, gen de la familia GT61, y donde se vio que menores que menores cantidades de FA y xilosa estaban relacionadas con un mayor grado de sacarificación [4, 49]. Se planteó la hipótesis de que la reducción observada en el contenido de FA se debe a la pérdida de sustituciones de xilosa que se requieren para la unión son los residuos de arabinosilo, lo que resulta en la disminución de la actividad de la enzima feruloiltransferasa, aunque esta hipótesis no se ha validado experimentalmente. En el trabajo de Bartley et al. [50], la sobreexpresión en arroz de la aciltransferasa OsAT10, condujo a una

disminución de FA y aumento de pCA, resultando finalmente en una mayor digestibilidad de pared. Un efecto similar se observó en líneas silenciadas para el gen Bradi5g24290, con una disminución en el contenido de AX asociado a un contenido de FA más bajo. Nuestros resultados confirman pues, la importancia de los AX en la determinación de la digestibilidad de la lignocelulosa en gramíneas.

Finalmente, podemos decir que en este trabajo hemos aunado el potencial de distintas herramientas a nuestro alcance para conseguir dar respuesta a nuestros objetivos: la mejora genética clásica, la biotecnología y la teledetección. Este trabajo da importantes indicaciones de hacia donde podrían dirigirse nuevas investigaciones para mejorar la viabilidad y eficiencia de la producción de bioetanol. Se trata de un hecho muy relevante, ya que la población continúa creciendo e industrializándose a un ritmo acelerado, y por otro lado las reservas energéticas fósiles decrecen y su uso intensivo afecta muy negativamente al medio ambiente. El bioetanol lignocelulósico tiene el potencial de proporcionarnos energía renovable que sustituya parcialmente a los combustibles líquidos procedentes del petróleo. Personalmente, creo que el bioetanol lignocelulósico tiene potencial para contribuir a que la transición hacia el uso de energías menos contaminantes, renovables y sostenibles llegue a ser realidad en un futuro no muy lejano.

Referencias

[1] Fernando Piston, Cristobal Uauy, Lianhai Fu, James Langston, John Labavitch, and Jorge Dubcovsky. Down-regulation of four putative arabinoxylan feruloyl transferase genes from family PF02458 reduces ester-linked ferulate content in rice cell walls. *Planta*, 231(3):677–691, 2010. 00048.

[2] Poppy E. Marriott, Leonardo D. Gómez, and Simon J. McQueen-Mason. Unlocking the potential of lignocellulosic biomass through plant science. *New Phytologist*, 209(4):1366–1381, March 2016. 00007.

[3] Caragh Whitehead, Francisco J. Ostos Garrido, Matthieu Reymond, Rachael Simister, Assaf Distelfeld, Sergio G. Atienza, Fernando Piston, Leonardo D. Gomez, and Simon J. McQueen-Mason. A glycosyl transferase family 43 protein involved in xylan biosynthesis is associated with straw digestibility in Brachypodium distachyon. *New Phytologist*, 218(3):974–985, May 2018.

[4] Dawn Chiniquy, Vaishali Sharma, Alex Schultink, Edward E. Baidoo, Carsten Rautengarten, Kun Cheng, Andrew Carroll, Peter Ulvskov, Jesper Harholt, Jay D. Keasling, Markus Pauly, Henrik V. Scheller, and Pamela C. Ronald. XAX1 from glycosyltransferase family 61 mediates xylosyltransfer to rice xylan. *Proceedings of the National Academy of Sciences of the United States of America*, 109(42):17117–17122, October 2012.

[5] Jane Lindedam, Sander Bruun, Henning Jørgensen, Stephen R. Decker, Geoffrey B. Turner, Jaclyn D. DeMartini, Charles E. Wyman, and Claus Felby. Evaluation of high throughput screening methods in picking up differences between cultivars of lignocellulosic biomass for ethanol production. *Biomass and Bioenergy*, 66:261–267, July 2014. 00004.

[6] Jacob Wagner Jensen, Jakob Magid, Jens Hansen-Møller, Sven Bode Andersen, and Sander Bruun. Genetic variation in degradability of wheat straw and potential for improvement through plant breeding. *Biomass and Bioenergy*, 35(3):1114–1120, March 2011. 00009.

[7] E. R. Ørskov, W. J. Shand, D. Tedesco, and L. a. F. Morrice. Rumen degradation of straw. 10. Consistency of differences in nutritive value between varieties of cereal straws. *Animal Science*, 51(1):155–162, August 1990. 00031.

[8] Larry M. White, Glenn P. Hartman, and Jerald W. Bergman. In Vitro Digestibility, Crude Protein, and Phosphorus Content of Straw of Winter Wheat, Spring Wheat, Barley, and Oat Cultivars in Eastern Montana. *Agronomy Journal*, 73(1):117–121, 1981. 00084.

[9] A. Kleinhofs, A. Kilian, M. A. Saghai Maroof, R. M. Biyashev, P. Hayes, F. Q. Chen, N. Lapitan, A. Fenwick, T. K. Blake, V. Kanazin, E. Ananiev, L. Dahleen, D. Kudrna, J. Bollinger, S. J. Knapp, B. Liu, M. Sorrells, M. Heun, J. D. Franckowiak, D. Hoffman, R. Skadsen, and B. J. Steffenson. A molecular, isozyme and morphological map of the barley (Hordeum vulgare) genome. *Theoretical and Applied Genetics*, 86(6):705–712, July 1993. 00683.

[10] A. Tondelli, E. Francia, D. Barabaschi, A. Aprile, J. S. Skinner, E. J. Stockinger, A. M. Stanca, and N. Pecchioni. Mapping regulatory genes as candidates for cold and drought stress tolerance in barley. *Theoretical and Applied Genetics*, 112(3):445–454, November 2005. 00099.

[11] L. Arru, E. Francia, and N. Pecchioni. Isolate-specific QTLs of resistance to leaf stripe (Pyrenophora graminea) in the 'Steptoe' x 'Morex' spring barley cross. *Theoretical and applied genetics.*, 106(4):668–675, February 2003. 00000.

[12] J. Lindedam, S.B. Andersen, J. DeMartini, S. Bruun, H. Jørgensen, C. Felby, J. Magid, B. Yang, and C.E. Wyman. Cultivar variation and selection potential relevant to the production of cellulosic ethanol from wheat straw. *Biomass and Bioenergy*, 37(0):221–228, February 2012.

[13] G. Caruso, L. D. Gomez, F. Ferriello, A. Andolfi, C. Borgonuovo, A. Evidente, R. Simister, S. J. McQueen-Mason, D. Carputo, L. Frusciante, and M. R. Ercolano. Exploring tomato Solanum pennellii introgression lines for residual biomass and enzymatic digestibility traits. *BMC Genetics*, 17:56, 2016. 00000.

[14] Fang Chen and Richard A. Dixon. Lignin modification improves fermentable sugar yields for biofuel production. *Nature Biotechnology*, 25(7):759–761, July 2007. 00769.

[15] Rebecca Van Acker, Ruben Vanholme, Véronique Storme, Jennifer C. Mortimer, Paul Dupree, and Wout Boerjan. Lignin biosynthesis perturbations affect secondary cell wall composition and saccharification yield in Arabidopsis thaliana. *Biotechnology for Biofuels*, 6:46, 2013. 00066.

[16] Andrea Bellucci, Anna Maria Torp, Sander Bruun, Jakob Magid, Sven B. Andersen, and Søren K. Rasmussen. Association Mapping in Scandinavian Winter Wheat for Yield, Plant Height, and Traits Important for Second-Generation Bioethanol Production. *Frontiers in Plant Science*, 6, November 2015. 00000.

[17] A. J. Travis, S. D. Murison, D. J. Hirst, K. C. Walker, and A. Chesson. Comparison of the anatomy and degradability of straw from varieties of

wheat and barley that differ in susceptibility to lodging. *The Journal of Agricultural Science*, 127(1):1–10, August 1996.

[18] Ye Chen, Ratna R. Sharma-Shivappa, Deepak Keshwani, and Chengci Chen. Potential of agricultural residues and hay for bioethanol production. *Applied Biochemistry and Biotechnology*, 142(3):276–290, September 2007.

[19] Ye Chen, Ratna R. Sharma-Shivappa, and Chengci Chen. Ensiling agricultural residues for bioethanol production. *Applied Biochemistry and Biotechnology*, 143(1):80–92, October 2007.

[20] S. (Polska Akademia Nauk Jezowski. Variation correlation and heritability of characters determining lodging of spring barley (Hordeum vulgare L.). 2. Analysis of relationship between lodging grade and some morphological characters of spring barley varieties. *Polish Journal of Theoretical and Applied Genetics*, 1981. 00009.

[21] JP Tandon and KBL Jain. Relationship between lodging resistance and some morphological characters in barley, 1973. 00008.

[22] J. Brady. Some factors influencing lodging in cereals. *The Journal of Agricultural Science*, 24(02):209–232, 1934. 00048.

[23] José Luis Araus and Jill E. Cairns. Field high-throughput phenotyping: the new crop breeding frontier. *Trends in Plant Science*, 19(1):52–61, 2014. 00191.

[24] Sindhuja Sankaran, Lav R. Khot, Carlos Zúñiga Espinoza, Sanaz Jarolmasjed, Vidyasagar R. Sathuvalli, George J. Vandemark, Phillip N. Miklas, Arron H. Carter, Michael O. Pumphrey, N. Richard Knowles, and Mark J. Pavek. Low-altitude, high-resolution aerial imaging systems for row and field crop phenotyping: A review. *European Journal of Agronomy*, 70:112–123, October 2015. 00012.

[25] Yeyin Shi, J. Alex Thomasson, Seth C. Murray, N. Ace Pugh, William L. Rooney, Sanaz Shafian, Nithya Rajan, Gregory Rouze, Cristine L. S. Morgan, Haly L. Neely, Aman Rana, Muthu V. Bagavathiannan, James Henrickson, Ezekiel Bowden, John Valasek, Jeff Olsenholler, Michael P. Bishop, Ryan Sheridan, Eric B. Putman, Sorin Popescu, Travis Burks, Dale Cope, Amir Ibrahim, Billy F. McCutchen, David D. Baltensperger, Robert V. Avant Jr, Misty Vidrine, and Chenghai Yang. Unmanned Aerial Vehicles for High-Throughput Phenotyping and Agronomic Research. *PLOS ONE*, 11(7):e0159781, July 2016. 00000.

[26] Guijun Yang, Jiangang Liu, Chunjiang Zhao, Zhenhong Li, Yanbo Huang, Haiyang Yu, Bo Xu, Xiaodong Yang, Dongmei Zhu, Xiaoyan Zhang, Ruyang Zhang, Haikuan Feng, Xiaoqing Zhao, Zhenhai Li, Heli Li, and Hao

Yang. Unmanned Aerial Vehicle Remote Sensing for Field-Based Crop Phenotyping: Current Status and Perspectives. *Frontiers in Plant Science*, 8, 2017.

[27] B. S. Capper. Genetic variation in the feeding value of cereal straw. *Animal Feed Science and Technology*, 21(2):127–140, October 1988. 00062.

[28] J. Torres-Sánchez, J. M. Peña, A. I. de Castro, and F. López-Granados. Multi-temporal mapping of the vegetation fraction in early-season wheat fields using images from UAV. *Computers and Electronics in Agriculture*, 103:104–113, April 2014.

[29] Zhenghong Yu, Zhiguo Cao, Xi Wu, Xiaodong Bai, Yueming Qin, Wen Zhuo, Yang Xiao, Xuefen Zhang, and Hongxi Xue. Automatic image-based detection technology for two critical growth stages of maize: Emergence and three-leaf stage. *Agricultural and Forest Meteorology*, 174-175:65–84, June 2013.

[30] Christelle Lequart, Jean-Marc Nuzillard, Bernard Kurek, and Philippe Debeire. Hydrolysis of wheat bran and straw by an endoxylanase: production and structural characterization of cinnamoyl-oligosaccharides. *Carbohydrate Research*, 319(1–4):102–111, June 1999.

[31] William S York and Malcolm A O'Neill. Biochemical control of xylan biosynthesis — which end is up? *Current Opinion in Plant Biology*, 11(3):258–265, June 2008. 00130.

[32] T. Kondo, K. Mizuno, and T. Kato. Cell wall-bound p-coumaric and ferulic acids in Italian ryegrass. *Canadian journal of plant science = Revue canadienne de phytotechnie*, 1990.

[33] K. J. Biggs and S. C. Fry. Phenolic cross-linking in the plant cell wall. *In Physiology of cell expansion during plant growth. American Society of Plant Physiologists., , eds d. j. cosgrove and d. p. knievel edition.*, 1987. 00000.

[34] T. Ikegawa, S. Mayama, H. Nakayashiki, and H. Kato. Accumulation of diferulic acid during the hypersensitive response of oat leaves to Puccinia coronata f.sp. avenae and its role in the resistance of oat tissues to cell wall degrading enzymes. *Physiological and Molecular Plant Pathology*, 48(4):245–256, April 1996. 00000.

[35] John H. Grabber, John Ralph, and Ronald D. Hatfield. Ferulate Cross-Links Limit the Enzymatic Degradation of Synthetically Lignified Primary Walls of Maize. *Journal of Agricultural and Food Chemistry*, 46(7):2609–2614, July 1998.

[36] Nathan Mosier, Charles Wyman, Bruce Dale, Richard Elander, Y. Y. Lee, Mark Holtzapple, and Michael Ladisch. Features of promising technologies for pretreatment of lignocellulosic biomass. *Bioresource Technology*, 96(6):673–686, April 2005. 03830.

[37] L. Scobbie, W. Russell, G. J Provan, and A. Chesson. The newly extended maize internode: a model for the study of secondary cell wall formation and consequences for digestibility. *Journal of the Science of Food and Agriculture*, 61(2):217–225, 1993.

[38] John H. Grabber. How do lignin composition, structure, and cross-linking affect degradability? A review of cell wall model studies. *Crop Science*, 45:820–831, 2005.

[39] Javier Gil-Humanes, Fernando Pistón, Alberto Hernando, Juan B. Alvarez, Peter R. Shewry, and Francisco Barro. Silencing of gamma-gliadins by RNA interference (RNAi) in bread wheat. *Journal of Cereal Science*, 48(3):565–568, 2008. 00061.

[40] John Vogel. Unique aspects of the grass cell wall. *Current Opinion in Plant Biology*, 11(3):301–307, June 2008. 00284.

[41] Daisuke Miki, Rika Itoh, and Ko Shimamoto. RNA silencing of single and multiple members in a gene family of rice. *Plant Physiology*, 138(4):1903–1913, 2005. 00294.

[42] Scott M. Hammond, Emily Bernstein, David Beach, and Gregory J. Hannon. An RNA-directed nuclease mediates post-transcriptional gene silencing in Drosophila cells. *nature*, 404(6775):293–296, 2000. 03368.

[43] Emily Bernstein, Amy A. Caudy, Scott M. Hammond, and Gregory J. Hannon. Role for a bidentate ribonuclease in the initiation step of RNA interference. *Nature*, 409(6818):363–366, 2001. 05038.

[44] Fernando Piston, Cristobal Uauy, Lianhai Fu, James Langston, John Labavitch, and Jorge Dubcovsky. Down-regulation of four putative arabinoxylan feruloyl transferase genes from family PF02458 reduces ester-linked ferulate content in rice cell walls. *Planta*, 231(3):677–691, December 2009. 00046.

[45] Javier Gil-Humanes, Fernando Pistón, Stig Tollefsen, Ludvig M. Sollid, and Francisco Barro. Effective shutdown in the expression of celiac disease-related wheat gliadin T-cell epitopes by RNA interference. *Proceedings of the National Academy of Sciences*, 107(39):17023–17028, 2010. 00073.

[46] Rowan A. C. Mitchell, Paul Dupree, and Peter R. Shewry. A Novel Bioinformatics Approach Identifies Candidate Genes for the Synthesis and Feruloylation of Arabinoxylan. *Plant Physiology*, 144(1):43–53, May 2007.

[47] John P. Vogel, David F. Garvin, Todd C. Mockler, Jeremy Schmutz, Dan Rokhsar, Michael W. Bevan, Kerrie Barry, Susan Lucas, Miranda Harmon-Smith, Kathleen Lail, Hope Tice, Jeremy Schmutz (Leader), Jane Grimwood, Neil McKenzie, Naxin Huo, Yong Q. Gu, Gerard R. Lazo, Olin D. Anderson, John P. Vogel (Leader), Frank M. You, Ming-Cheng Luo, Jan Dvorak, Jonathan Wright, Melanie Febrer, Dominika Idziak, Robert Hasterok, Erika Lindquist, Mei Wang, Samuel E. Fox, Henry D. Priest, Sergei A. Filichkin, Scott A. Givan, Douglas W. Bryant, Jeff H. Chang, Todd C. Mockler (Leader), Haiyan Wu, Wei Wu, An-Ping Hsia, Patrick S. Schnable, Anantharaman Kalyanaraman, Brad Barbazuk, Todd P. Michael, Samuel P. Hazen, Jennifer N. Bragg, Debbie Laudencia-Chingcuanco, Yiqun Weng, Georg Haberer, Manuel Spannagl, Klaus Mayer (Leader), Thomas Rattei, Therese Mitros, Sang-Jik Lee, Jocelyn K. C. Rose, Lukas A. Mueller, Thomas L. York, Thomas Wicker (Leader), Jan P. Buchmann, Jaakko Tanskanen, Alan H. Schulman (Leader), Heidrun Gundlach, Michael Bevan, Antonio Costa de Oliveira, Luciano da C. Maia, William Belknap, Ning Jiang, Jinsheng Lai, Liucun Zhu, Jianxin Ma, Cheng Sun, Ellen Pritham, Jerome Salse (Leader), Florent Murat, Michael Abrouk, Klaus Mayer, Remy Bruggmann, Joachim Messing, Noah Fahlgren, Christopher M. Sullivan, James C. Carrington, Elisabeth J. Chapman, Greg D. May, Jixian Zhai, Matthias Ganssmann, Sai Guna Ranjan Gurazada, Marcelo German, Blake C. Meyers, Pamela J. Green (Leader), Ludmila Tyler, Jiajie Wu, James Thomson, Shan Chen, Henrik V. Scheller, Jesper Harholt, Peter Ulvskov, Jeffrey A. Kimbrel, Laura E. Bartley, Peijian Cao, Ki-Hong Jung, Manoj K. Sharma, Miguel Vega-Sanchez, Pamela Ronald, Christopher D. Dardick, Stefanie De Bodt, Wim Verelst, Dirk Inzé, Maren Heese, Arp Schnittger, Xiaohan Yang, Udaya C. Kalluri, Gerald A. Tuskan, Zhihua Hua, Richard D. Vierstra, Yu Cui, Shuhong Ouyang, Qixin Sun, Zhiyong Liu, Alper Yilmaz, Erich Grotewold, Richard Sibout, Kian Hematy, Gregory Mouille, Herman Höfte, Todd Michael, Jérome Pelloux, Devin O'Connor, James Schnable, Scott Rowe, Frank Harmon, Cynthia L. Cass, John C. Sedbrook, Mary E. Byrne, Sean Walsh, Janet Higgins, Pinghua Li, Thomas Brutnell, Turgay Unver, Hikmet Budak, Harry Belcram, Mathieu Charles, Boulos Chalhoub, and Ivan Baxter. Genome sequencing and analysis of the model grass Brachypodium distachyon. *Nature*, 463(7282):763–768, February 2010. 00000.

[48] Ai-Min Wu, Emma Hörnblad, Aline Voxeur, Lorenz Gerber, Christophe Rihouey, Patrice Lerouge, and Alan Marchant. Analysis of the Arabidopsis IRX9/IRX9-L and IRX14/IRX14-L pairs of glycosyltransferase genes reveals critical contributions to biosynthesis of the hemicellulose glucuronoxylan. *Plant Physiology*, 153(2):542–554, June 2010. 00107.

[49] Poppy E. Marriott, Richard Sibout, Catherine Lapierre, Jonatan U. Fangel, William G. T. Willats, Herman Hofte, Leonardo D. Gómez, and Simon J.

McQueen-Mason. Range of cell-wall alterations enhance saccharification in Brachypodium distachyon mutants. *Proceedings of the National Academy of Sciences*, 111(40):14601–14606, October 2014.

[50] Laura E. Bartley, Matthew L. Peck, Sung-Ryul Kim, Berit Ebert, Chithra Manisseri, Dawn M. Chiniquy, Robert Sykes, Lingfang Gao, Carsten Rautengarten, Miguel E. Vega-Sánchez, Peter I. Benke, Patrick E. Canlas, Peijian Cao, Susan Brewer, Fan Lin, Whitney L. Smith, Xiaohan Zhang, Jay D. Keasling, Rolf E. Jentoff, Steven B. Foster, Jizhong Zhou, Angela Ziebell, Gynheung An, Henrik V. Scheller, and Pamela C. Ronald. Overexpression of a BAHD Acyltransferase, OsAt10, Alters Rice Cell Wall Hydroxycinnamic Acid Content and Saccharification. *Plant Physiology*, 161(4):1615–1633, April 2013. 00050.

Capítulo 6

CONCLUSIONES

I El método de sacarificación puesto a punto en el IAS-CSIC fue útil en la cuantificación de variabilidad del potencial de producción de bioetanol a partir de biomasa lignocelulósica.

II De forma general, los genotipos de cebada muestran una biomasa lignocelulósica menos reclacitrante que el trigo y el triticale, que estuvieron al mismo nivel.

III El ranking de genotipos descritos por el método de IAS-CSIC fue ligeramente distinto al obtenido en el CNAP (UK). Sin embargo, ambos métodos identificaron las líneas más constrastantes que fueron: Steptoe x Morex y OWB Dominant x OWB Recessive.

IV Por las correlaciones observadas entre el contenido de lignina y el grosor de los tallos, este último podría usarse para una estimación de la degradabilidad de la biomasa en programas de mejora. Habría que destacar también la importancia de la falta de correlación entre el factor del potencial de etanol a partir de la biomasa lignocelulósica y la producción de grano, implicando que se podrían conseguir líneas con un alto rendimiento en grano y buena degradabilidad de la paja.

V El fenotipado masivo basado en imágenes tomadas a lo largo del desarrollo del cultivo en el espectro del visible así como del infrarrojo cercano, mediante una plataforma UAV, ha demostrado ser un método relativamente preciso en la estimación de variables relacionadas con la cantidad de biomasa, potencial de etanol de esta biomasa así como de etanol teórico.

VI Los datos estimados con la plataforma UAV fueron siempre mejores considerando escenarios multi-temporales que los que tomaron datos en fechas individuales.

VII De forma general los índices basados en NIR (NDVI, GNDVI, MCARI y MSR) fueron más apropiados en las estimaciones de biomasa, mientras que

los basados en el visible (EXG, VIgreen y TCI) lo fueron para liberación de azúcar.

VIII La plataforma UAV obtuvo los mejores valores de predicción para el factor conocido como etanol teórico, obtenido por combinación lineal de la biomasa producida y la liberación de azúcares a partir de esta. En este caso el mejor índice predictor del factor etanol teórico fue NDVI (R2=0.66) bajo el escenario multi-temporal TS-3.

IX A partir del índice NDVI en el escenario multi-temporal TS-3 se construyó un ranking de genotipos para el factor del etanol teórico, se observaron importantes diferencias entre los parentales de cebada OWB dominant x OWB recessive y Franklin x OWB dominant, que podrían ser interesantes para el desarrollo de futuros programas.

X La población RIL generada a partir de los parentales Bd3-1 x Bd21 reveló un QTL significativo en la evaluación del grado de sacarificación a partir de su biomasa, concretamente a partir del tallo de la planta. En el análisis de QTLs, en el cromosoma 5 se identificaron varios genes candidatos con funciones conocidas en la pared celular.

XI Las plantas transgénicas en las que el gen Bradi5g24290.1 fue silenciado mediante miRNA mostraron incrementos significativos para el grado de sacarificación frente a las plantas no silenciadas. En el análisis de los componentes de pared celular, se observó que las plantas transgénicas tienen una menor concentración de xilosa, arabinosa y FA. Se puede sugerir por tanto que esta diferencia de componentes de pared sea la probable responsable del incremento de digestibilidad.